



FEASIBILITY STUDY OF CST TECHNOLOGIES FOR THE LOW TEMPERATURE REQUIREMENTS OF THE BAYER ALUMINA PROCESS

August 2019



About ITP

The ITP Energised Group, formed in 1981, is a specialist renewable energy, energy efficiency and carbon markets consulting company. The group has offices and projects throughout the world.

IT Power (Australia) was established in 2003 and has undertaken a wide range of projects, including designing grid-connected renewable power systems, providing advice for government policy, feasibility studies for large, off-grid power systems, developing micro-finance models for community-owned power systems in developing countries and modelling large-scale power systems for industrial use.

ITP Thermal Pty Ltd was established in early 2016 as a new company within the ITP Energised group, with a mandate to lead solar thermal projects globally. In doing so it accesses staff and resources in the other ITP Energised group companies as appropriate.

About this report

ITP Thermal and CSIRO are participants in the project funded by ARENA as part of ARENA's Research and Development Program and led by the University of Adelaide Centre for Energy Technology. This report records ITP's and CSIRO's contributions to Program 1 of the project, which also received valuable input from the Steering Committee, comprising members of all parties in the project. The mechanical vapour recompression concept and examples in this study were provided by 'Alcoa of Australia' under the umbrella of the RND054 Program study for the purposes of comparing relative economics to concentrated solar thermal options.

Disclaimer

The views expressed herein are not necessarily the views of the Australian Government, and the Australian Government does not accept responsibility for any information or advice contained herein.

Report Control Record

Document prepared by:

ITP Thermal Pty Ltd
 Level 1, 19 Moore Street, Turner ACT 2612
 PO Box 6127, O'Connor, ACT, 2602, Australia
 Tel. +61 2 6257 3511
 E-mail: info@itpau.com.au
 http://www.itpthermal.com.au

| Document Control | | | | | |  |
|---------------------|---------------|---|--|-----------------|----------------------|---|
| Report title | | Feasibility study of CST technologies for the low temperature requirements of the Bayer Alumina Process | | | | |
| Client Contract No. | | ARENA RND 054 | ITP Project Number | | T0031 | |
| File path | | G:\ITPThermalWork\0Projects\T0031\work | | | | |
| Client | | University of Adelaide | Client Contact | | Professor Gus Nathan | |
| Rev | Date | Status | Author/s | Project Manager | Approved | |
| 1.0 | 1 July 2018 | Draft | R Bader, K Lovegrove, A Bayon, A Beath | R Bader | K Lovegrove | |
| 2.0 | December 2018 | Final draft | R Bader, K Lovegrove, A Bayon, A Beath | R Bader | K Lovegrove | |
| 2.2 | August 2019 | Final, updated | R Bader, K Lovegrove, A Bayon, A Beath | R Bader | K Lovegrove | |

A person or organisation choosing to use documents prepared by IT Power (Australia) Pty Ltd accepts the following:

- a) Conclusions and figures presented in draft documents are subject to change. IT Power (Australia) Pty Ltd accepts no responsibility for their use outside of the original report.
- b) The document is only to be used for purposes explicitly agreed to by IT Power (Australia) Pty Ltd.
- c) All responsibility and risks associated with the use of this report lie with the person or organisation who chooses to use it.

LIST OF ABBREVIATIONS

| | |
|------|--|
| AUD | Australian Dollar |
| BOM | The Australian Bureau of Meteorology |
| BOP | Balance of Plant |
| CPC | Compound Parabolic Concentrator |
| CSP | Concentrating Solar Power |
| CST | Concentrating Solar Thermal Energy |
| EUR | Euro |
| HRSG | Heat Recovery Steam Generator |
| HTF | Heat Transfer Fluid |
| ITP | IT Power (Australia) Pty Ltd |
| kW | Kilowatt, unit of power – subscript e for electric, th for thermal |
| kWh | Kilowatt-hour, unit of energy (1 kW generated/used for 1 hour) |
| LCOH | Levelised Cost of Heat |
| MVR | Mechanical Vapour Recompression |
| MW | Mega Watt, unit of power = 1000kW |
| NPV | Net Present Value |
| O&M | Operations and Maintenance |
| PTC | Parabolic Trough Collector |
| PV | Photovoltaic |
| RET | Renewable Energy Target |
| SF | Solar field |
| SM | Solar Multiple |
| TES | Thermal Energy Storage |
| USD | US Dollar |
| WACC | Weighted Average Cost of Capital |

CONTENTS

| | |
|---|-----------|
| EXECUTIVE SUMMARY | 7 |
| 1. INTRODUCTION | 11 |
| 2. BACKGROUND | 12 |
| 2.1. The Bayer process | 12 |
| 2.2. Alumina refineries in Australia | 14 |
| 3. SITE ASSESSMENT | 16 |
| 3.2. Other potential sites | 22 |
| 4. THERMAL ENERGY DEMAND AND SUPPLY | 23 |
| 5. SOLAR PLANT DESIGN | 26 |
| 5.1. CST plant design variants | 27 |
| 5.2. Nominal temperature ranges | 29 |
| 5.3. Design point specification | 30 |
| 6. TECHNOLOGIES FOR SOLAR THERMAL PROCESS HEAT | 31 |
| 6.1. Solar collector technology options | 31 |
| 6.2. Storage options | 42 |
| 6.3. Possible CST system layouts | 43 |
| 6.4. Combined Heat and Power configurations | 44 |
| 7. COST DATA COLLECTION | 45 |
| 7.1. Overview of technology suppliers | 45 |
| 7.2. Cost data format | 45 |
| 8. INPUT PARAMETERS FOR SAM | 47 |
| 8.1. Summary of inputs for SAM | 47 |
| 9. FEASIBILITY ANALYSIS | 51 |
| 9.1. Methods and Parameters | 51 |
| 9.2. Base case economics | 54 |
| 9.3. Plant operability | 66 |
| 9.4. Parametric design optimisation | 71 |
| 9.5. Alternative scenarios | 81 |
| 9.6. Resource requirements | 96 |
| 9.7. Environmental impact | 99 |

| | |
|---|------------|
| 9.8. Discussion and Recommendations..... | 100 |
| 10. MECHANICAL VAPOUR RECOMPRESSION | 104 |
| 10.1. Overview of MVR..... | 104 |
| 10.2. Application to reference refinery | 105 |
| 10.3. Analysis | 107 |
| 10.4. Results and Discussion..... | 108 |
| 10.5. Next steps..... | 110 |
| 11. CONCLUSIONS | 112 |
| APPENDIX A. STEAM GENERATION HEAT EXCHANGERS | 115 |
| APPENDIX B. COST MODELING | 117 |
| B.1. Methodology | 117 |
| B.2. Component cost modelling | 120 |
| B.3. Operation and Maintenance costs | 129 |
| B.4. Model verification | 131 |

EXECUTIVE SUMMARY

As part of the ARENA R&D project 2015/RND054, ITP Thermal and CSIRO have assessed the techno-economic viability of integrating low- or medium-temperature process heat generated with concentrated solar thermal energy (CST) into the Bayer alumina production process. Alumina refineries are among the largest industrial natural gas users in Australia and, as such, are particularly exposed to changes in natural gas prices. In this study, we aimed to determine whether integration of CST into one of the world's largest alumina refineries is a viable option to reduce energy-related costs and lower the exposure to increasingly volatile gas prices and increasingly stringent carbon emissions regulations. More generally, this study aims to provide a reference case for CST integration into the Australian industry sector.

The present study has evolved in collaboration our industrial partner and academic partner University of Adelaide. The industrial partner currently operates three alumina refineries in Australia, all located within an area of about 100 km, near the coast in the southwest of Western Australia. This region has a direct solar irradiation >2000 kWh/m²/year, suitable for CST.

Based on the reference plant's current steam demand and supply infrastructure, three potential ways to integrate CST have been identified:

- 1) displacing gas boilers by producing up to 500 tph of steam at 470°C and 8 MPa for power generation via existing steam turbines followed by steam introduction to the digestion process at 210°C, 0.8 MPa;
- 2) providing up to 100 tph of steam generation at 210°C, 0.8 MPa to replace the current steam which is currently produced by the gas boilers at 470°C/8 MPa and directly throttled to 210°C/0.8 MPa for introduction to the digestion process;
- 3) providing up to 500 tph of steam generation at 210°C, 0.8 MPa for direct introduction to the digestion process in combination with electric energy supply from a new solar photovoltaic system or purchase of additional electricity off the grid to offset the loss in steam turbine power output as a result of a reduced steam flow rate through the turbine.

While all three scenarios have their advantages and disadvantages, we have focussed our work on scenario 1 addressing greatest compatibility with thermal storage. This requires the CST system to operate between around 300 and 500°C. This temperature range is achievable with trough, Fresnel and tower technology.

A request for information was issued to commercial CST technology providers to provide up-to-date preliminary cost estimates for the three CST technologies. Received cost information from CST companies was combined with literature and NREL SAM's default data to derive size-

dependent component cost models for the three main system components; solar field, thermal energy storage and balance of plant. O&M cost data was reviewed from a wide range of plants and a size (capex) dependent O&M percentage (ref.: 2.05% of capex pa. at \$100m capex) was determined.

The resulting component cost models were used with NREL's SAM model to evaluate the annual thermal output and total installed costs (including 25% indirect) for a range of pilot and large-scale CST system configurations. CST system configurations considered included the technologies of linear Fresnel, parabolic trough and solar tower, with thermal storage capacities of 0, 8 and 14 hours. The solar multiple (solar field size) was optimised in each case to minimise the resulting LCOH.

The economic viability of a CST system was evaluated at the reference refinery. Target criteria for a full-scale 392 MW_{th} CST system, capable of providing 500 t/h of steam during peak irradiation, were prescribed as NPV>AUD20m with a WACC of 12% and a solar share of 29-45%. We additionally considered IRR and LCOH to guide the economic evaluation of different system designs.

The results of our analysis show that, based on current commercial costs and the solar resource in the region South-west of Perth, no CST system configuration could be identified that meets the NPV target. However, all large-scale system configurations are found to yield positive IRRs. Using the average of the cost estimates provided by suppliers, which represent a conservative estimate for today's costs, the IRR values were found to range from 3.5 to 7%, while the low cost estimates of suppliers, which represent the lowest available cost opportunities, IRR was found to range from 6 to 13.5%. Values of LCOH are estimated to be in the range of 22 to 30 \$/GJ_{th} based on the average costs and in the range of 14 to 24 \$/GJ_{th} based on the low cost estimates. Nevertheless, the viability is expected to increase rapidly as the costs of CST technologies continue to fall, as discussed in more detail below, and at sites with a better solar resource.

The two linear technologies were found to yield similar economic results. Tower technology tends to be somewhat more economical than linear technology with current average cost estimates. On the other hand, low-cost data from linear technology providers suggests that costs significantly below the average cost estimates may be achievable. The economics generally improve with decreasing storage size, due to the large added capital cost of a large thermal energy storage system. However, to reach a solar share (fraction of annual thermal energy demand provided by the CST system) in the range of 29 to 45%, around 7 and 14 hours of full-load thermal energy storage will be required.

In addition to the full-scale plant, we considered the possibility of an initial 20 MW_{th} pilot system, built before the large-scale plant, for de-risking and gaining experience and confidence with the technology, and potentially for further testing of new solar thermal technologies in the future. The economics of a pilot plant is assessed similarly to the actual full-scale plant. As with the full-scale

system, NPVs are negative in most cases considered. Grant support from the Australian Renewable Energy Agency could be sought to reduce the required investment and risk for the investors.

Several factors could reduce LCOH and increase IRR and NPV of a large-scale plant: CST cost reductions (capex and opex), better plant location, lower solar share, longer projected system lifetime and higher gas price.

CST technology is currently in a phase of rapid price declines. From 2010 to 2017, CST costs have decreased by approximately 25% and a further cost decline of approximately 20% has been predicted for the next five years, based on projected growth and learning rates. We estimated that this cost reduction could yield NPV > AUD20m for a large-scale system without TES.

Significantly better economics could also be reached with today's CST technology in locations with significantly better solar resource than at the reference location. To illustrate this, we have shown for the location of Learmonth at the western tip of WA, where DNI levels are approximately 30% higher than at the reference location, that NPV of nearly AUD100m and IRR of around 14% may be achieved with large-scale systems with up to 14 hours of thermal energy storage and solar capacity factors of 65 to 70%. These economic figures will further increase as costs of CST technologies continue to decline.

Based on these results, we conclude that while a CST system is currently not fully economical under the given target criteria at the reference location, it does offer potentially positive IRR that may be sufficient for other investors. Also, there is a high probability that a CST system will meet the investment criteria in the future, as cost reductions continue, and under alternative investment scenarios with other types of investors.

Further, we have assessed potential CST technology suppliers, resource requirements and environmental impact of a CST system. We found the site at the reference location refinery to be suitable and to be sufficiently large for the construction of a large-scale 392 MW_{th} CST plant.

For comparison, we have screened potential alternative renewable technology options besides CST for steam generation. While the potentials of bioenergy and geothermal have been deemed low for this large-scale application, mechanical vapour recompression of waste steam currently discarded at around 53°C and 0.14 bar, driven by renewable grid electricity, has been identified as a potentially viable alternative. Further development of this technology is considered to be needed to meet the requirements for an alumina refinery.

Consequently, the economics of MVR have been assessed and compared to CST. We found that the economics of MVR strongly depend on the assumed average electricity price over the plant operation life. If low average electric energy prices below ~7 c\$/kWh are expected, MVR may be more economical at the reference location in the short- to medium-term than CST. On the other

hand, above ~8 c\$/kWh, CST with storage may be more cost effective than MVR even at today's costs of CST energy at the reference location.

Electrically driven grid connected MVR has potential to offer a higher renewable share than an on-site CST system alone when the electrical grid becomes sufficiently decarbonised. However, reliance on the electrical grid alone would make the plant subject to intermittently high grid prices for electricity, due to the large fluctuations in electricity price with the time of day, weather and season. This, together with the low cost of thermal energy storage, suggests that the most cost-effective 100% renewable energy system for delivering steam at sites with solar resources comparable with, or better than, Pinjarra is likely to be achieved with a hybrid MVR and CST system in which the CST plant is used to provide process heat for stored thermal heat during periods of relatively high electricity prices. For full renewable operation it seems likely that an optimised combination of the two will offer the best financial performance. Further work to analyse this approach is recommended.

1. INTRODUCTION

Alumina refineries using the Bayer process are together the largest overall users of natural gas in Australia at approximately 160PJ pa and the dominant contributor to Australia's greenhouse gas emissions from the mining and minerals processing sector, being responsible for approximately 40% of Australia's minerals CO₂ emissions (Clean Energy Regulator, 2010).

The energy is used approximately half at temperatures below 280°C and half at above 800°C.

The individual refineries have thermal loads that are in the 100s MW_{th} range. The low temperature step is amenable to the application of lower temperature and more cost effective solar thermal technologies and the large scale means that considerable cost efficiencies should in principle be possible.

This project has been funded by ARENA as project no. 2015/RND054. The contracting party is the University of Adelaide (UoA). The UoA has subsequently entered into a collaboration agreement with the other parties. The project is comprised of three separate programs. Program 1 deals with the use of solar thermal technologies for the lower temperature heat requirement of the Bayer process, Program 2 examines the integration of solar reforming of natural gas and Program 3, investigates application of solar thermal to the high temperature calcination step.

This report is a deliverable for program 1 and examines the feasibility of a solar thermal solution with particular focus on application to a reference refinery in Western Australia.

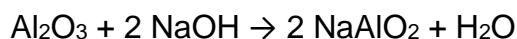
The project definition specifies that the solar thermal system designed in Program 1 reaches a solar share of 29 to 45%.

2. BACKGROUND

2.1. The Bayer process

The Bayer process converts bauxite into alumina, which is the feedstock for the subsequent stage of aluminium production. Only about 8% of Australia's alumina is converted into aluminium within Australia, with 92% exported as alumina (Armitage, 2013). The key stages of the Bayer process, which are illustrated in Figure 1 and Figure 2 are:

- **Grinding:** The raw bauxite is ground to a fine powder with a diameter of ~100 µm (depending on the raw material and the downstream process).
- **Predesilication:** The material is heated in a slurry to approximately 80°C and agitated for several hours in a holding tank.
- **Silication:** The material is mixed with spent liquor at similar temperatures and under moderate pressure, to leach out the aluminium-bearing minerals as a soluble sodium aluminate. This is then reprecipitated to form a complex sodium aluminosilicate;
- **Digestion:** Depending on the composition of the bauxite, the digestion can be undertaken at temperatures of either 140-150 °C or 220-260 °C. In this step the bauxite is washed with a hot solution of [sodium hydroxide](#), NaOH, under pressure. This converts the aluminium oxide in the ore to soluble [sodium aluminate](#), 2NaAlO_2 , according to the [chemical equation](#):



- **Clarification:** The impurities are then removed in several stages. The liquor is first cooled and a flocculent is added to remove some of the impurities by precipitation, a process that involves lime. Further impurities are removed by filtration. The residue is termed "red mud", while the product is alumina tri-hydrate, $\text{Al}(\text{OH})_3$.
- **Drying and preheating:** The moist $\text{Al}(\text{OH})_3$ is dried and preheated before calcination.
- **Calcination:** The alumina tri-hydrate is then heated to temperatures of ~1000°C, to thermally decompose it to form aluminium oxide, a highly endothermic reaction that releases water as per the following equation:



The calcination was traditionally performed in rotary kilns, but these have mostly been replaced by the "flash" calciner, which heats the material as powder of diameter ~100µm, which is conveyed in high temperature air at velocities of ~20m/s, at which conditions the powder remains in suspension. The calcination process is complex, with several phases of alumina being

possible. The quality of the fuel is also important, so that natural gas is mostly the fuel of choice since it yields the lowest impact on product quality.

Approximately half of the thermal energy to the process is expended in the low temperature processes and half in the high temperature calcination process.

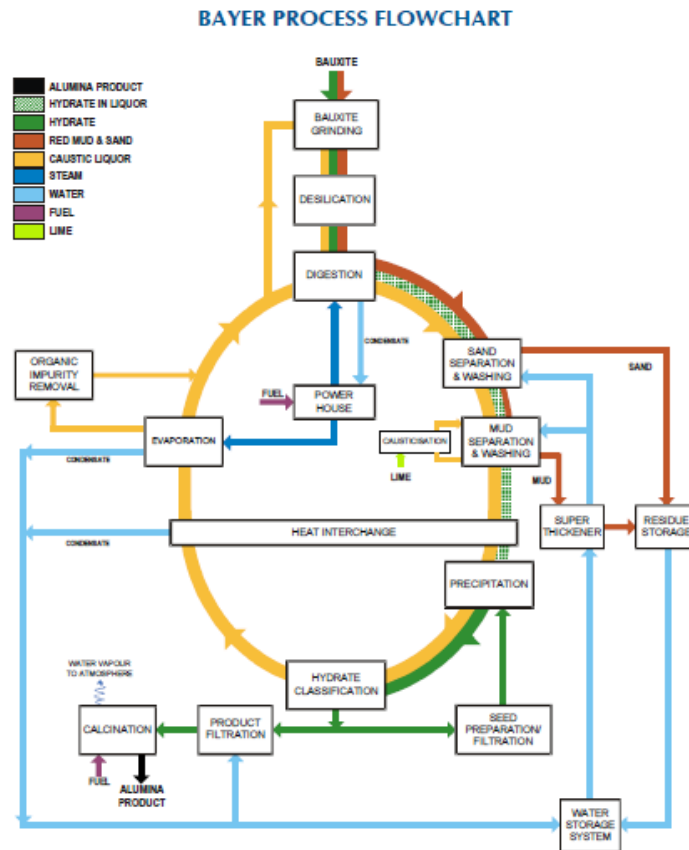


Figure 1: A schematic diagram of the Bayer refining process, which converts Bauxite to alumina via the key stages of digestion, precipitation, classification and calcination (Source: Hatch).

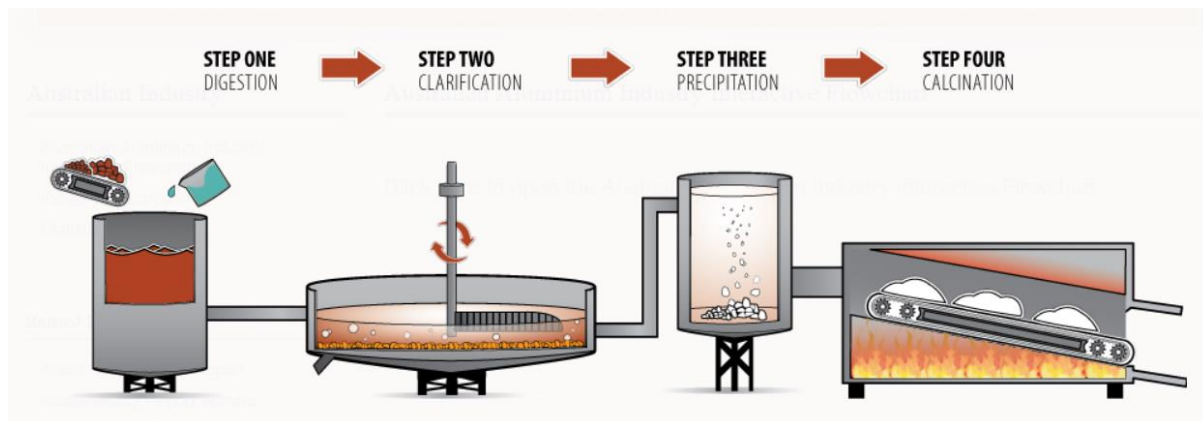


Figure 2: Schematic illustration of the Bayer process.

2.2. Alumina refineries in Australia

According to the Australian Aluminium Council, there are six alumina refineries operating in Australia producing mostly smelter grade alumina for both the domestic and export markets. Australia is the world's second largest producer and exporter of alumina, with 22% of global production. In 2011 Australia produced 19.1 million tonnes of metallurgical (smelter grade) alumina and around 0.5 Mt of chemical grade alumina.¹ Four alumina refineries are located in the southwest of Western Australia and two near Gladstone, QLD (Figure 3):

- Yarwun (Queensland) - Rio Tinto Alcan
- Kwinana (Western Australia) - Alcoa of Australia
- Pinjarra (Western Australia) - Alcoa of Australia
- Queensland Alumina Ltd (QAL) (Queensland) - Rio Tinto Alcan, Rusal
- Wagerup (Western Australia) - Alcoa of Australia
- Worsley (Western Australia) - South32 - Worsley Alumina

A seventh at Gove (Northern Territory) - Pacific Aluminium - suspended operations in 2014. As can be seen from Figure 4, these alumina refineries are typically located where they are readily accessible from the bauxite mines. Notable exceptions are the mine at Weipa that is not close to a refinery and the refineries in Gladstone that in turn are reliant on bauxite delivered by ship.

¹ <http://aluminium.org.au/australian-alumina/australian-alumina>

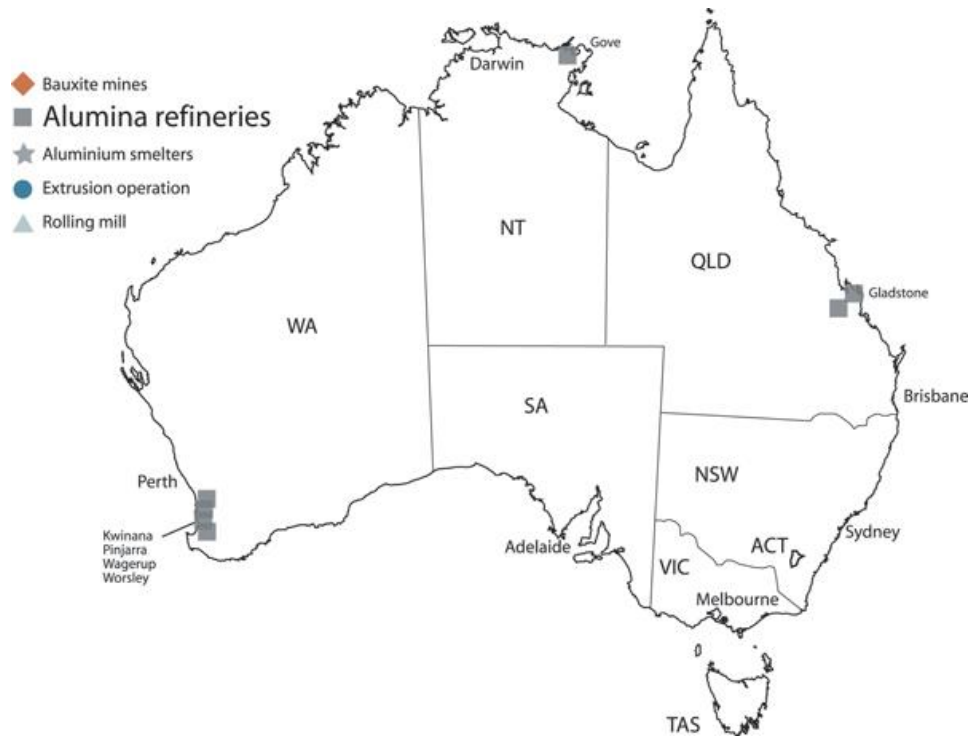


Figure 3: Overview of existing alumina refineries in Australia.



Figure 4: Overview of existing bauxite mines in Australia.

3. SITE ASSESSMENT

An important consideration in the planning of a CST system is the available local solar resource. Table 1 compares long-term average daily DNI and GHI for the reference facility in southwestern WA with those for the two other locations of alumina refining, Gladstone, QLD and Gove, NT, as well as with those of two other locations of potential interest: Learmonth WA and Alice Springs, NT. Learmonth lies at the lower north western corner of WA and is about 10° closer to the equator. Learmonth is also on the coast and hence is a potential example location for delivery of bauxite by ship as well as export of alumina for a future export-oriented green field industrial plant. There are no identified locations where a major known bauxite deposit coincides with best available DNI. Alice Springs is chosen as a reference location as it is near the centre of the Australian continent and generally associated with very high solar resources, it is not proposed as a realistic alumina refining site however.

It can be seen that both locations near Gladstone and Gove exhibit lower DNI and higher GHI. This is likely due to a higher frequency of clouds in these near-tropical/tropical regions. In contrast, Learmonth, WA and Alice Springs Airport, NT exhibit significantly higher annual DNI and GHI. Higher DNI is likely to be due to lower atmospheric attenuation due to higher latitude and may also be due to fewer clouds, as indicated by the lower amount of average annual rain. GHI is also influenced, to a lesser degree than DNI, by atmospheric attenuation and clouds. In addition, GHI incorporates a component of cosine losses, which increases with increasing distance from the equator.

Table 1. Comparison of long-term average daily DNI and GHI for reference site in WA and four alternative reference locations. For Gladstone, QLD and Gove, NT, locations slightly off the coast were chosen because a CST plant built directly at the coast would be likely to suffer from increased corrosion due to the high humidity and salt content in the air and to be exposed to increased wind loads. Percentage differences between the reference location in WA and the other locations are also tabulated.²

| Parameter | DNI, MJ/m ² /day (kWh/m ² /day) | Difference, % | GHI, MJ/m ² /day (kWh/m ² /day) | Difference, % |
|---------------------------|--|---------------|--|---------------|
| Reference location, WA | 20.8 (5.8) | - | 18.8 (5.2) | - |
| Gladstone, QLD (10 km W) | 20.6 (5.7) | -1.0% | 20.2 (5.6) | +7.4% |
| Gove, NT (20 km SW) | 18.4 (5.1) | -11.5% | 20.3 (5.6) | +8.0% |
| Learmonth, WA | 25.9 (7.2) | +24.5% | 22.6 (6.3) | +20.2% |
| Alice Springs Airport, NT | 26.4 (7.3) | +26.9% | 22.1 (6.1) | +17.6% |

² AREMI; <https://nationalmap.gov.au/renewables/>

Since CST plant performance is approximately proportional to the available DNI (or GHI in case of stationary collectors), it can be concluded that same CST plant operated in Learmonth or Alice Springs would generate at least ~20% more thermal energy due to higher DNI (GHI), with an additional performance advantage due to lower cosine losses.

3.1.1. Solar resource

Surface-based one minute direct normal irradiation measurement data is available from the Australian Bureau of Meteorology (BOM) for a few (~30) weather stations in Australia.³ The BOM has derived a grid of hourly irradiation data for Australia based on satellite images. This data is gridded with a resolution corresponding to a ground area of $1.25 \times 1.25 \text{ m}^2$ at the equator (larger away from the equator) and is available for the period 1990–2015 through the website of AREMI (The Australian Renewable Energy Mapping Infrastructure).⁴ Hence, for the present project, hourly DNI and GHI data was obtained through AREMI. Up-to-date weather data for a dense grid of Australian weather stations was obtained directly from the BOM on a hard drive. The BOM estimated the error in satellite-derived daily global solar exposure by comparison with 9 surface-based pyranometer measurements. In clear sky conditions, the difference was at most 7%, with average difference of 0.17% and most measurements with difference < 6%.

ITP's in-house software was used to process the raw radiation and weather data to create real-year TMY3 (typical meteorological year) format files with hourly data for GHI, DNI, dry bulb temperature, dew point temperature, relative humidity, ambient pressure, wind speed and wind direction. These files can be directly used in NREL's SAM model. Data files were created for the 10 years 2004–2008 and 2011–2015, which are the 10 recent years with the lowest number of hours with missing weather or DNI data (less than 100 hours).

Figure 5 shows monthly average daily DNI (a) and GHI (b) for the reference location in WA. Red bars are averages over the 10 selected years of data, while blue and green bars represent minimum and maximum values over the ten years. The monthly average daily DNI is highest in January at a long-term average of $32.9 \text{ MJ/m}^2/\text{day}$ and lowest in July with a long-term average of $11.5 \text{ MJ/m}^2/\text{day}$. The variation for a specific month between best and worst year is around 50% in summer and up to 150% in winter. The average yearly total DNI is $7.5 \text{ GJ/m}^2/\text{yr}$ and varies by 16.6% between best and worst year. Based on the yearly average daily DNI, best, worst and "closest to average" years are, respectively, 2015 ($6.25 \text{ kWh/m}^2/\text{day}$), 2012 ($5.36 \text{ kWh/m}^2/\text{day}$) and 2013 ($5.65 \text{ kWh/m}^2/\text{day}$).

³ Definitions and how solar radiation is measured: <http://www.bom.gov.au/climate/austmaps/solar-radiation-glossary.shtml#globalexposure>

⁴ <https://nationalmap.gov.au/renewables/>

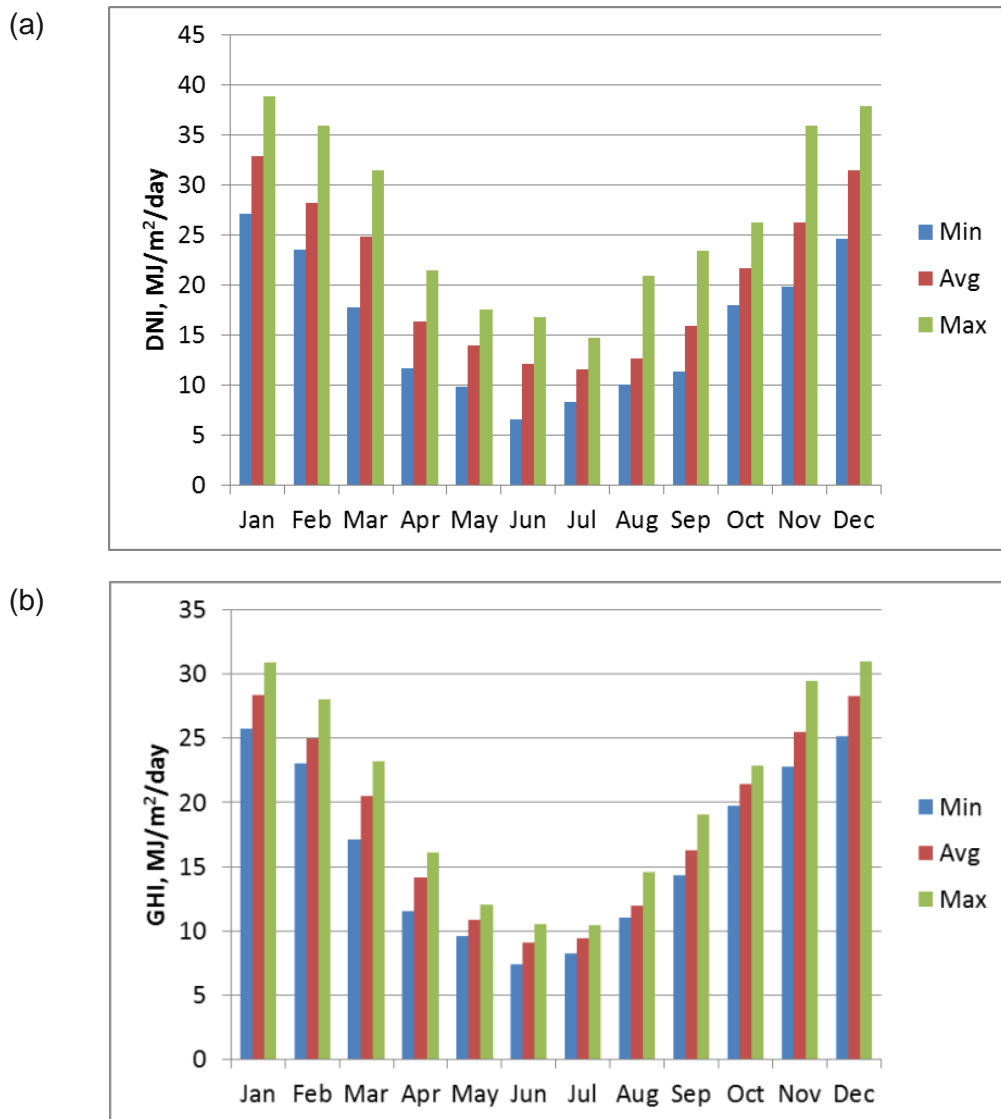


Figure 5. Monthly average daily DNI (a) and GHI (b) for the reference location in WA: Min: year with lowest monthly average DNI/GHI; Max: year with highest monthly average DNI/GHI; Avg: Average over 10 years (data source: AREMI).

Similarly, GHI varies from a long-term average of 28.4 MJ/m²/day in summer to 9.1 MJ/m²/day in winter. On the other hand, the variation for a specific month between best and worst year is only around 16% (October) to 42% (June) for GHI. This is attributed to the fact that GHI comprises both direct and diffuse components of sunlight. Hence, while clouds strongly reduce the DNI, they lead to a shift from direct to diffuse radiation and hence tend to affect GHI less than DNI. Hence, systems that use global solar radiation rather than only the DNI will experience lower variation in their performance output from year to year than systems that only use DNI. The average yearly total GHI is 6.7 GJ/m²/yr and varies by 7.4% between best and worst year. In summary, the reference location experiences large variation in both DNI and GHI over the course of a year,

which results in strong performance variations of CST plants. Additionally, the variation in available DNI for a specific month and hence CST system performance also strongly varies from year to year.

Shading is not expected to be an issue at the reference site. The site and its surroundings are fairly flat with no high mountains, tall buildings or trees in the area.

To provide a reference, Figure 6 shows the annual DNI and GHI maps for Australia. As can be seen, the southwest of WA is an intermediate location for solar energy, with best locations in Australia receiving up to 40% more direct normal sunlight.

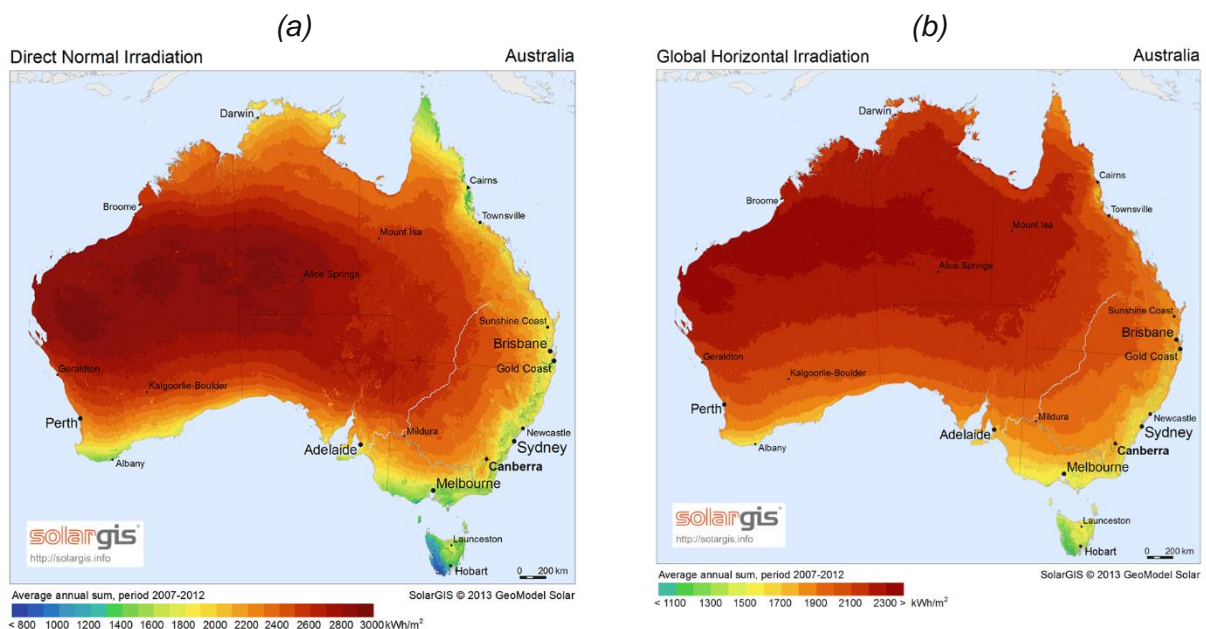


Figure 6: (a) DNI and (b) GHI maps of Australia.

3.1.2. Weather

High wind speeds may lead to tracking inaccuracies and hence lower optical efficiency of the solar thermal system. At very high wind speeds (above ~ 15 m/s⁵), CST systems need to be stowed. As can be seen from Figure 7 below, the reference region very rarely experiences hourly average wind speeds of more than 14 m/s (probability of $\sim 0.25\%$). Hence, high wind speeds are not expected to be a problem for a CST plant in this region and would not affect the plant output significantly. Further, Figure 7b shows the frequency distribution of wind directions. If dust is emitted by the refinery, CST plant locations in direction of the wind relative to the refinery may experience increased levels of soiling. Predominant overall wind direction is from south to north with most frequent wind directions between south-southeast and south. Based on this data, a

⁵ http://www.sbp.de/fileadmin/sbp.de/Presse/Downloads/150819_Stellio_Heliostat_Press_Release_2.pdf (retrieved 2017-11-22).

CST plant located directly north/north-northwest of the refinery would be most exposed to dust emitted by the plant, while a CST plant located between east and west-southwest relative to the refinery would likely experience lowest dust exposure from the plant (not considering any other nearby dust sources other than the refinery).

Figure 8 shows the distribution of monthly rain for the reference site. Rain is concomitant with clouds and hence a drop in DNI. On the other hand, regular rain can help keep collector surfaces free from dust and reduce the O&M costs for system cleaning. The reference location experiences non-uniform rain distribution over the year, with highest amounts of rain in winter and very little rain during the summer months. Average yearly rainfall is nearly twice as high as the long-term average for Australia.⁶

Temperatures in the reference location are moderate with average min. and max. temperatures of 14.8 and 23.3°C and absolute min. and max. temperatures of 5.4 and 39.4°C over the course of the year. Hence, there is no significant freeze risk for water.

The list of assessment criteria should be completed and expanded as new information and new aspects emerge from future site inspections and discussions with the end user and potential technology providers. An inquiry with one LFR technology supplier about their specific site requirements for a pilot-size system (design variant 4 below) yielded the following response: “The plot should be rectangular, and north south length not less than 350 meters (ideally 470 m). The maximum slope of final topography (after cut and fill activities) should be less than 5%. We can deal with all types of soil conditions, unless it is natural ground, free of soil contamination.

⁶ <http://www.abs.gov.au/ausstats/abs@.nsf/Lookup/by%20Subject/1301.0~2012~Main%20Features~Australia's%20climate~143>

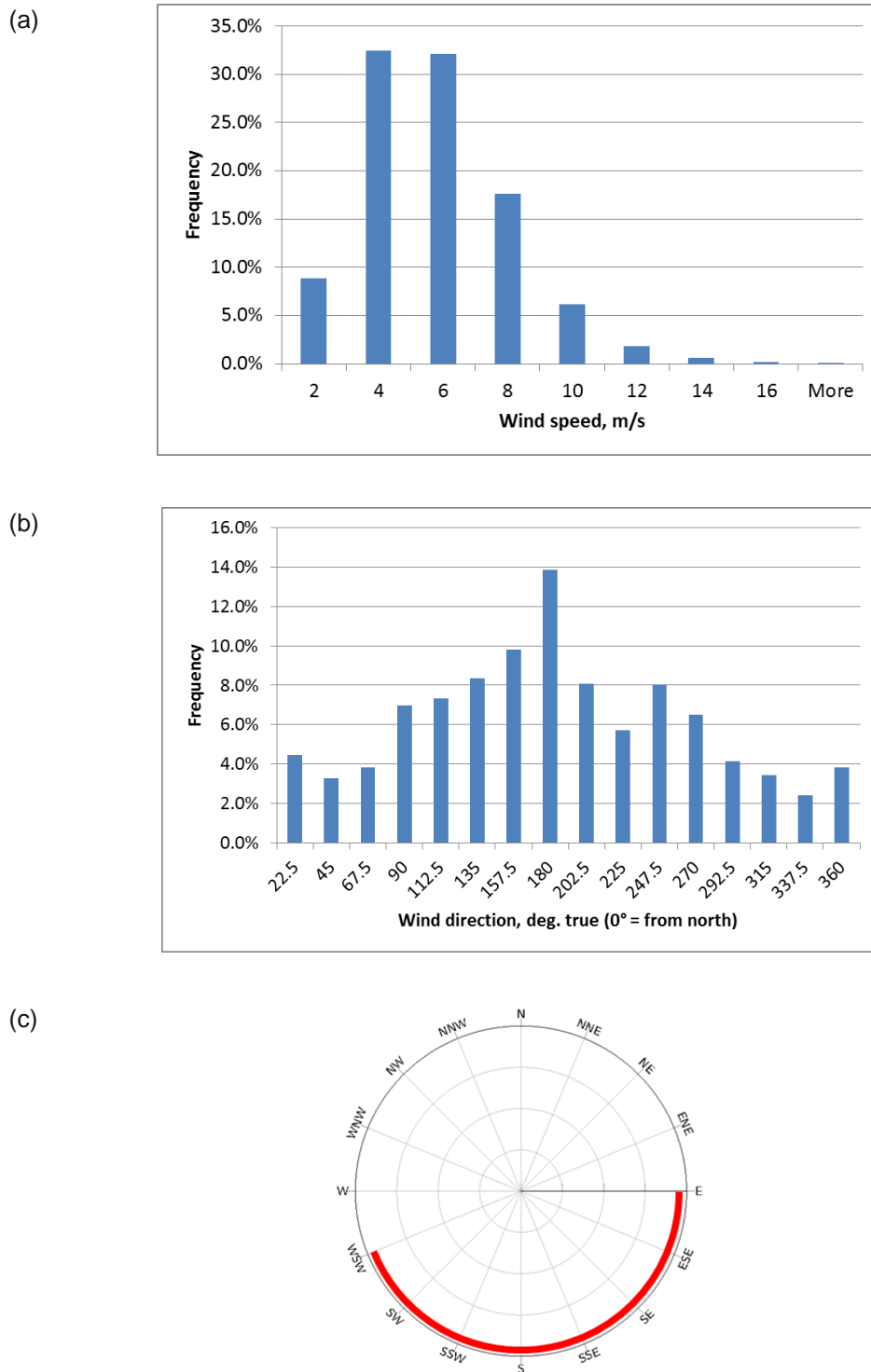


Figure 7. Frequency distributions of wind speeds (a) and directions (b) occurring at the reference location in WA and best plant locations with regard to wind direction relative to the refinery (indicated in red) (c)

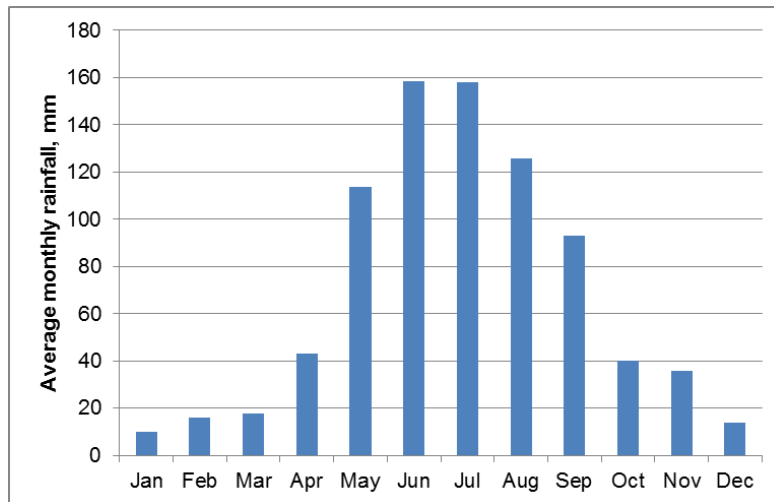


Figure 8. Long-term mean monthly rainfall at the reference location in WA.

3.2. Other potential sites

As shown in section 2.2, beside the three plants in the southwest of WA, the only other region in Australia with operational alumina refineries is near Gladstone, QLD. This region only offers slightly better solar conditions, due to its location closer to the equator. There is slow growth in alumina refining in Australia. Hence, a greenfield plant is most likely to be considered when one of the current plants is retired. Currently, there are no known plans for a new refinery.

Nevertheless, we have looked at potential sites for a new greenfield plant for any industrial process that requires significant quantities of process heat. A good region for CST in WA appears to be Learmonth, due to its location at the coast, high DNI and relatively high latitude of (-22° S). This site should be considered more closely. Aspects to consider should include accessible land, port/sea access (Exmouth), solar and weather data, existing flora and fauna, sensitive habitats, risk of cyclones and high winds, availability of other existing infrastructure, e.g. access to power lines, access to fresh water, existing nearby townships (building a new remote community lead to high shipping costs of goods).

In addition, the potential for CST in existing minerals processing centres should be considered. The location should involve a high demand for process heat at temperatures accessible for CST and good solar conditions. One example could be Kalgoorlie, WA.

4. THERMAL ENERGY DEMAND AND SUPPLY

Based on the total energy consumption of all alumina refineries in Australia of ~160 PJ and their combined annual alumina production of ~20 Mt pa, the energy intensity of alumina refining is around 8 GJ/t of alumina produced. Further assuming the plants to operate round-the-clock and at a constant rate and assuming that the specific energy consumption per unit mass of alumina produced is uniform across all plants, the reference facility's energy demand would be estimated to be in the order of 1GW_{th}. About half of this energy is used to produce steam for electricity production and as low-temperature process heat in the digestion process, while the other half is used for the high-temperature calcination process.

The project team visited the reference facility on 12 May 2017 and considered the plant's energy flows in detail. The detailed arrangements are complex and specific. The underlying structure however is that gas is used as the primary energy source in a combined heat and power mode for electricity and the low temperature process heat.

Two 100 MW_e gas turbines supply electricity to the grid and provide waste heat which is used to generate steam. The heat recovery steam generators are estimated to produce 400–600 tph of steam, approximately half (~500 tph) of the plant's steam demand. They have additional gas fired duct heaters such that they can supply steam somewhat independently of the gas turbine operation. The other half (~500 tph) of the steam required by the plant is produced by six gas-fired boilers. Boiler thermal (HHV) efficiency is 82% and remains approximately constant at part load. The boilers produce steam at nominal conditions of 470°C and 8 MPa. The steam from either or both sources is directed to the power house where it is used to generate electricity using a single stage back pressure steam turbine. The digestion process requires a steam mass flow rate of 900 to 1100 tph (250 to 306 kg/s). 900 tph of steam are passed through the steam turbine to produce ~137 MW_e of electricity (assuming an isentropic turbine efficiency of 95%) before being used in the digestion process, while any excess steam beyond 900 tph (up to 200 tph) by-passes the steam turbine and is directly throttled in a pressure reducer and de-superheater system to the conditions required by the digestion process. In average, around 10% (approx. 100 tph / 75 MW_{th} of energy supplied to the digestion process) of the produced steam by-passes the steam turbine. State points of the steam are indicated in Figure 9.

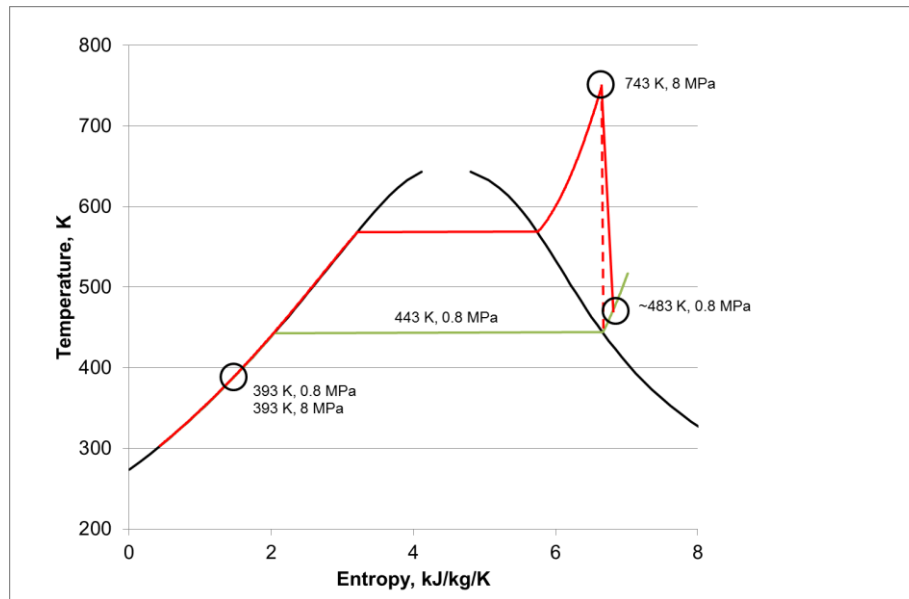


Figure 9. T-s diagram for water/steam: Black: saturation curves; green: isobaric line for 0.8 MPa; red: isobaric line for 8 MPa; indicated are the state points for feedwater (~393 K and 0.8/8 MPa), superheated steam at the boiler outlet (~743 K, 8 MPa), and at the digester inlet at around 483 K/0.8 MPa.

A Microsoft Excel model was developed to calculate the energy demand for the steam required at the reference facility. The CoolProp database (2014 version) was used to obtain the thermodynamic properties of steam and water with direct linkage into Excel. The final energy required to produce 500 tph of steam from liquid water exiting the evaporation at 120 °C to 470 °C and 8 MPa is 392 MW_{th}. In this calculation it is considered that the water at 120 °C requires a pressure of 0.198 MPa or more to remain in liquid state and 0.2 MPa pressure inlet is considered.

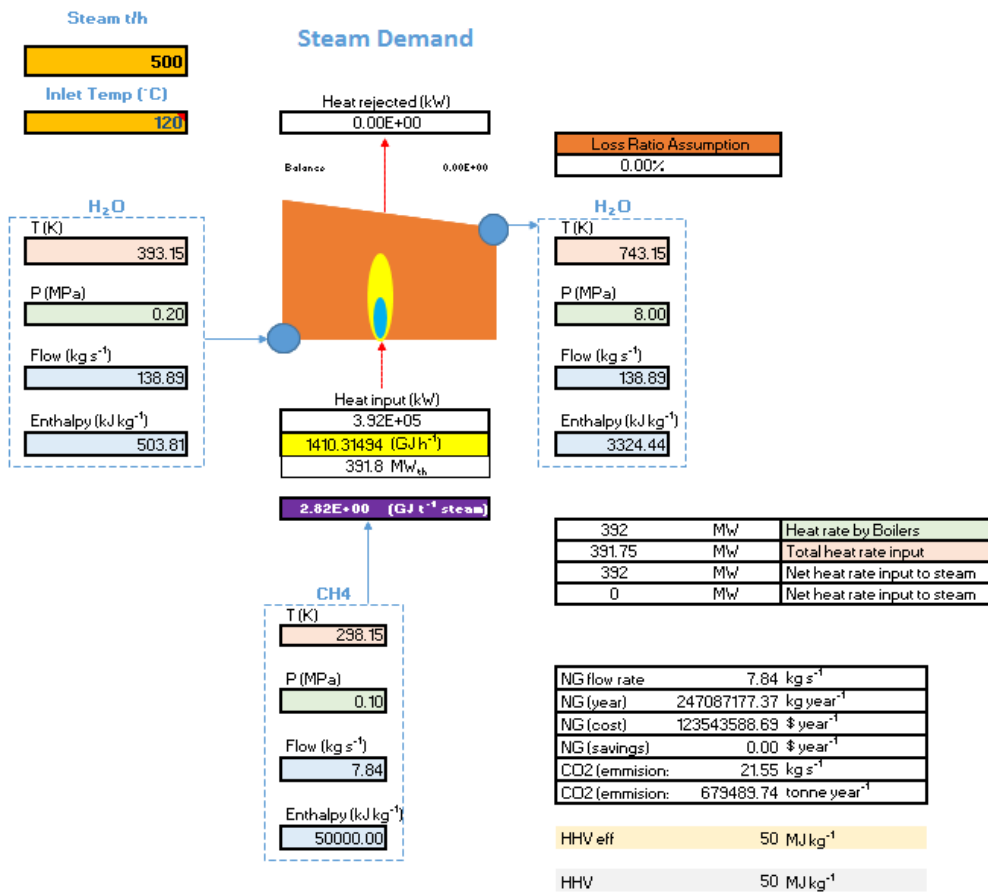


Figure 10 Excel model for the calculation of the steam on demand to the low temperature stage at the reference facility.

5. SOLAR PLANT DESIGN

The gas use for the combined facilities in the reference facility can be divided into three categories:

- a) Gas that is used to first drive gas turbines, with exhaust heat recovered as steam for power generation in steam turbines, followed by use of the exhaust steam for process heat. This is the most thermodynamically and economically optimal use of gas.
- b) Gas that is used to produce high T high P steam in boilers. With the steam first used in the steam turbines followed by low temperature exhaust used for process heat. This is intermediate in terms of thermodynamic and economic performance.
- c) Gas that is used in the boilers to make high pressure/temperature steam that is then throttled and de-superheated to process steam conditions. This is the least optimal path for use and represents the most expensive route to providing the process heat.

In regard to each of these categories a solar thermal solution could be suggested for each of these as follows:

- a) Disregarding the mixed ownership of assets, the only feasible way of addressing the gas turbine firing with a solar component is via the use of Solar Reformed Methane as discussed in detail in Program 2. The syngas produced can in principal be used a gas turbine fuel. This would be limited to an approximately 25% solar share. It would presumably use a tower and heliostat system to drive the steam reforming process. Dish arrays could also be considered.
- b) A CST array could be used to produce 470°C and 8 MPa steam. This could be either by direct steam production or via intermediate thermal storage using molten salts. Tower plus heliostat field CST plants exist at the multi 100 MW_t scale to produce steam via either of these routes. Trough plants have been tested at pilot scale with both direct steam or direct molten salt heating. They would however be unable to reach the temperature needed in there most commercially proven configuration using oil heat transfer fluid. Linear Fresnel systems have also been operated at pilot scale with either direct steam or molten salt at the desired temperature. Dish concentrators are less commercially mature but have been configured for superheated steam production. Dishes are unlikely to be compatible with molten salt but are investigated for application to ammonia based thermochemical energy storage systems that could deliver the superheated steam needed.
- c) Producing steam directly for use at 210°C is easily achievable with either trough or linear Fresnel collectors. Either direct steam production or oil heat transfer fluid could be applied. Operating such concentrators at such a modest temperature represents an underuse of their capabilities but it would achieve very high thermal efficiencies in operation. This

temperature is however just within reach of advanced non-tracking solar thermal systems based around evacuated tube or evacuated flat plate units with non-tracking partial solar concentration.

Each of these technical possibilities could have a role in alumina refineries in general and in a future hypothetical greenfield ‘solar alumina’ plant. In the context of the reference refinery they can be refined to the following solar plant draft specifications for further investigation, where only categories b) and c) will be further investigated under the low temperature Program 1.

5.1. CST plant design variants

Based on these considerations, the reference facility’s steam demand, the existing steam and power supply infrastructure and several discussions about the possibilities of integrating low- to medium-temperature CST into the reference facility among the project team, we have developed ten potential CST plant design variants, summarised in Table 2 for the purposes of requesting cost estimates from suppliers.

Table 2. CST plant specifications for 10 different design variants of the solar energy system, grouped in five pairs of two with equal nominal output and with or without energy storage. “Est. heat rate”: the estimated heat rate required to produce the given steam rate at given conditions (T, p) from water at 120°C; TBD: to be determined; sh: superheated; sat: saturated; PV: photovoltaic.

| Parameter | 1 | 2 | 3 | 4 | 5 | 6 | 7 | 8 | 9 | 10 |
|---|-----|-----|-----|-----|-----|-----|-----|-----|-----|-----|
| Steam rate, tph | 500 | 500 | 25 | 25 | 100 | 100 | 30 | 30 | 500 | 500 |
| Est. heat rate required, MW _{th} | 392 | 392 | 20 | 20 | 66 | 66 | 20 | 20 | 328 | 328 |
| Steam temperature, °C | 470 | 470 | 470 | 470 | 210 | 210 | 210 | 210 | 210 | 210 |
| Steam pressure, MPa | 8 | 8 | 8 | 8 | 0.8 | 0.8 | 0.8 | 0.8 | 0.8 | 0.8 |
| Steam quality | sh | sh | sh | sh | sat | sat | sat | sat | sat | sat |
| Storage capacity, hours | 0 | 15 | 0 | 15 | 0 | 15 | 0 | 15 | 0 | 15 |
| Solar multiple | 1 | TBD |
| PV power, MW _e | 0 | 0 | 0 | 0 | 0 | 0 | 0 | 0 | 50 | 50 |

The design variants are described as follows:

1) Fully displace gas boilers at the design point (summer solstice, solar noon): Produce 500 tph of steam at 470°C / 8MPa with commercially proven CST arrays.

- 2) Fully displace gas boilers at the design point (summer solstice, entire day): Produce 500 tph of steam at 470°C / 8MPa with commercially proven CST arrays, with 15 hours of full-load thermal energy storage.
- 3) Pilot-scale demonstration of medium-temperature solar energy integration (without storage): Produce 20 tph of steam at 470°C/8MPa with demonstration phase CST arrays.
- 4) Pilot-scale demonstration of medium-temperature solar energy integration (with storage): Produce 20 tph of steam at 470°C/8MPa with demonstration phase CST arrays, with 15 hours of full-load thermal energy storage.
- 5) Replace steam that currently by-passes steam turbine (without storage): Produce 100 tph of steam at 210°C/0.8MPa with commercially proven CST arrays.
- 6) Replace steam that currently by-passes steam turbine (with storage): Produce 100 tph of steam at 210°C/0.8MPa with commercially proven CST arrays, with 15 hours of full-load thermal energy storage.
- 7) Pilot-scale demonstration of low-temperature solar energy integration (without storage): Produce 25 tph of steam at 210°C/0.8MPa with demonstration phase CST arrays.
- 8) Pilot-scale demonstration of low-temperature solar energy integration (with storage): Produce 25 tph of steam at 210°C/0.8MPa with demonstration phase CST arrays, with 15 hours of full-load thermal energy storage.
- 9) Fully displace gas boilers and steam turbine at the design point (summer solstice, solar noon) with low-temperature solar energy and photovoltaic system: Produce 500 tph of steam at 210°C/0.8MPa with commercially proven CST arrays and 50 MW_e of electric power with commercially proven photovoltaic system.
- 10) Fully displace gas boilers and steam turbine at the design point (summer solstice, entire day) with low-temperature solar energy and photovoltaic system: Produce 500 tph of steam at 210°C/0.8MPa with commercially proven CST arrays and 50 MW_e of electric power with commercially proven photovoltaic system, with 15 hours of full-load thermal and electric energy storage.

Both, systems with and without energy storage are considered and their economic benefits are compared. Generally, thermal storage can be viable to store heat for continuous 24/7 operation during sunny periods, with full-load storage capacity of up to around 15 hours. Thermal storage is not usually designed for longer periods without sun due to cloudy weather and periods with low solar irradiation due to the variation of DNI, GHI and incidence angle over the course of a year. Therefore, the gas-fired boilers need to be retained in all scenarios of CST integration. The gas boilers will need to be controlled actively to balance the variable heat rate supplied by the CST system. Stockpiling within refinery processing steps was considered as an alternative to thermal

energy storage, but was discarded after discussions with the industrial partner for practical reasons.

To displace a significant portion of the natural gas used for steam production and minimise the unit cost of thermal energy produced by the solar plant, a large scale solar thermal system is considered. This system would need to provide 500 tph of superheated steam at 470°C and 8 MPa. This steam would be first expanded in the steam turbine to generate electricity for the plant before being used in the digestion process (design variants 1 and 2). The required heat rate to generate this steam flow rate is estimated to be ~450 MW_{th}.

As a lower-risk and more short-term alternative and pre-cursor to a full-sized system, a pilot-scale system has also been considered. After discussions, the target design point for the pilot plant was selected to be 20 MW_{th} (design variants 3 and 4).

Another possibility would be to displace steam that is currently supplied by the gas boilers and directly throttled to the digestion process inlet conditions (without generating any mechanical work in the turbine). In this case, the solar thermal system were to provide 100 tph of saturated steam at 210°C and 0.8 MPa (design variants 5 and 6). Again, a lower-risk pilot-scale system of this concept is considered with 20 MW_{th} nominal heat rate is considered (variants 7 and 8).

Finally, the possibility of substituting the gas boilers by low-temperature steam at 210°C and 0.8 MPa produced with solar thermal energy, combined with a 50 MW_e PV system to substitute the electric energy currently generated by the steam turbine will be considered (design variants 9 and 10). In this scenario, the electric power output of the existing steam turbine would decrease with increasing solar irradiation levels. This correlation of solar irradiation and electricity demand may lend itself to the use of solar power via PV. The possibility of a hybrid solar thermal/PV collector operating at up to 210°C could be an appropriate solution. However, this would likely require a system with beam-splitting and separate PV and thermal receivers, as PV cells are not operable at up to 210°C.

5.2. Nominal temperature ranges

For all CST systems not operating with steam as the heat transfer fluid, heat transfer from a heat transfer fluid to the steam needs to be accomplished in one or multiple steam generation heat exchangers. Figure 11 shows the heating curves of steam at 0.8 MPa heated to 210°C (blue, solid) and 8 MPa (red solid) heated to 470°C. Dashed lines are indicative cooling curves of the heat transfer fluid, assuming constant c_p , to estimate the heat transfer fluid (HTF) and hence the solar field operating temperature range. The low temperature solar field operating range was set to 200-300°C, the high temperature range to 300 to 500°C. An allowance of 5° is included for heat

losses between solar field and heat exchange and inlet/outlet temperatures for low- and high-temperature cases are 295/205°C and 495/305°C, respectively.⁷

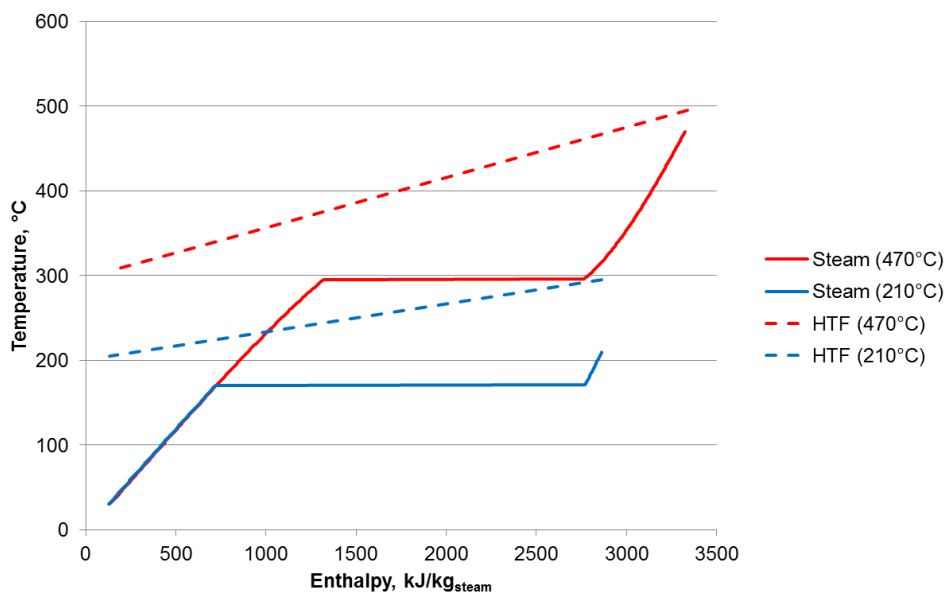


Figure 11: Temperature vs. enthalpy curves for low- and high-temperature steam and indicative cooling curves of heat transfer fluid (dashed lines).

5.3. Design point specification

For system variants without storage, the design point is defined at summer solstice, solar noon, with a nominal DNI of 1 kW/m² / GHI of 1 kW/m² and zenith angle of 9.21°. For systems with energy storage, the design point is defined at summer solstice (entire day) with a daily DNI of 40 MJ/m²/day / GHI of 30 MJ/m²/day. The ambient temperature is defined constant at 30°C.

In addition, hourly weather and irradiation data files for the reference location have been created for the ten years 2004 to 2008 and 2011 to 2015. The average daily DNI and GHI for these ten years are 5.73 kWh/m²/day and 5.10 kWh/m²/day, respectively. In terms of average daily DNI, best, worst and “closest to average” years are 2015 (6.25 kWh/m²/day), 2012 (5.36 kWh/m²/day) and 2013 (5.65 kWh/m²/day), respectively. The “closest to average” year 2013 was used to estimate the performance of CST systems with numerical simulations.

⁷ Note that these temperature ranges were fixed with low pressure steam outlet temperature of 170°C and feedwater inlet temperature of 160°C in mind. These conditions were later changed to 210°C and 30°C, respectively. With the new steam specifications, the solar field operating temperature ranges could be reduced to around 150-250°C and 200-500°C for low- and high-temperature cases, respectively, resulting in slightly increased solar field efficiency (order of 2-3%).

6. TECHNOLOGIES FOR SOLAR THERMAL PROCESS HEAT

6.1. Solar collector technology options

Solar thermal collectors convert solar radiation into heat. Their efficiency is limited by heat losses from the hot collector surfaces that increase with temperature and with the area of the hot surface. Solar thermal technology solutions must be optimised for the temperature range needed. Various approaches are used to reduce thermal losses and so improve efficiencies and these increase the complexity and cost of the system. Low temperature heat (e.g. for pool heating) can be provided by black, uninsulated rubber or PVC tubes laid flush on a rooftop. At the other extreme, temperatures of over 1,000°C are possible with point focus concentrators such as heliostat tower systems or paraboloidal dishes. The range of options available is summarised in Table 3.

Table 3. Solar thermal technologies & key characteristics.

| Collector Technology | Tracking | Concentration Ratio ⁸ | Temperature Range, °C | Usual heat transfer fluid |
|---|-------------|----------------------------------|-----------------------|------------------------------------|
| Unglazed | Nil | 1 | 20-40 | Water, air |
| Glazed Flat Plate (FPC) | Nil | 1 | 30-85 | Water, air, glycol |
| Evacuated Tube (ETC) | Nil | 1 | 50-150 | Water, glycol |
| Compound Parabolic Concentrator with evacuated tube (CPC) | Nil | 1-5 | 60-200 | Water, glycol |
| Linear Fresnel (LFR) | Single axis | 10-40 | 100-400 (-500) | Water, steam, HT oil (molten salt) |
| Parabolic Trough (PTC) | Single axis | 15-50 | 100-400 (-500) | Water, steam, HT oil (molten salt) |
| Paraboloidal Dish (PDC) | Double axis | 500-2,000 | 300-2,000 | Steam, chemical process |
| Heliostat Power Tower Concentrators (CRS) | Double axis | 500-1,500 | 300-2,000 | Steam, molten salt |

Non concentrating systems are mounted to rigid frames and convert the radiation that is incident on them, whether it is direct beam or diffused by clouds or dust. Concentrating systems use mirrors to concentrate only the direct beam component of solar radiation. The greater the

⁸ Concentration ration is the ratio of the intensity of radiation after concentration compared to incident sunlight.

concentration ratio, the smaller the hot area that is subject to thermal losses and hence the higher the achievable operating temperature. Concentrators must track the sun such that incident radiation is perpendicular to the plane of the collector. Those that focus on a linear receiver need to track on a single axis only, while point focus concentrators need to track in two axes.

With very few exceptions, a fluid medium is required to pass through the collector and absorb the heat. This Heat Transfer Fluid (HTF) can then be transported to a point of use where some form of heat exchanger is applied to extract useful heat. The boiling and freezing points, the heat capacity, and the chemical stability of the material are major factors in HTF selection.

Solar heat can be stored in tanks of heated HTF, or via heat exchangers to other thermal energy storage mediums. New approaches to HTF, solar collectors and storage mechanisms are the subject of ongoing research and development.

It is apparent that the low temperature requirements of the Bayer process may possibly be met by low-concentration evacuated tube based systems. Either PTC or LFR linear concentrators are easily capable of providing the temperatures needed. The following sections provide more detail on the relevant solar collector types.

6.1.1. Evacuated Tube Collectors

Evacuated tube collectors involve a series of individual tubes mounted together in panels as shown in Figure 12.



Figure 12. Evacuated tube collector array.⁹

A single evacuated tube is constructed in similar manner to a thermos flask, as shown in Figure 13 and Figure 14. An inner and outer glass tube are fabricated as a continuous unit with one open

⁹ www.sustainablebuildingconstruction.blogspot.com (Accessed 01-09-14)

end and the annular space between them evacuated. The inner tube is coated with a selective surface for preferentially absorbing solar radiation. Inside the inner tube a heat transfer mechanism is installed to collect the heat by conduction from the hot inner tube surface. Figure 13 shows one method employed which is a sealed heat pipe based on a standard refrigerant material that boils and moves the heat by natural convection and then condensation to the inside of a storage tank or water heat exchanger. Figure 14 shows an alternative of a basic 'U' tube HTF heat exchange unit that sits within the tube. Direct heating of the HTF within a tube is also possible.

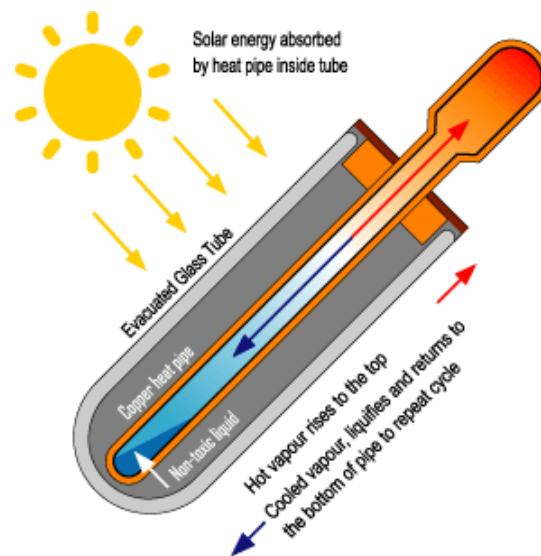


Figure 13. Working principle of an evacuated tube with heat pipe based heat transfer.¹⁰



Figure 14. Exploded view of an evacuated tube with internal U-tube heat exchanger.¹¹

¹⁰ www.reuk.co.uk (Accessed 19-08-14)

¹¹ www.andyschroder.com (Accessed 19-08-14)

Annual output will be maximised if the collector is tilted toward the equator at an angle equal to the latitude of the site. However, in Australia, the low thermal losses of evacuated tube collectors make them prone to summer overheating. To mitigate this risk, collectors will often be mounted at greater angles, levelling seasonal output by increasing winter output at the expense of summer output. Increased tilt angles will also increase hail resistance of the tubes, which are typically designed to withstand 25mm diameter hail stones incident at 90km/h.

6.1.2. CPC Collectors

Compound Parabolic Concentrators (CPC) are an example of a non-tracking concentrator. They utilise evacuated tube receivers with an arrangement of stationary mirrors to gather more radiation than is directly incident on the tube. The optical principles are illustrated in Figure 15.

Concentration levels of around two times are possible and so have the effect of boosting operating temperatures up to around 150°C. Multiple tubes are again arranged in panels as illustrated in Figure 15.

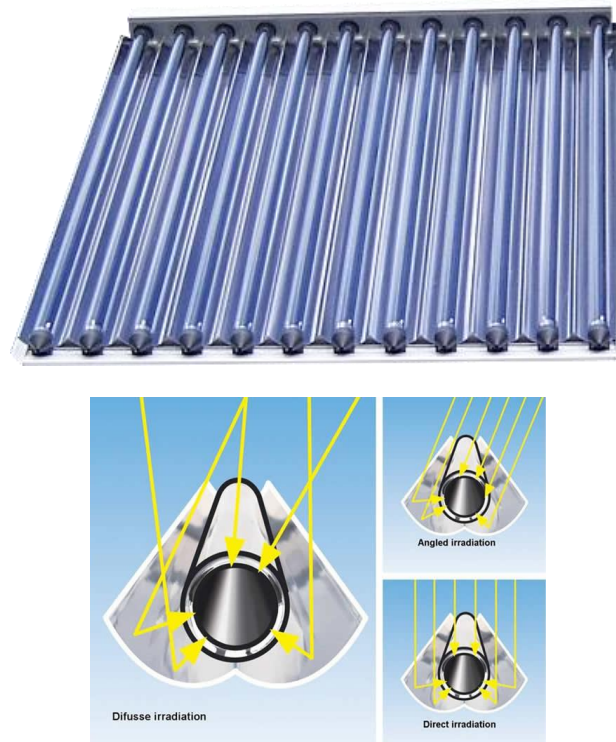


Figure 15. Top: Evacuated tube plus CPC collector assembly.¹² Bottom: Working principle of a CPC collector.¹³

¹² www.andyschroder.com (Accessed 18-08-14)

¹³ www.jrsolar.co.za (Accessed 19-08-14)

6.1.3. Parabolic Trough Collectors

The focal properties of the parabola are utilised in trough concentrator systems. The tubular receiver is fixed to the focal line of the array of mirrors, which track the sun along one axis throughout the day. Trough systems can heat a HTF such as synthetic oil, or generate steam for process heat or power generation. Modern systems are capable of reaching up to 500°C but are typically used for temperatures between 150° to 400°C. PTCs operated up to 400°C usually use synthetic oil as HTF, which is the most mature PTC technology, proven over many years in many CST power plants with arrays of several 100 MW_{th}. For temperatures above 400°C, oil cannot be used as HTF as it becomes chemically unstable. Molten salt has been used at higher temperatures. This approach has been demonstrated at pilot scale and is a less mature technology than PTC with synthetic oil.

PTCs are normally installed with tracking axis oriented N-S, as this normally maximizes their yield, while their thermal output over the year is more uniform with a E-W orientation.

Key components are illustrated in Figure 16. As tracking occurs, the receiver at the focal point of the trough must also move. This creates the necessity for dynamic joints through which the HTF must be circulated, adding complexity.

The receiver tubes can be simple metal tubes. Adding a glass tube cover to limit convection losses improves performance, more usually they use an evacuated tube as the receiver gives the best possible performance. The evacuated tube receivers differ from those used in panels in that they are usually direct flow-through units made from a central metal tube with a surrounding glass tube joined by a bellows unit to maintain the sealed evacuated space.

Whilst parabolic troughs could be made in any length and aperture width, there has been an evolution in commercially available products in two directions; large aperture units for solar thermal power generation, and smaller systems for process heat.

Use of large troughs with aperture widths of around 5.8m and high quality evacuated tube receivers has become standard practice for concentrated solar power generation. These large trough arrays use heat transfer oil in the receivers and collect heat at around 400°C. Arrays with peak thermal capacities between 30MW_{th} to 1GW_{th} have become a mature technology, with the hot oil used to raise steam for power generation, (Figure 17).

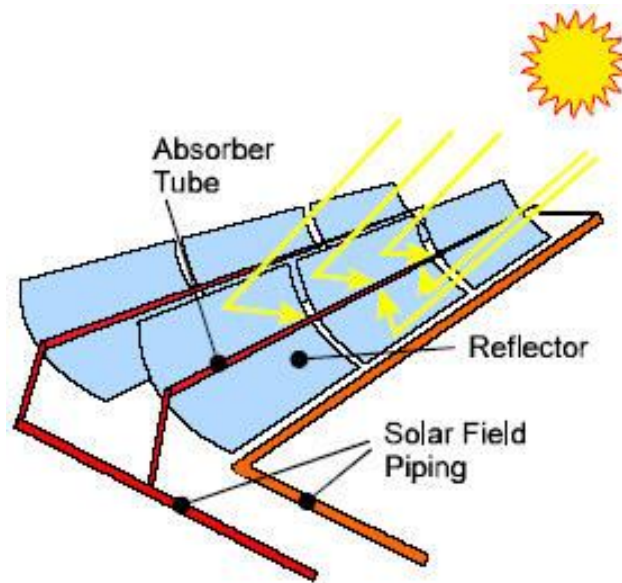
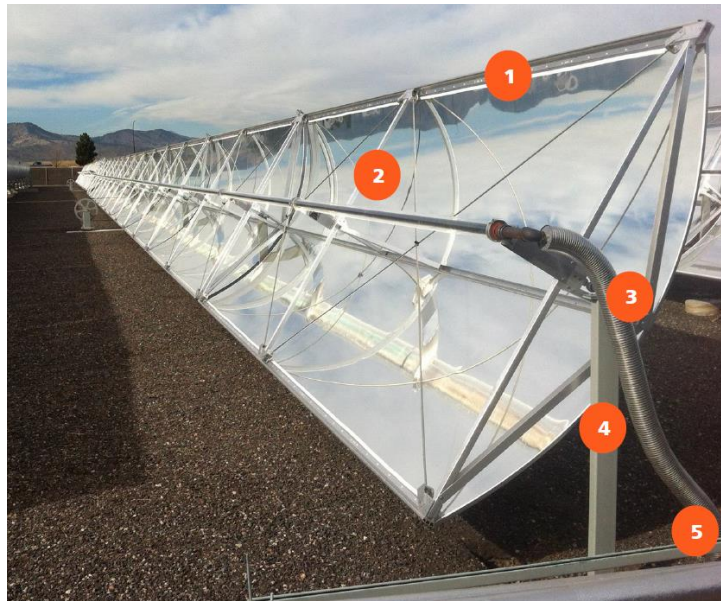


Figure 16. Top: Parabolic trough collector construction, 1 Concentrator with aluminium or glass mirror, 2 Receiver tube, 3 Flexible coupling, 4 Pylons, 5 Header piping (picture from Abengoa). Bottom: Working principle of PTC collectors (picture from <http://www.solarpaces.org>).

Large trough collectors can also be used for process heat. Arrays down to 1MW_{th} are technically feasible, however large trough suppliers typically have less interest in such small systems. Globally there are a number of companies who offer small aperture, lightweight troughs specifically for mid-range process heat, as illustrated in Figure 18.



Figure 17. Parabolic trough field in a large CSP plant (picture K. Lovegrove)



Figure 18. Small aperture parabolic trough collector (picture from NEP)

6.1.4. Linear Fresnel Reflectors

A linear Fresnel system is an analogue of a trough concentrator and provides heat over the same temperature range. Long semi flat mirror strips laid out in parallel rows are each rotated independently so as to focus direct beam radiation on a linear focus that is fixed on a non-moving tower (Figure 19). Manufacturers of LFR systems claim that they offer advantages over trough concentrators via having reduced structural costs, mirrors that are easier to manufacture and

clean plus the benefits of a fixed focus that does not require flexible coupling for the HTF. Against these advantages their overall average optical efficiency is lower.

LFR has been mostly used for direct steam generation (DSG) within the solar receiver, typically at temperatures up to $\sim 300^{\circ}\text{C}$. At higher temperatures, molten salt can also be used. Similar as for PTC, this approach is also still in the demonstration phase, although already at the MW-scale.

As with troughs, receivers can be evacuated or non-evacuated. Whilst less commercially mature than troughs, the split of commercial offerings into large scale units used for power generation (but also available for process heat) and smaller units particularly aimed at medium temperature process heat can be observed.



Figure 19. Top: Linear Fresnel Collector (courtesy of Industrial Solar). Bottom: Working principle of LFR collectors (picture from <http://www.frenell.de/>)

LFR systems are also produced in larger scale for power production. There are three utility scale systems in the world to date. One of these is the Kogan Creek solar boost project that is to

provide steam at 334°C to Kogan Creek power station near Chinchilla in Queensland. The solar thermal array will have a capacity of 130 MW_{th} when complete.

6.1.5. Heliostat Power Tower Collectors

In the concentrated solar power sector, the heliostat field / central receiver approach is gaining wider support. It offers higher temperatures (matching any available steam turbine technology) and can also utilise the molten salt energy storage solution more effectively because of the higher temperature difference.

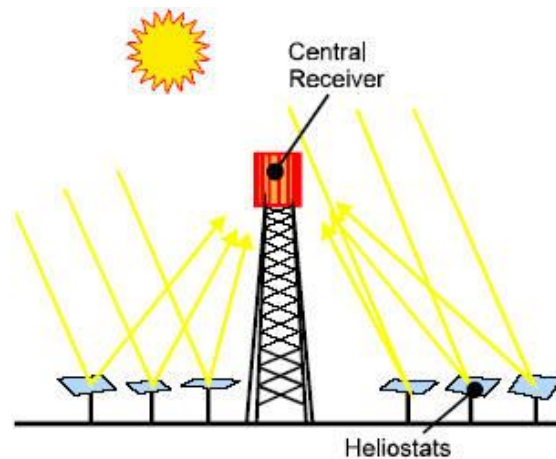


Figure 20. Top: Aerial view of the Gemasolar heliostat power tower plant in Spain, thermal capacity 400 MW_{th} (courtesy of Torresol Energy). Bottom: Working principle of heliostat power tower systems (picture from <http://www.solarpaces.org>).

The most commercially mature systems are large in thermal capacity (over 50 MW_{th}). However there are also commercial players developing smaller systems down to a few MW_{th} in size. For a process heat application the use of molten salt as both a HTF and thermal storage medium is readily adaptable and offers heat at temperatures up to 580°C. Even higher temperatures up to

~1000°C are reachable with CRS systems. Systems without TES usually generate steam directly in the solar receiver.

There is ongoing work at the pilot stage on applying tower systems to directly drive high temperature chemical processes. A key relevant example is the solar driven steam reforming of methane to produce hydrogen or syngas mixtures. The CSIRO solar group in Newcastle is a pioneer in this area.

6.1.6. Paraboloidal Dish Collectors

Paraboloidal dishes are the least mature of the large scale solar concentrator technologies but also provide high concentration ratios and low thermal losses. Dishes are double axis tracking and have the highest concentration levels and efficiencies of the concentrator system options. Dishes are also modular and have the capacity to be mass manufactured to minimise project engineering costs. They are mentioned here for completeness as there is no real commercial provider in a position to offer solutions for immediate application to industry for process heat as yet.

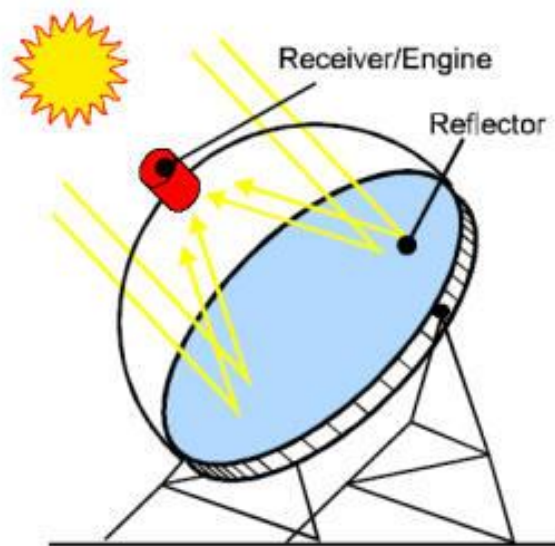


Figure 21. Top: Australian National University's prototype 500m² paraboloidal dish concentrator (picture K Lovegrove). Bottom: Working principle of paraboloidal dish concentrator (picture from <http://www.solarpaces.org>).

6.1.7. Selection of collectors

The target temperatures of steam in this project are 210°C and 470°C. 210°C is near the upper limit of CPC collectors or could easily be achieved with simple PTC or LFR systems. 470°C is near the upper limit of PTC and LFR concentrators. These concentrators can be operated up to ~500°C, but experience at these temperatures with molten salt HTF is rather limited, in particular for PTC. CRS and PDC can readily reach temperatures in excess of 500°C and would hence be

somewhat underused for the present project. However, the lower DNI and higher cosine losses with linear concentrators at the reference location compared to locations closer to the equator tend to favour a CST collector technology with two axis tracking in order to operate efficiently. The rather low latitude of the reference location leads to relatively strong variation of CST system output over the course of a year. This trend is more pronounced for linear concentrators than for point-focussing concentrators. For these reasons, CRS systems are also considered in this study. On the other hand, PDC are disregarded due to their lower level of commercial maturity for process heat applications.

Based on their operating temperature ranges, CPC collectors are suitable for design variants 5 to 10, PTC and LFR collectors are suitable for design variants 5 to 10 and potentially also for design variants 1 to 4 (at the pilot stage), and CRS collectors are suitable for design variants 1 to 4.

6.2. Storage options

There are a range of options available for thermal energy storage applied to energy collected from solar thermal systems. Such systems would represent a significant extra investment that is additional to the solar collector field. In principle, an alternative to storing energy in a separate system is to convert the process to a batch based operation, whereby energy consuming steps are carried out when the solar energy is available.

Examination of the Bayer process as it is implemented at the reference refinery, suggest that this is not particularly feasible. The digestion process is carried out in a complex system of thermally interconnected vessels and components. Heat is recuperated between cooling digested material and newly mixed material entering the process in multiple steps. The plant as designed is not designed for other than very infrequent shut downs and start-ups.

It is clear that any initial application of solar thermal should be applied without change to the process, meaning solar thermal must provide heat in an interchangeable manner as it is currently supplied via gas. Thus separate energy storage needs to be considered if the solar share is to be boosted beyond that corresponding to immediate use during solar availability.

Options for energy storage are interlinked with the options for heat transfer fluid for use in the solar field. The practical choices for heat transfer fluid are:

- Heat transfer oil
- Pressurised water
- Saturated steam

Thermal storage can then be achieved via either of:

- Storage of large volumes of heated heat transfer fluid

- Storage of heat in volumes filled with a matrix of rock or ceramic material in direct contact with the heat transfer fluid.
- Transfer of heat via heat transfer tubes to large volumes of solid heat storage material (eg concrete)

If the option of operating the solar field at the higher temperatures needed for steam turbine power generation is followed, with the process heat then extracted from a back pressure turbine, the favoured approach would be to use molten salt as both the heat transfer fluid and the thermal storage medium.

A new system for thermal energy storage is the EnergyNest system. This system uses a block of concrete which is heated by the heat transfer fluid. This could result in cost reductions in the thermal storage, particularly for large storage systems. One advantage of a solid storage system is that it doesn't require heat tracing as in molten salt systems. Another advantage is that it can be combined with different heat transfer fluids (steam, oil, compressed gas, etc.).¹⁴

6.3. Possible CST system layouts

Depending on heat transfer fluid (HTF) used in the solar collectors and the energy storage medium used in the thermal energy storage (TES) system, three main CST plant configurations result, as shown schematically in Figure 22. If synthetic oil (e.g. Therminol VP-1®) is used as HTF, as in most existing large-scale solar parabolic trough power plants, heat is stored in a separate storage medium, typically molten salt, as the costs of a direct oil storage would be rather high. In this case, a heat exchanger is needed to transfer heat between oil and molten salt during charging and discharging of the TES (configuration 1 in Figure 22). In addition, a heat exchanger steam generator is required to generate steam for the alumina plant.

If molten salt is used as the HTF, the heat exchanger between HTF and TES becomes obsolete. During charging of the TES, molten salt is drawn from the cold salt storage, heated in the solar field, and then stored in the hot salt storage. During discharge, hot salt is drawn from the hot salt storage and used to generate steam via the heat exchanger steam generator (configuration 2 in Figure 22).

If steam is produced directly in the solar field (DSG), there is no need for any heat exchanger. In this case, a steam buffer may be included to bridge shorter periods of clouds up to ~1 hour (configuration 3 in Figure 22). However, steam storage is usually not suitable for longer periods of TES and DSG with molten salt TES is not currently an available technology option. Therefore,

¹⁴ <http://www.energy-nest.com/>.

DSG technology is expected to be unable to achieve the desired solar share of 29 to 46% specified in this project (typical solar shares are <20% without TES).

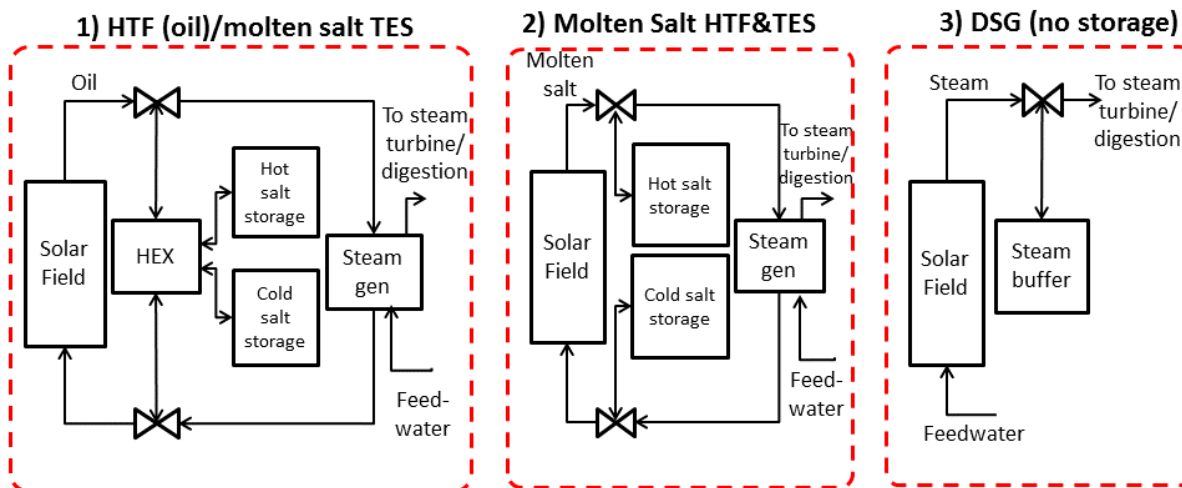


Figure 22. Common system configurations for CST plants.

6.4. Combined Heat and Power configurations

Due to the high exergy content of concentrated solar energy, systems can be designed to cover both electric power and low- to intermediate-temperature process heat demands.¹⁵ One such system is the 1.5MW_e/36MW_{th} CST system built by Aalborg CSP to provide energy to generate power, heat and desalinated water for the Sundrop Farms in Port Augusta, SA. Their system uses a tower system to generate storable heat. The heat is used 1) to generate superheated steam to generate power with a steam turbine; 2) desalinate water via seawater distillation to irrigate the horticulture; 3) generate heat to heat the greenhouse during cold periods at night-time and in winter.

Another combined heat and power system is offered by the company RayGen. Their system is a concentrated photovoltaic system, using a heliostat field to focus direct solar radiation onto a high-efficiency PV cell. The waste heat from cell cooling is collected and delivered as additional energy output.

¹⁵ The sun is a heat source at 5777 K. After concentrating sunlight on earth, temperatures of up to ~1500 K can be generated. Hence, up to 80% of concentrated solar energy collected can theoretically be converted into work (e.g. electricity).

7. COST DATA COLLECTION

7.1. Overview of technology suppliers

A total of 17 CST technology suppliers have been contacted with a request for information (RFI) on their technology's cost for the present project. Suppliers have been asked to provide information for the respective design variants (Table 2) they would be expected to be able to deliver on, based on their technology and their previous project experience.

It should be noted that in the RFI to suppliers, an estimated full-scale steam rate of 340 tph was used, as opposed to our latest estimates listed in Table 2. However, cost data can be scaled within reasonable limits to larger and smaller plant sizes with reasonable confidence. In addition to the design specifications tabulated in Table 2, suppliers were provided with a short description of the project overall. In addition, we provided them with the solar design point specifications described in section 5.3 and, upon request, with hourly weather and solar irradiation data files for 10 recent years at the reference location, including an indication of best, worst, and "closest to average year" in terms of average DNI.

7.2. Cost data format

Typical categories for CST system costs (without power block) are:

1) Capital costs:

Direct capital costs:

- Engineering and site preparation/improvements
- Solar field
- Thermal energy storage
- Balance of plant (BOP)
- Contingency

Indirect capital costs:

- EPC and Owner costs
- Land costs

2) O&M costs:

- fixed

- variable

Different studies report costs in somewhat different categories and different units (e.g. \$/kW, \$/kWa, \$/m² land, \$/m² solar field, etc.). For PTC systems, solar field costs include the reflectors and receivers and the additional category “heat transfer fluid and system” is added. For CRS systems, solar field costs are further divided into “heliostat field”, “receiver system”, and “tower”. O&M costs can be divided into fixed and variables O&M costs. In addition to these CST plant-specific costs, costs for heat exchanger steam generator and piping between CST and alumina refinery plants are to be added in the present project. An example of a cost breakdown for a 50 MW_e PTC plant in Spain is found in IRENA, 2012¹⁶. Recent cost analyses of PTC and CRS technologies can be found in NREL Report No. 65688 (2016).¹⁷

¹⁶ IRENA, CSP Cost Analysis, 2012.

¹⁷ NREL, Report No. 65688, Advancing Concentrating Solar Power Technology, Performance, and Dispatchability, 2016.

8. INPUT PARAMETERS FOR SAM

8.1. Summary of inputs for SAM

Based on the collected cost data, component cost models were developed. The models have been implemented in Excel to calculate SF, TES and BOP costs as functions of their sizes.

To use the cost models with SAM, the component costs have been recast into a form that allows direct input to SAM. The resulting SAM cost model parameters for trough, Fresnel and tower are listed in Table 4 to Table 6 for the reference system (section B.1.2) with temperature range 200-300°C.

As no site preparation data could be singled out from the available cost data set, the SAM default parameters are retained.

The total solar field costs are the product of unit solar field costs (in AUD/m²) for the given solar field design size (in MW_{th}) times the solar field reflective area determined by SAM's solar field models.

Table 4. Parabolic trough, SAM input parameters for reference system, in AUD (¹low-cost SF and BOP models, average cost TES model; ²SAM default parameter).

| SAM parameters | Average cost models | Low cost models | Mixed cost models ¹ |
|---|---------------------|-------------------|--------------------------------|
| Site Preparation, \$/m ² (reflective area) | \$33 ² | \$33 ² | \$33 ² |
| Solar field, \$/m ² (reflective area) | \$310.56 | \$163.49 | \$163.49 |
| HTF and system, \$/m ² (reflective area) | \$124.23 | \$65.40 | \$65.40 |
| Thermal energy storage, \$/kWh _{th} | \$80.68 | \$11.92 | \$80.68 |
| Balance of Plant, \$/kW _{th} | \$86.73 | \$55.62 | \$55.62 |
| Spec. power block cost, \$/kW _e (gross) | \$0 (na) | \$0 (na) | \$0 (na) |
| Contingency (% of direct capital cost) | 0% | 0% | 0% |
| EPC and Owner cost (% of direct costs) | 25% | 25% | 25% |
| Total spec. land cost, \$/acre | \$0 | \$0 | \$0 |
| Sales tax (% on 80% of direct cost) | 0% | 0% | 0% |
| O&M, fixed, \$/kW _e /yr | \$0 | \$0 | \$0 |
| O&M, variable, \$/MWh _{th} | \$12.35 | \$12.35 | \$12.35 |

For linear concentrating systems, the solar field costs are split into two contributions in SAM, categories “solar field” and “HTF and system”. The solar field unit costs have been split into these two categories using SAM’s default fractions of 71%/29% for trough and 76%/24% for Fresnel.

Table 5. Linear Fresnel, SAM input parameters for reference system, in AUD (¹low-cost SF and BOP models, average cost TES model; ²SAM default parameter).

| SAM parameters | Average cost models | Mixed cost models ¹ |
|---|---------------------|--------------------------------|
| Site Preparation, \$/m ² (reflective area) | \$27 ² | \$27 ² |
| Solar field, \$/m ² (reflective area) | \$264.18 | \$136.45 |
| HTF and system, \$/m ² (reflective area) | \$82.78 | \$42.76 |
| Thermal energy storage, \$/kWh _{th} | \$80.68 | \$80.68 |
| Balance of Plant, \$/kW _{th} | \$86.73 | \$55.62 |
| Spec. power block cost, \$/kW _e (gross) | \$0 (na) | \$0 (na) |
| Contingency (% of direct capital cost) | 0% | 0% |
| EPC and Owner cost (% of direct costs) | 25% | 25% |
| Total spec. land cost, \$/acre | \$0 | \$0 |
| Sales tax (% on 80% of direct cost) | 0% | 0% |
| O&M, fixed, \$/kWe/yr | \$0 | \$0 |
| O&M, variable, \$/MWh _{th} | \$12.35 | \$12.35 |

For tower systems, the solar field costs are split into “solar (heliostat) field”, “tower” and “receiver” models in SAM. Again, the solar field unit costs have been split into these three categories using SAM’s default fractions of 62%, 9% and 29%, respectively.

The “heliostat field” cost parameter is simply the product of solar field unit costs (in AUD/m²) times the above fraction (62%).

The costs of the tower structure are calculated within SAM by an exponential law, tower costs grow exponentially with the tower height. In addition, the model takes into account the receiver and heliostat heights. The pre-exponential cost factor is the only external input to the tower cost model in SAM. It is calculated in the Excel cost model spreadsheet by solving the tower cost

model equation. The inputs to the Excel spreadsheet for the calculation of the pre-exponential factor are the tower, receiver and heliostat heights from the SAM heliostat field optimisation.

Table 6. Tower, SAM input parameters for reference system, in AUD (¹low-cost SF and BOP models, average cost TES model; ²SAM default parameter).

| SAM parameters | Average cost models | Mixed cost models ¹ |
|---|---------------------|--------------------------------|
| Site Preparation, \$/m ² (reflective area) | \$21 ² | \$21 ² |
| Solar (heliostat) field, \$/m ² (reflective area) | \$252.74 | \$215.48 |
| Tower, fixed cost factor, \$/m | \$1,508,500 | \$1,286,115 |
| Tower scaling exponent | 0.01130 | 0.01130 |
| Receiver ref. cost, \$ | \$75,101,920 | \$64,030,285 |
| Receiver reference area, m ² | 1,571 | 1,571 |
| Receiver cost scaling exponent | 0.7 | 0.7 |
| Thermal energy storage, \$/kWh _{th} | \$80.68 | \$80.68 |
| Balance of Plant, \$/kW _{th} | \$86.73 | \$55.62 |
| Spec. power block cost, \$/kW _e (gross) | \$0 (na) | \$0 (na) |
| Contingency (% of direct capital cost) | 0% | 0% |
| EPC and Owner cost (% of direct costs) | 25% | 25% |
| Total spec. land costs, \$/acre | \$0 | \$0 |
| Sales tax (% on 80% of direct cost) | 0% | 0% |
| O&M, variable, \$/MWh _{th} | \$12.35 | \$12.35 |

The average cost models represent the average deduced from all responses. The low-cost models are deduced from the most cost competitive responses and the mixed models combine the most competitive solar field cost responses with averaged TES and BOP estimates. In this way results obtained with average cost models are more conservative whereas the low-cost models are used to indicate a likely but not certain cost performance that might be expected from a competitive tender process for a real project.

As no site preparation data could be singled out from the available cost data set, the SAM default parameters are retained.

The total solar field costs are the product of unit solar field costs (in AUD/m²) for the given solar field design size (in MW_{th}) times the solar field reflective area determined by SAM's solar field models.

For linear concentrating systems, the solar field costs are split into two contributions in SAM, categories "solar field" and "HTF and system". The solar field unit costs have been split into these two categories using SAM's default fractions of 71%/29% for trough and 76%/24% for Fresnel.

For tower systems, the solar field costs are split into "solar (heliostat) field", "tower" and "receiver" models in SAM. Again, the solar field unit costs have been split into these three categories using SAM's default fractions of 62%, 9% and 29%, respectively.

The "heliostat field" cost parameter is simply the product of solar field unit costs (in AUD/m²) times the above fraction (62%).

The costs of the receiver are calculated within SAM by a 0.7 power laws. The only external input to the receiver cost model is the pre-power cost factor. It is calculated in the Excel cost model spreadsheet by solving the receiver cost model equation. The input to the Excel spreadsheet for the calculation of the pre-power factor is the receiver area calculated by the SAM heliostat field optimisation algorithm.

The TES cost model is in AUD/MWh_{th} and can be directly entered to SAM.

To model a process heat system in SAM, the thermal efficiency of the power block can be set to 1. In this case the BOP cost units correspond to \$/kW_{th}.

Contingencies and indirect costs are rolled into a single factor corresponding to 25% of direct costs that can be included in the EPC and Owner cost category of the SAM cost model.

Sales tax and land costs are not technology specific and are currently not taken into account, but can be included as appropriate.

O&M costs are wrapped into a size (capex) dependent percentage of capex pa.

9. FEASIBILITY ANALYSIS

9.1. Methods and Parameters

In this analysis several parameters are examined to gauge the economic performance of CST system options:

- Total installed cost (direct and indirect),
- levelised cost of heat (LCOH),
- net present value (NPV),
- internal rate of return (IRR). and,
- the required grant amount is estimated to reach positive NPV with the pilot systems.

Selected system configurations are discussed here, with parameters summarized in Table 7. These parameters are considered the most relevant for the reasons described next. Further parametric analyses focussed on NPV maximisation is presented in section 9.4.

Table 7. CST system parameters used in economic analysis.

| Parameter | Value |
|---------------------------------------|---|
| System rating (thermal design output) | 20 MW _{th} (pilot) 392 MW _{th} (large-scale) |
| Thermal storage size | 0, 8, 14 hours |
| Solar multiple | optimised |
| Technology | trough, Fresnel, tower |
| Operating temperature range | 300-500°C |
| Cost model used | SF: average, low TES: average BOP: average, low |

The analysis is focused on the two most likely scenarios: a 20 MW_{th} pilot system for demonstration purposes followed by a large-scale 392 MW_{th} system that produces up to 500 t/h of steam and hence can completely displace the gas boilers during peak irradiation.

To explore the effect of the TES on the economics, we have selected three TES sizes of 0, 8 and 14 hours. The thermal storage size influences a CST system's capacity factor, dispatchability/controllability and costs.

A CST system without TES would reach a solar share of around 15-20% – below the target of 29 to 45% in this project. In addition, a system without TES would impose added challenges in the control of the process due to the low level of dispatchability of a system without TES. However, since the TES does not generate additional thermal energy, 0 hours of TES should lead to close to minimum costs (LCOH) of delivered steam.

On the other hand, the TES can also eliminate energy dumping during periods of overproduction and allow larger solar field which can benefit from economies of scale. In case of tower systems, there is the additional effect that its performance decreases at small scales (such as the 20 MW_{th} pilot scale), according to our SAM simulations.

A system with an intermediate TES capacity of 8 hours is likely to meet the target solar share (29–45%) and leads to good operability of the CST plant. A system with TES capacity of 14 hours would likely lead to a solar share of around 45–50%, at the upper limit of the target band in this project, and would allow for full solar operation (without gas boilers) during peak solar periods. This case is included to give an indication of the development of the economics of CST systems with large TES. Increasing the TES capacity beyond 14 hours is unlikely to be economical, as its utilisation starts to decrease over significant periods of the year.

The solar multiple (ratio of solar field capacity to system design output capacity) is optimised in each case (rate system thermal power output, fixed TES capacity) to minimize LCOH and maximize IRR. For TES = 0 hours, SM = 1 is used, as oversizing the solar field is unlikely to be economically beneficial for a system with low BOP costs.

Since all three solar field technologies considered (trough, Fresnel, tower) are readily capable of reaching temperatures of around 500°C, we have focused on the scenarios where the CST system operates in the temperature range 300–500°C, to generate steam at the same conditions as the gas boilers. This ensures that the electricity generation remains unchanged and minimises the disruption of the current steam turbines¹⁸ and of the overall plant operations. Lower temperature CST integration with a CST system operating in the temperature range of 200–300°C to generate steam at 0.8 MPa and 210°C is currently omitted from consideration as it would lead to additional power purchases off the grid or additional power generation e.g. via photovoltaics during operation hours of the CST system (due to a reduction in the steam mass flow rate through the turbine). The economics of this scenario are uncertain.

As discussed in the previous chapter, average and low-cost models can be derived from the available component cost data for SF, TES and BOP. We use and compare both average and low-cost models. Average cost estimates are considered the most likely and a conservative estimate of today's component costs, while low-cost estimates are considered today's "best case" costs.

¹⁸ Reduced mass flow through the steam turbine would likely come at the additional expense of a reduced part-load turbine efficiency.

The base case studied in section 9.2 uses today's CST cost estimates. In section 9.4, we explore alternative scenarios, including the effects of a future cost reduction in CST technology and of an alternative plant location with better solar resource compared to the reference location.

The economic parameters entering the economic analysis in this chapter are summarised in Table 8. For pilot systems with construction start set to 2020, today's cost models are used. For large-scale systems with construction start set to 2023, both today's costs as well as predicted future costs are used. Future costs are estimated based on the historical growth rate of CST of around 20% pa since the first CST plants were built in the mid-1980s and a learning rate of 15% per doubling in capacity. These assumptions yield a cost reduction of around 20% between 2018 and 2023 for CST technology.

Table 8. Parameters for economic calculations (all financial parameters are in terms of real AUD)

| Parameter | Pilot system | Large-scale system |
|--|---|----------------------------|
| Project life/depreciation period | 20 year | 20 years |
| Construction start | 2020 | 2023 |
| Time for construction | 1 year | 3 years |
| Operation start | 2021 | 2026 |
| WACC | 5% | 12% |
| Capital expenditure distribution over construction period: | year 1: 100% | year 1:2:3: 10%:30%:60% |
| O&M cost of CST system | $2.05 \times (\text{capex}/\$100\text{m})^{-0.3}$ % pa. | |
| Salvage value of CST system | \$0 | |
| Natural gas cost | 10 \$/GJ _{HHV} / 12.2 \$/GJ _{th} | |
| CO2 emissions costs (tax) | escalating from 29 \$/t _{CO2} in 2020 to 131 \$/t _{CO2} in 2050 | |
| CO2 emissions from NG combustion | 51.4 kg/GJ _{HHV} | |

Amortisation period of 20 years for both pilot and large-scale systems is used. For proven CST technology, a 25 years lifetime can be expected, based on data from systems operating since the mid-1980s. Current development goal for the lifetime of CST technology is even 30+ years (US DoE SunShot 2020 target).

The WACC values used for the reference location are based on risk assessment and valuation of a pilot system. A value of 5% is used for the pilot CST system. For the large-scale system, a value of 12% is applied. This value is higher than the industry-average WACC for renewable

energy projects of ~7%, as the CST system is considered to be linked to the additional risk associated with its coupling to the refinery.

Salvage value is set to \$0, disregarding the possibility of any revenue from further operations or sales of the CST system beyond its depreciation period.

A fixed natural gas price of 10 AUD/GJ_{HHV} (real) is used, which is an expected long-term average estimate over the course of the CST system life. A gas boiler efficiency of 82% is used to convert costs based on the HHV of NG to costs per unit of thermal energy generated.

CO₂ emissions are expected to be costed at an increasing price, starting at 29 AUD/t in year 2020 and increasing to 131 AUD/t in year 2050 (real; growth rate of 5.2% pa). This is the estimate obtained from the Australian Treasury modelling. Typical CO₂ emissions from NG combustion of 51.4 kg/GJ_{HHV} are used.

The resulting mitigated direct gas costs per unit of thermal energy are 12.2 AUD/GJ_{th}. For the periods 2023-2042 and 2026-2045, the additional mitigated CO₂ emission costs are estimated to be 3.2 and 4.1 AUD/GJ_{th}, respectively. Potential additional economic benefits of O&M cost savings on the gas boilers and LGCs are currently omitted.¹⁹ Income taxes are not taken into account in this study.

All CST systems are modelled and optimised using NREL's System Advisor Model, which returns total installed CST system costs and annual system output.

9.2. Base case economics

9.2.1. Total installed cost

Total installed costs for all system configurations considered are shown in Figure 23. Results are shown at (a) 20 MW_{th} and (b) 392 MW_{th} system size for all technologies (trough, Fresnel, tower), with 0, 8, and 14 hours of TES, using *i*) the average cost models for all three system components (SF, TES, BOP; labelled as "avg.") and *ii*) using the low-cost models for SF and BOP and the average cost model for TES (labelled as "low").

Similar costs can be observed for the two linear technologies (trough and Fresnel). With the low cost estimates, linear technologies significantly underbid the cost of tower technology. Note, however, that higher installed costs may be compensated by higher annual thermal energy output (see next section).

¹⁹ An added economic benefit of a solar thermal system using proven technology is that it provides relatively firm energy costs over time. In contrast, natural gas prices in Australia are subject to increasing volatility and projected to grow over the coming years.

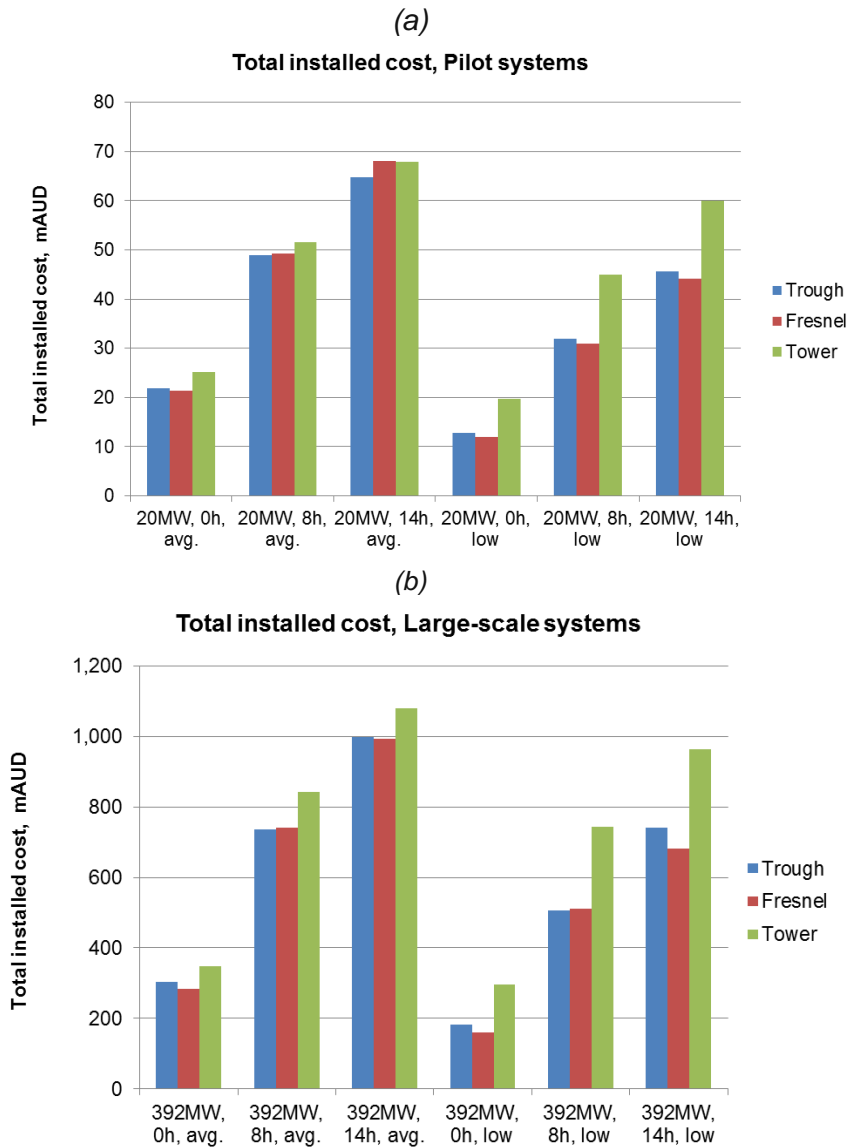


Figure 23: Total installed cost estimates for a) pilot and b) large-scale CST systems.

9.2.2. Annual thermal energy output

Annual steam production of CST systems is estimated using NREL’s System Advisor Model (SAM) for each technology and system configuration. An estimation of the average annual output of the CST system is obtained with a 1-year hour-by-hour system performance simulation with SAM using an average meteorological year (in terms of annual DNI) for the location. SAM system model parameters include:

- Technology (Fresnel, trough, tower, exact solar field components used)
- Rated (design) system output, MW_{th}

- Thermal energy storage capacity, in hours of full-load generation capacity
- Solar multiple
- System operating temperature range

Annual thermal energy generation for all cases is shown in Figure 24. Owing to the different costs represented by the “average” and “low” cost models, slight differences in the optimum solar multiple values can lead to small variations between annual output of “average” and “low cost” systems of equal size and equal TES capacity.

As can be seen from Figure 25, for similar sized systems tower technology results in the highest annual energy collection (except with small 20 MW_{th} solar fields). This is due to the lower optical and thermal losses achieved with tower technology due to its lower “cosine” (optical) losses as well as its higher solar concentration compared to linear systems. Where results for Fresnel technology show higher annual output than trough this is due to slightly higher optimum solar multiple. For equal solar multiple, trough technology yields higher annual output than Fresnel. This is due to trough’s superior optics resulting in lower optical losses at the concentrators as well as lower thermal losses from the receiver (due to smaller receiver size and lower radiation spillage at the receiver).

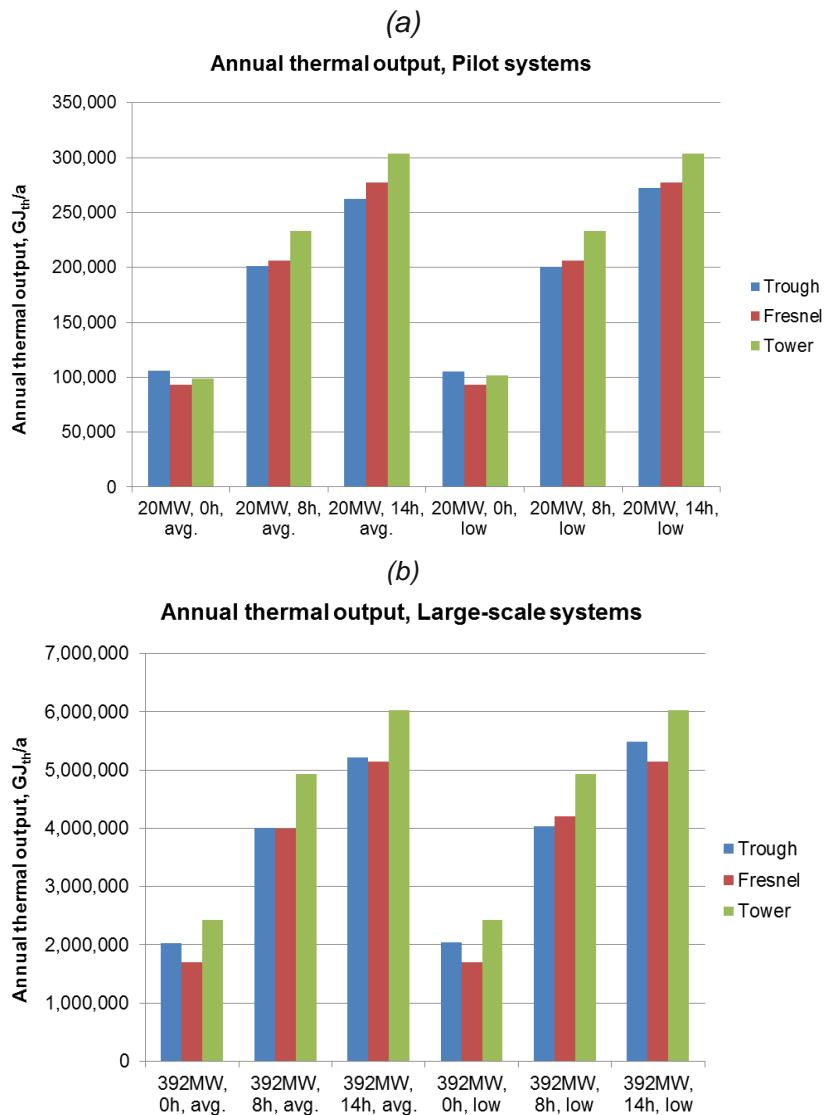


Figure 26: Annual thermal output estimates for a) pilot and b) large-scale CST systems.

9.2.3. Levelised Cost of Heat

The levelised cost of heat (LCOH) from a CST system can be calculated, given:

- Total installed cost (and expenditure distribution)
- Salvage value
- O&M costs
- WACC
- Annual thermal energy (heat) generation (assumed constant from year to year)

- System operating lifetime

LCOH are calculated as:

$$LCOH = \frac{\sum_{t=1}^{t_{\text{project}}} \frac{C_t}{(1+WACC)^t}}{\sum_{t=1}^{t_{\text{project}}} \frac{Q_{\text{annual}}}{(1+WACC)^t}}$$

where C_t are costs in year t , including initial investments and annual O&M costs and Q_{annual} is the annual thermal energy generation in year t .

Resulting LCOH values are shown in Figure 27. The average cost model can be considered the best estimator of current costs of state-of-the-art technology. Using low-cost models for SF and BOP (results labelled “low”) provides an estimate of potential “best case” costs today and in the near future.

Despite the size effect, overall higher LCOH are obtained for the large-scale systems, due to the higher WACC assumed.

The two linear technologies yield very similar LCOH, except for systems without TES, in which case LCOH for trough are lower due to the higher annual output.

With average cost estimates, tower technology yields up to about 10-15% lower LCOH than linear technologies, except for a 20 MW_{th} system without TES due to the lower predicted thermal performance of tower technology at this scale. Hence, the higher installed costs of tower systems are typically outweighed by their higher thermal output.

Due to the large difference between average and low-cost estimates for the linear technologies, with low cost estimates they result in around 15-35% lower LCOH than tower technology. In part, this result may be due to a lack of current cost data from tower technology providers. In an actual bidding environment, more interest and more competitive cost data may be obtained for tower technology.

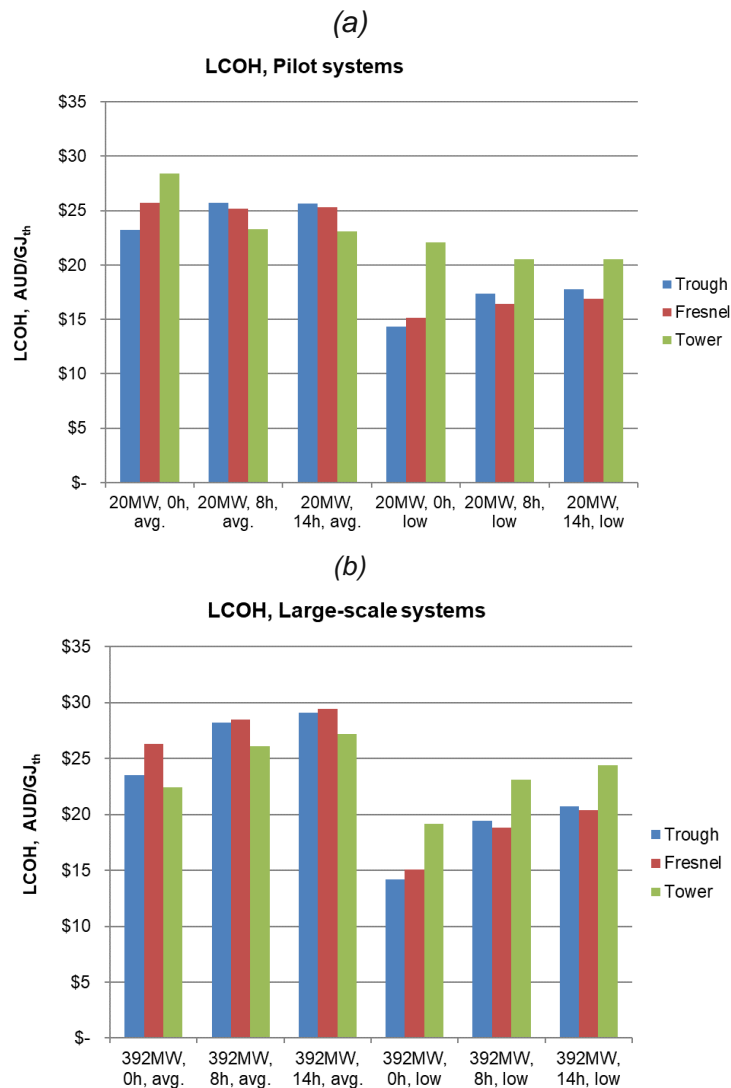


Figure 27: Levelised cost of heat estimates for a) pilot and b) large-scale CST systems.

9.2.4. Net Present Value and Internal Rate of Return

The CST system aims to displace thermal energy currently generated with natural gas fired boilers to produce superheated steam at conditions of 8MPa/470°C. To determine the economic viability of the CST system, its costs need to be compared to those created by the current energy supply system.

The CST system mitigates (potential) costs associated with:

- natural gas consumption
- carbon (CO₂) emissions taxes
- operation and maintenance costs of boilers

In addition, the CST system may qualify for large generation certificates (LGCs), an additional incentive for renewable power production, for the share of electricity it is able to generate via the steam turbines.

On the other hand, a CST system will not be capable of replacing the gas boilers entirely. Hence, the gas boilers will need to be maintained to complement the CST system during off-peak solar irradiation and as a backup.

The economic viability of a CST system is determined by:

- total installed and O&M costs of the CST system
- annual thermal energy generated by the CST system
- CST system lifetime
- Natural gas and CO₂ costs mitigated by the CST system
- additional income generated (LGCs)
- any government grants, concessional loans or other incentives
- required IRR for investment

NPV and IRR are the primary metrics used to assess economic feasibility. They are defined by:

$$NPV = \sum_{t=0}^{t_{project}} \frac{F_t}{(1+WACC)^t}$$

$$IRR \Leftrightarrow NPV = \sum_{t=0}^{t_{project}} \frac{F_t}{(1+IRR)^t} = 0$$

where F_t is the net cash flow in year t .

The project construction periods are 1 year for pilot and 3 years for large-scale system, with capital expenditure distribution over the 3 years of construction of 10%, 30% and 60%, respectively. Payments and revenues are assumed to occur at the end of each year.

Full operation of the CST system is assumed to start in the first year after construction. Revenue is generated in terms of mitigated costs for natural gas and carbon taxes.

Additional cash flows are due to the O&M costs for the CST system.

The resulting NPV and IRR values are shown in Figure 28 and Figure 29. With given WACC (5% for pilot, 12% for large scale) and today's CST costs, nearly all configurations studied for the reference location yield negative NPVs. Exceptions are linear systems with no TES and low-cost estimations. Highest NPV of AUD16m is reached with a large-scale trough system without TES.

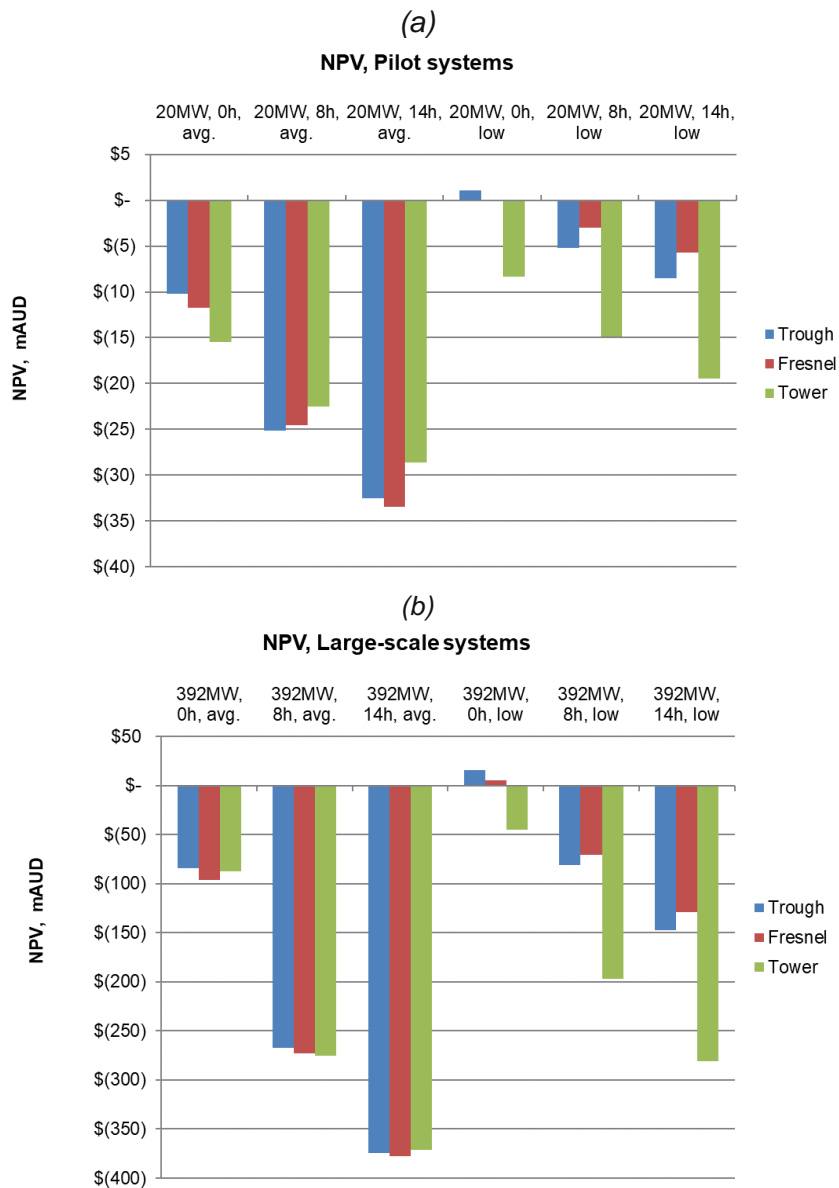


Figure 28: NPV estimates for a) pilot and b) large-scale CST systems.

Figure 29 shows that with average cost estimates, all pilot-scale systems have IRR values below zero, while the significant cost reductions for linear systems predicted with the low cost models lead to significantly higher “best case” IRR values for linear than for tower technologies, leading to IRR of around 3 to 6% even for pilot systems.

All large-scale system configurations are predicted to yield positive IRR. Using best case cost estimates indicates that best current/near term costs achievable may enable IRR values of up to 13%.

These results suggest that positive NPVs are most likely achieved with large-scale systems with no or small TES using linear technology from lowest cost suppliers. On the other hand, if the results based on the average cost estimates are used, large-scale tower technology with no or small TES would be most likely to reach the highest IRR.

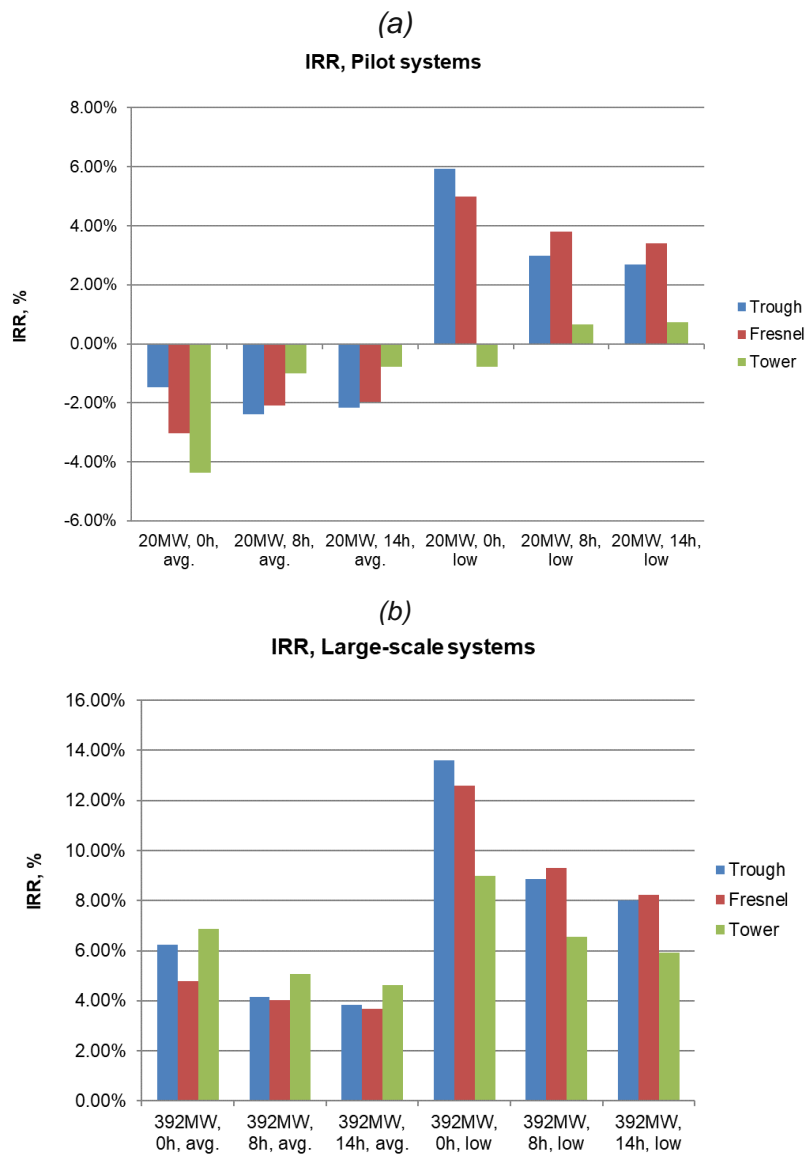


Figure 29: IRR estimates for a) pilot and b) large-scale CST systems.

9.2.5. Grant amount required for pilot plant

The economic viability of a CST system increases with increasing system size, due to the economy of scale size effect on the installed costs (and indirectly on the O&M costs). In addition, further cost

reductions in CST technology are likely to occur before a large-scale system will be built. Hence, while a large-scale system in a few years' time may be economically feasible, a pilot system in the near term may require some level of financial support, such as an ARENA grant, to reach positive NPV.

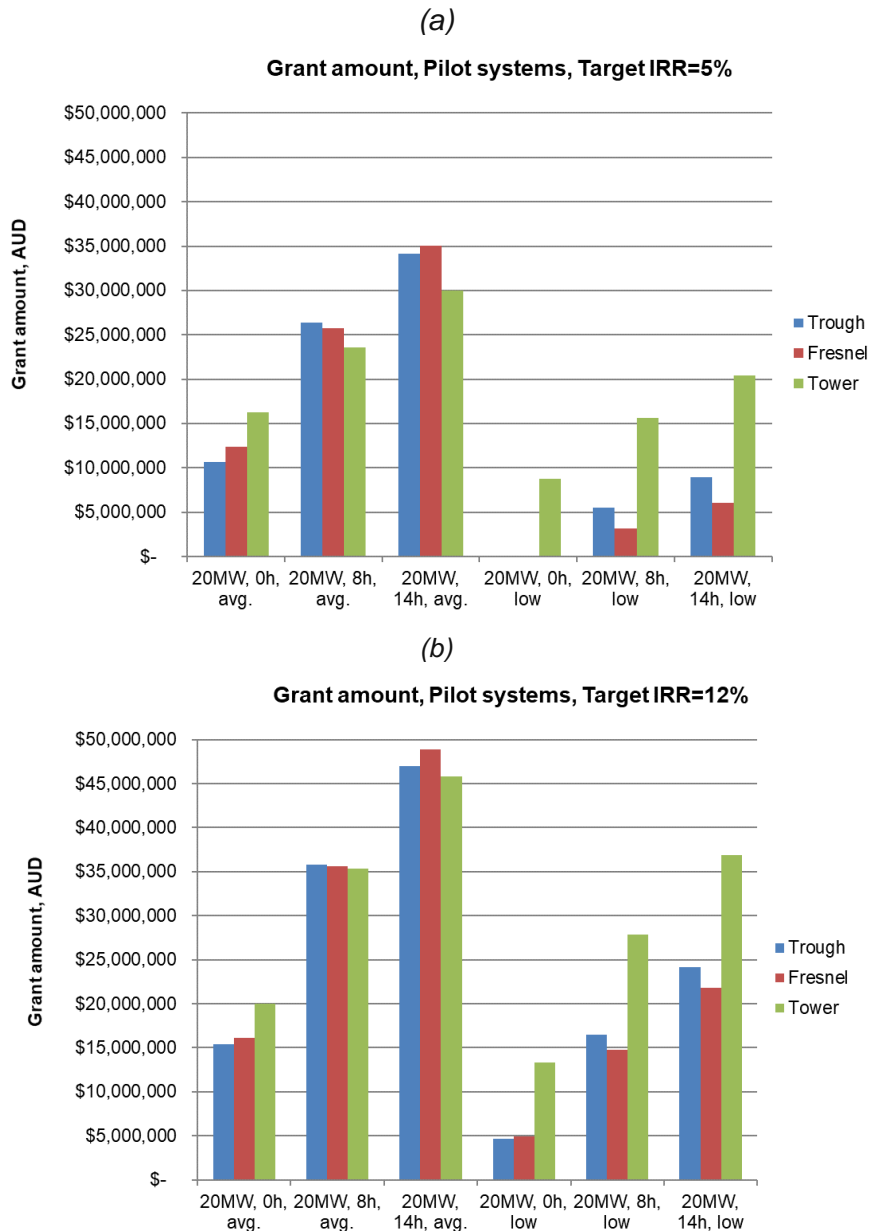


Figure 30: Estimates of required grant amounts for pilot systems to reach target IRRs of a) 5% and b) 12%.

In effect, a financial grant reduces the required capital investment by the investors, thus increasing their financial returns. Figure 30 shows the estimated grant amounts required to reach target IRRs of 5% and 12%, respectively, with a 20 MW_{th} pilot system.

With an IRR expectation of 5%, using average CST cost estimates, the required grant amount is around \$10m to \$16m for a system without TES, increasing to around \$30m to \$35m with 14 hours of TES. This clearly illustrates the increasing capital investment required for systems with increasing TES. On the other hand, if low cost estimates are used, a pilot system may be feasible without a grant or with only a small grant, for a linear system.

The required grant amount increases up to around \$15m to \$49m (depending on TES size) if the IRR expectation on the pilot is increased to 12% pa, using today's average cost estimates.

Based on average cost models, tower technology tends to require the lowest grant amount for systems with TES. With low cost estimates, the required grant amount for linear systems is substantially lower than for tower.

Based on these results, a 20 MW_{th} pilot system for demonstration purposes may likely only incorporate a small TES system (e.g. 2-4 hours) due to the strong increase in the required capital and hence grant amount with TES size. If a grant in the required magnitude cannot be raised, additional financial support, for example in the form of a concessional loan, may be sought.

9.2.6. Capacity factor

One of the project targets is to reach a solar share of the thermal energy provided to the low-temperature digestion process of between 29-45%, with the remainder further supplied by the gas boilers.

Here we report the capacity factors of both the pilot- and large-scale CST systems. The capacity factor is defined as a system's actual annual thermal output divided by the system's annual thermal output if it operated at the rated (design) thermal power output (e.g. 20 MW_{th} for a 20 MW_{th} pilot system) throughout the year. The large-scale system capacity of 392 MW_{th} approximately corresponds to the capacity of the boilers. Hence, for the large-scale CST systems, the capacity factor corresponds to the solar share.

As can be seen from Figure 31, systems without TES reach typical capacity factors of around 15-20%, below the target band defined in this project, while systems with 8 or more hours of TES are likely to fall into the target band. Systems with 14 hours of TES reach capacity factors between 40% and 50%, around the upper limit targeted in this project. Hence, to achieve the target solar share, a large-scale system with a TES capacity between around 7 and 14 hours of TES is required.

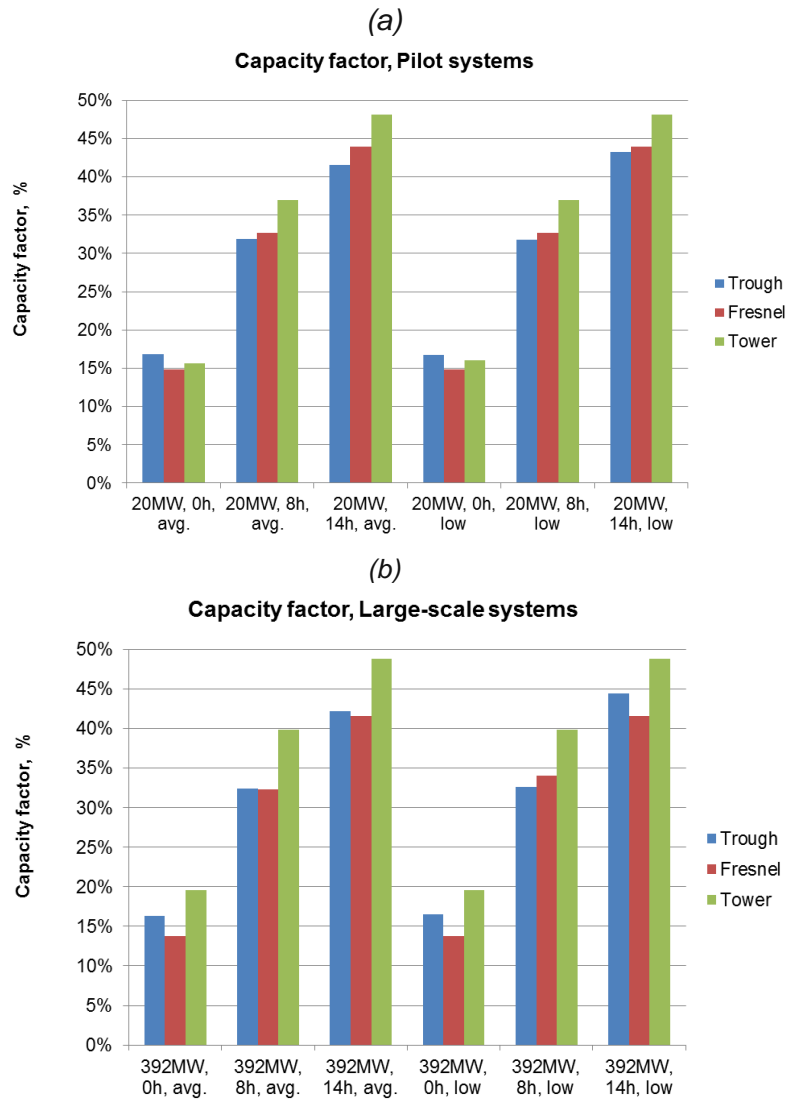


Figure 31: Capacity factor estimates for a) pilot and b) large-scale CST systems.

9.3. Plant operability

In the preceding analyses, solar thermal plant designs have been optimised to deliver the most cost-effective delivery of steam to meet the annual requirement of solar steam supplying at least 29% of the steam utilised in the low temperature bauxite digestion process. Due to the use of storage within the solar plant, delivery of this steam has considerable flexibility but it is worthwhile to consider how well this can be matched to variations in the plant demand and to provide the best possible operation of the existing steam generation equipment. In this regard, the reference facility has a considerable current surplus of steam generation capacity via two adjacent cogeneration units capable of producing 250t/h each (maximum 440t/h each), three onsite boilers capable of producing 250t/h each and three onsite boilers capable of producing 135t/h each. Consumption of steam within the reference Bayer plant is typically 1000t/h, which is considerably less than the maximum production capacity of 2,035t/h if all steam producers were operating at full capacity. Data supplied from 2 years of plant operation is presented in Figure 32, showing that plant operations are intermittently affected by unavailability of one or both of the cogeneration units, with the onsite boilers being used to match the plant steam demand.

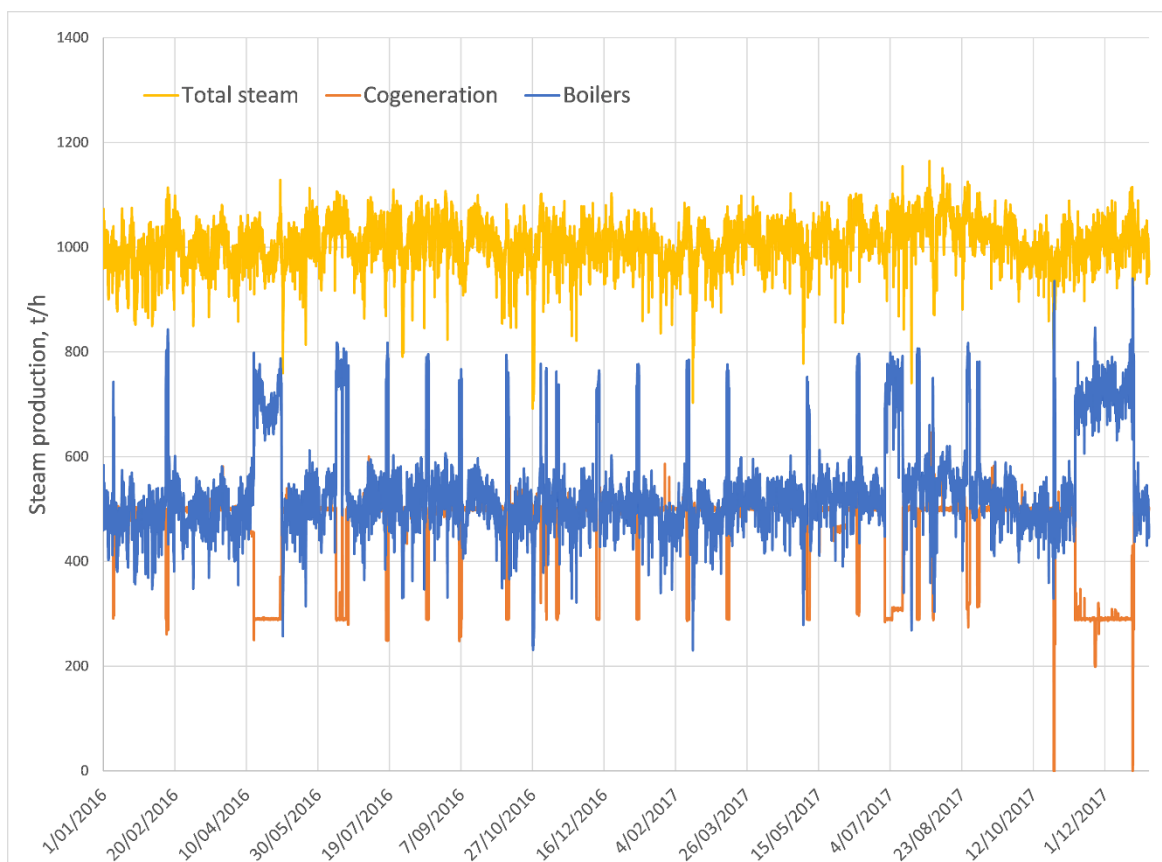


Figure 32: Hourly steam production data from the reference facility over a two-year period.

Additional data was provided for the daily average steam flows for the six onsite boilers over a one year period, as shown in Figure 33. While the operation of the gas turbine heat recovery steam generator (HRSG) units can be adjusted to increase the cogeneration steam production, normal operating procedure is for the onsite boilers to be used to account for any increase in demand over that provided by the CST system. This requires that significant additional capacity needs to be available if rapid increases in output are required, so boilers are rarely operated near full load. From the figure, a typical arrangement is for 3x250t/h and 1x135t/h boilers to be operating at approximately 50-60% load. This produces around 500t/h of steam, but with the potential to rapidly increase production if required. This could be, for example, to compensate for the loss of one or more cogeneration or onsite boilers. This is similar to a common electricity network specification of having surplus operational capacity of 150% of the largest unit in the network. In the case of steam boilers, maximum efficiency occurs at loads around the 50-70% of design capacity so this also minimises natural gas usage, although there is likely to be a slight increase in other operational costs when this strategy results in an extra boiler being in service.

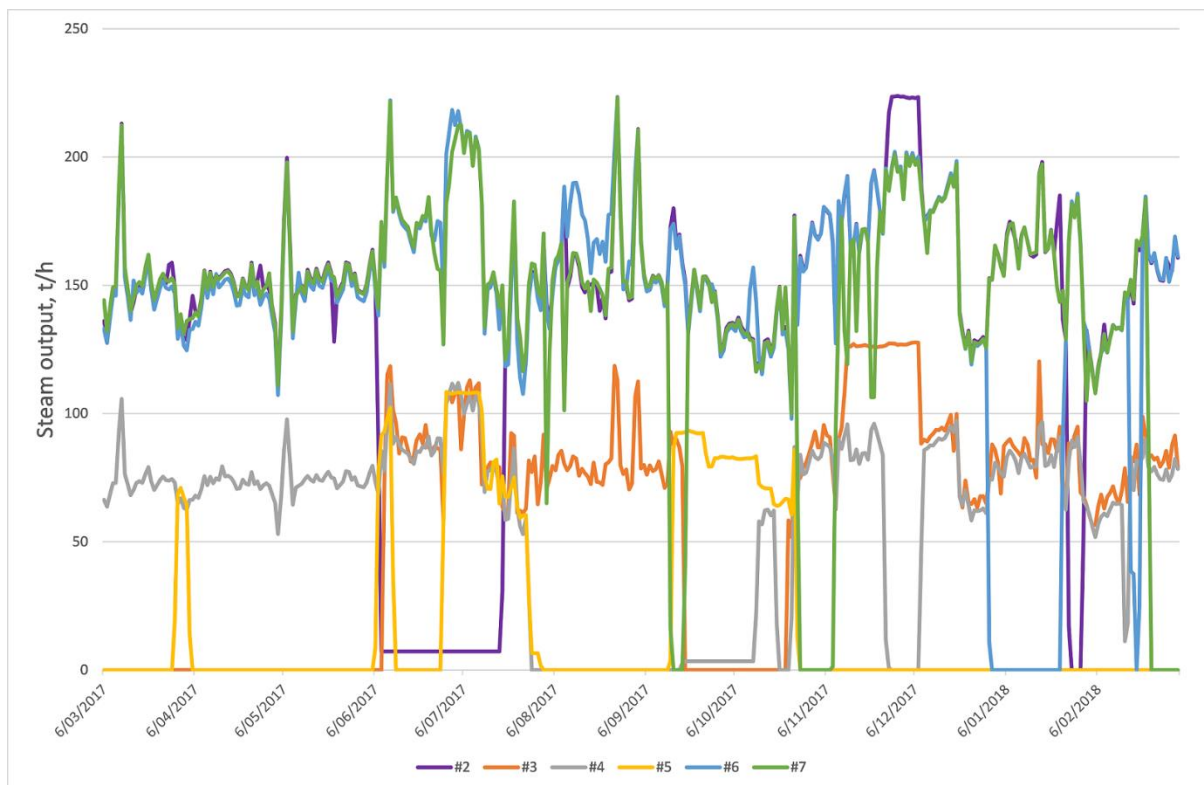


Figure 33: Daily average steam flow data for the onsite boilers at the reference facility over a one-year period.

Introducing an additional CST steam generation unit with design output of 500t/h into this plant configuration adds considerably to the complexity, due to the inability of the CST plant to always be available. Thermal storage will stabilise the CST steam output and allow for ramping up and

down of output to allow other plant sufficient time to respond to changing demand, but it is difficult to guarantee a continuous steam output, even at part load. The capacity factors achieved by the trough and tower plants throughout the year are shown in Figure 34, showing that the decreased and intermittent solar input in winter results in low capacity factors in the CST plant. The larger storage and better solar tracking technology of the tower plant results in significantly better capacity factors, but the winter results are still only approximately 20%.

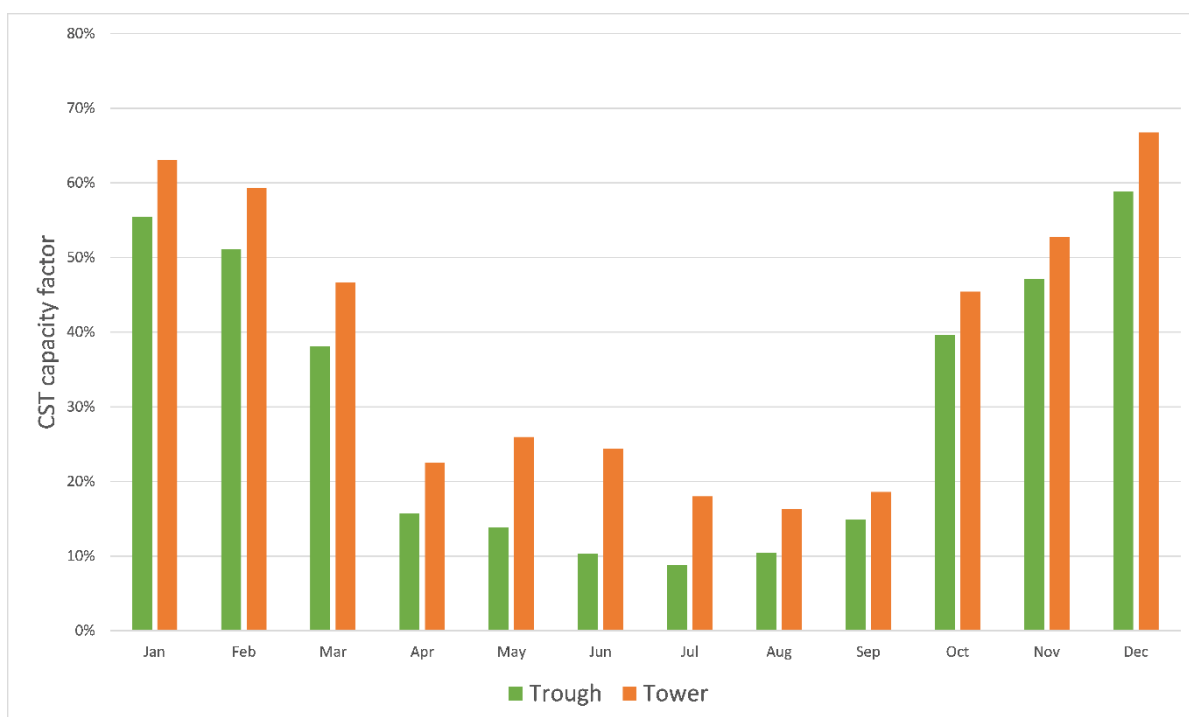


Figure 34: Capacity factors for trough and tower plants on a monthly basis.

In the costing assessment undertaken, a default operating schedule is assumed for the CST plants that essentially has the plant operating at either full or zero output. This is likely to be quite impractical for real applications, but establishes the amount of solar energy that can be collected, stored and converted to steam. The advantage of having a thermal storage of significant size is that the stored energy can be used to generate a wide range of steam output levels to match the plant demands without affecting the overall efficiency for the CST plant. In general, it would be expected that operation of the CST plant would be preferred to be a relatively constant output over extended periods, avoiding zero output periods if possible. Using the financially preferred designs at the reference location of solar multiple 2 and 6 hours of storage for the parabolic trough plant and solar multiple 2 with 8 hours of storage for the tower plant, an attempt was made to optimise the operating schedule to achieve longer periods of relatively constant operations. The operating schedule consists of a general set of rules regarding the fraction of design output the plant will attempt to produce during each hour of the day, with this being different for each month. An intelligent operator with information on weather forecasts and expected plant

behaviour (eg. boiler availability) should be able to improve on the CST plant operations considerably, and may be able to use the storage to reduce natural gas usage during periods of high demand to deliver increases financial benefits. The results of the adjusted CST steam output are shown for a week of summer operation of the trough and tower plants in Figure 35 and Figure 36, respectively. The main impact of the optimisation is to reduce the plant output to below design capacity for significant periods of operation in an attempt to maintain output for whole days. This is slightly more successful for the tower plant due to the larger size of the storage compared to the trough plant. It should be noted that an experienced operator should be able to adjust the daily plant operations to bridge the smaller gaps in output and to avoid the overproduction where the CST plant output exceeds the plant demand that is shown to occur on some days. It is likely that the plants could operate continuously at loads ranging from 40 to 100% without lengthy outages during summer.

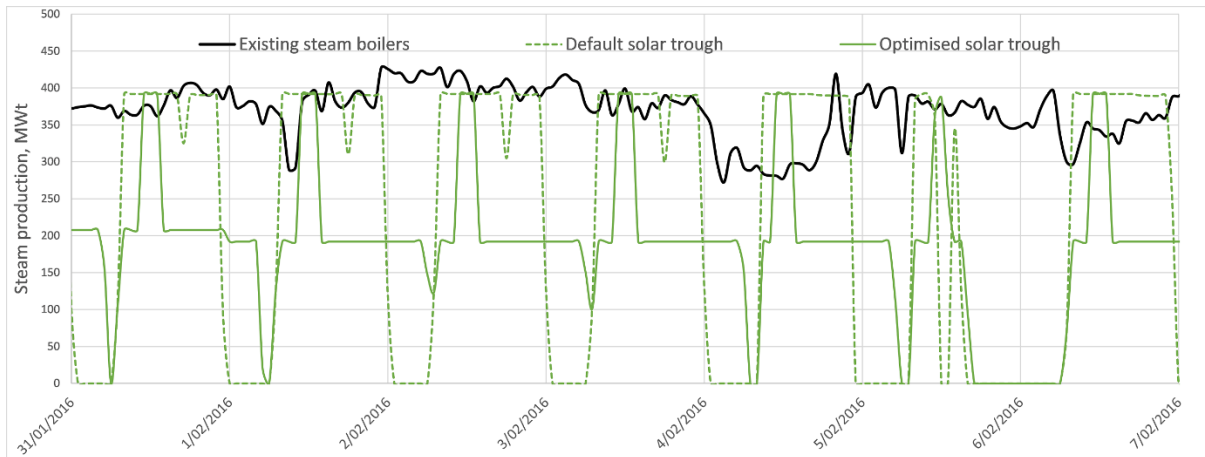


Figure 35: Operation of default and optimised solar trough plant in summer.

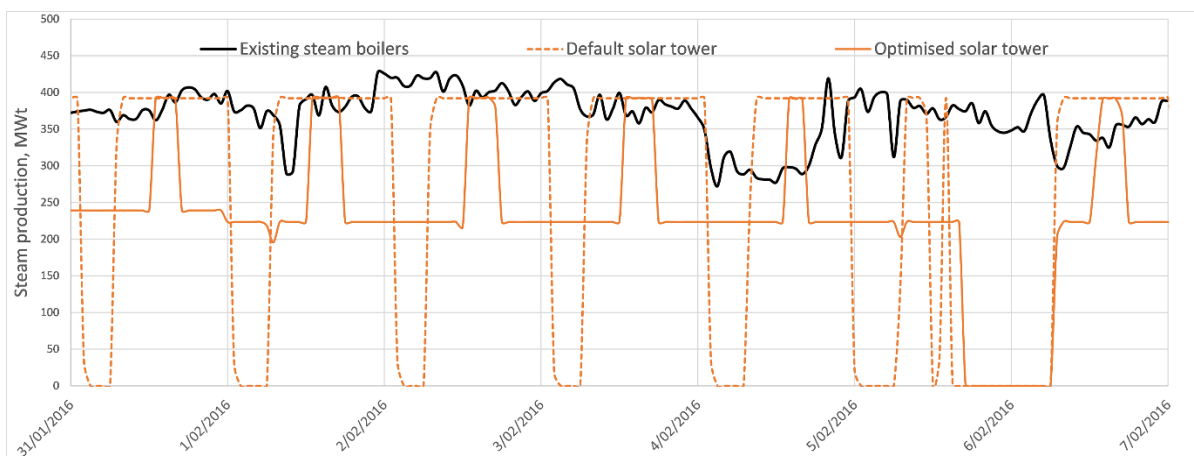


Figure 36: Operation of default and optimised solar tower plant in summer.

Operations of the trough and tower plants during a week in winter are shown in Figure 37 and Figure 38, respectively. Operations in this winter period are quite poor at this site, with the default operation only approaching full output for brief periods on some days. The benefits of optimisation of the operations are evident in both plants being able to achieve extended periods of output (although at low levels), but the capacity factor for the CST plants during winter is typically around 20% compared to the 50 to 70% achieved in summer. The tower technology has a noticeably better performance during winter months than trough technology, arising from the better optical efficiency of heliostat fields compared to linear concentrators at times when the sun is lower in the sky. Again, a skilled operator may achieve a better daily operation than the general optimisation approach that has been used, but one of the major disadvantages of the reference site is the poor solar availability during the winter months. To some extent, the viability of solar technologies at the site may be influenced by the benefits of the significant natural gas usage reductions that can be achieved in summer, when demand can be high for other users, with a consequently higher spot price, rather than the whole year performance of the CST plant.

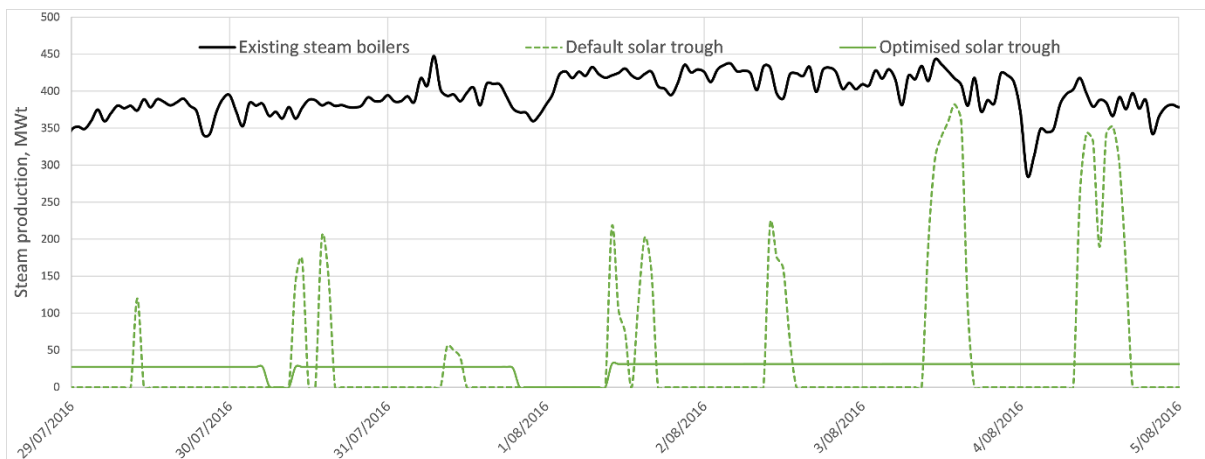


Figure 37: Operation of default and optimised solar trough plant in winter.

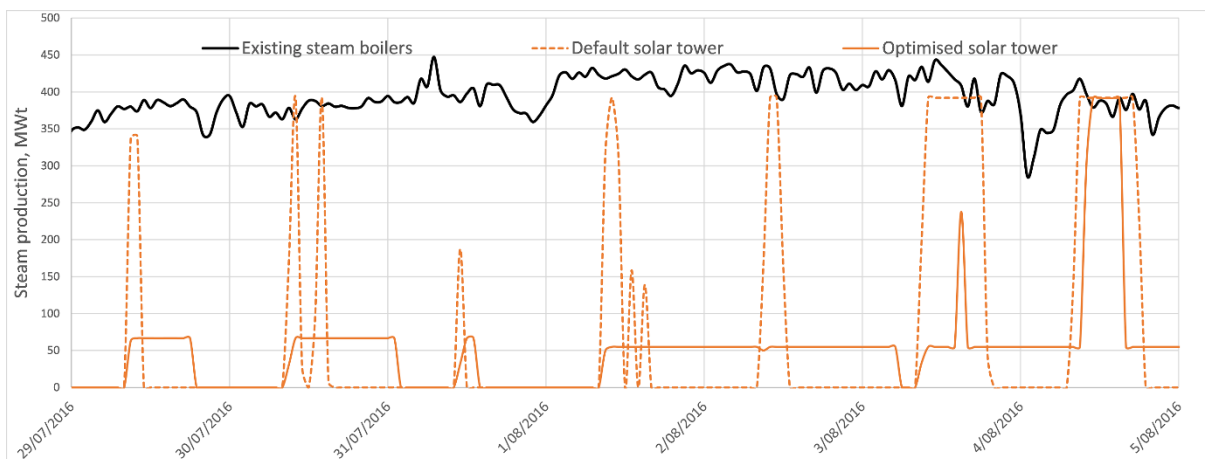


Figure 38: Operation of default and optimised solar tower plant in winter.

9.4. Parametric design optimisation

The variability in financial performance between different technologies and plant specifications warrants a more detailed assessment that identifies more precisely the combinations of solar multiple and storage capacity that achieve the highest NPV and IRR for each of the technology types. For all technologies, the plant design is to achieve a maximum output of 500t/h of steam, which matches the typical requirement for the onsite boilers when the cogeneration plant is producing another 500t/h. Based on the Bayer process model described in Section 4, this is equivalent to a 392 MWt input of steam from the CST plant. Besides the NPV target of \$20m, the CST plant is also required to produce greater than 29% of the steam used in the Bayer process over a year of operation.

The implementation of CST technology requires that a pilot plant of approximately 10% full scale be operated at greater than 40% capacity for at least 3 years before the full-scale plant is operated. This is a measure to improve operator confidence in the plant, optimise the design before construction of the full plant and to reduce the time taken for the full plant to achieve design output on commissioning. The pilot plant was assumed to operate at an average of 35% capacity in the first year, 70% capacity in the second year and 100% capacity in subsequent years, based on McNulty ("Developing innovative Technology", Mining Engineering, October 1998) which is commonly cited by companies implementing new technologies in the minerals industry. From the analysis undertaken by McNulty, the experience gained in the pilot plant should translate to the full plant achieving approximately 50% capacity in the first year and then 100% of design capacity for subsequent years. On this basis, the pilot plant is assumed to be built in 2020 and operated from 2021 to 2024. Engineering design of the full plant commences in 2023, leading to construction through 2024 and 2025 with operations from 2026 to 2045. While the cost per unit output for pilot plants is considerably higher than for a full-scale plant, it is considered by industry that pilot plants provide a significant benefit in risk reduction and smoothing the transition to successful adoption of any innovative technology at a large scale to the extent that it is likely to improve the real financial outcome. McNulty presents data from real plant installations that suggests that it is likely that failure to pilot new technology is often responsible for full plants never achieving full design capacity, when it is quite likely that they will exceed full design capacity if the pilot experience has been applied appropriately.

Three technology variants are considered for the parametric design optimisation, namely tower, trough and Fresnel systems, with the cost models developed above used to estimate component costs with the changes in sizes. The range of solar multiple and storage considered varies between technologies, but the general ranges applied are solar multiple from 1 to 3 and storage hours from 2 to 14 hours. At the reference location it is not possible to achieve the target CST

input of 29% with no storage, plus the use of significant storage capacity has been found to both improve the financial performance and operational stability of CST plants in prior analyses.²⁰

9.4.1. Trough system analysis

In Figure 39, the results of the financial analysis of the combined pilot and full scale plant construction and operation at the reference location are shown for parabolic trough plants using the three different cost estimation models summarised in Table 9. The values shown are based on the cost models defined earlier as applied to a plant design with solar multiple of 2 and storage capacity of 6 hours. The best estimate cost model in the figure as “a” represents the combination of component costs that appeared to be provide the most realistic estimates of technology cost and the financial analysis indicates that an NPV of \$-35m exists at approximately solar multiple 2 with 6 hours of storage. Given that the total plant cost exceeds \$400m, this may be improved through minor design improvements and negotiations with suppliers to a situation where the project parameters are met. The other cost models, namely a combined version of costs from different suppliers shown in “b” and an average of the costs from different suppliers shown in “c”, are less promising. For all cost models the best NPVs and IRRs are be achieved with systems that are smaller than required to deliver the target CST output, but with the combined and average cost models the NPVs and IRRs are lower in the region where CST output is greater than the 29% target and more significant cost reductions would be required to achieve the NV target. The capital expenditure variations between the three models is relatively minor (approximately \$10m in \$400m total), so this indicates the importance of optimising the design and supplier costs if the project is to be viable.

In Figure 40 the IRR of the best cost model at the reference location is displayed together with the CST share. As expected from the NPV values all the IRR are below 12%. Please, note that the IRR will be 12% when the NPV is 0 because the IRR will be the same as the discount rate. For NPV values of \$20m, the IRR needs to be at least 13.1%. Between 12 and 13.1% the NPV is positive and below \$20m. In all the cases under investigation for trough systems the IRR is located below the 12%. The maximum IRR is 10.69% for solar multiple 1 and 0 hours storage, however, CST share at that design conditions is 16.3%. At solar multiple 2 and 6 hours storage (which is the design conditions that achieve the minimum CST share) the IRR is 9.79%.

²⁰ eg. Meybodi &Beath (2016) “[Impact of cost uncertainties and solar data variations on the economics of central receiver solar power plants: An Australian case study](#)”, Renewable Energy 93, 510–524 and Lovegrove *et al.* (2012) “Realising the Potential for Concentrating Solar Power in Australia”, Prepare by IT Power for the Australian Solar Institute.

Table 9 Cost model values for full size plant – Trough systems

| Item | Best estimate “a” | Combined “b” | Average “c” | Units |
|------------------|----------------------|-----------------|----------------|--------------------------|
| Site preparation | 33 | 33 | 33 | \$/m ² (refl) |
| Field | 124.15 | 124.15 | 235.84 | \$/m ² (refl) |
| HTF system | 49.66 | 49.66 | 94.34 | \$/m ² (refl) |
| Thermal storage | 40.34 | 40.34 | 40.34 | \$/kWht |
| BOP | 22.78 | 35.52 | 35.52 | \$/kWt |
| EPC & Owner | 25 | 25 | 25 | % |
| O&M | 1-2 | 2 | 2 | % (CapEx) |

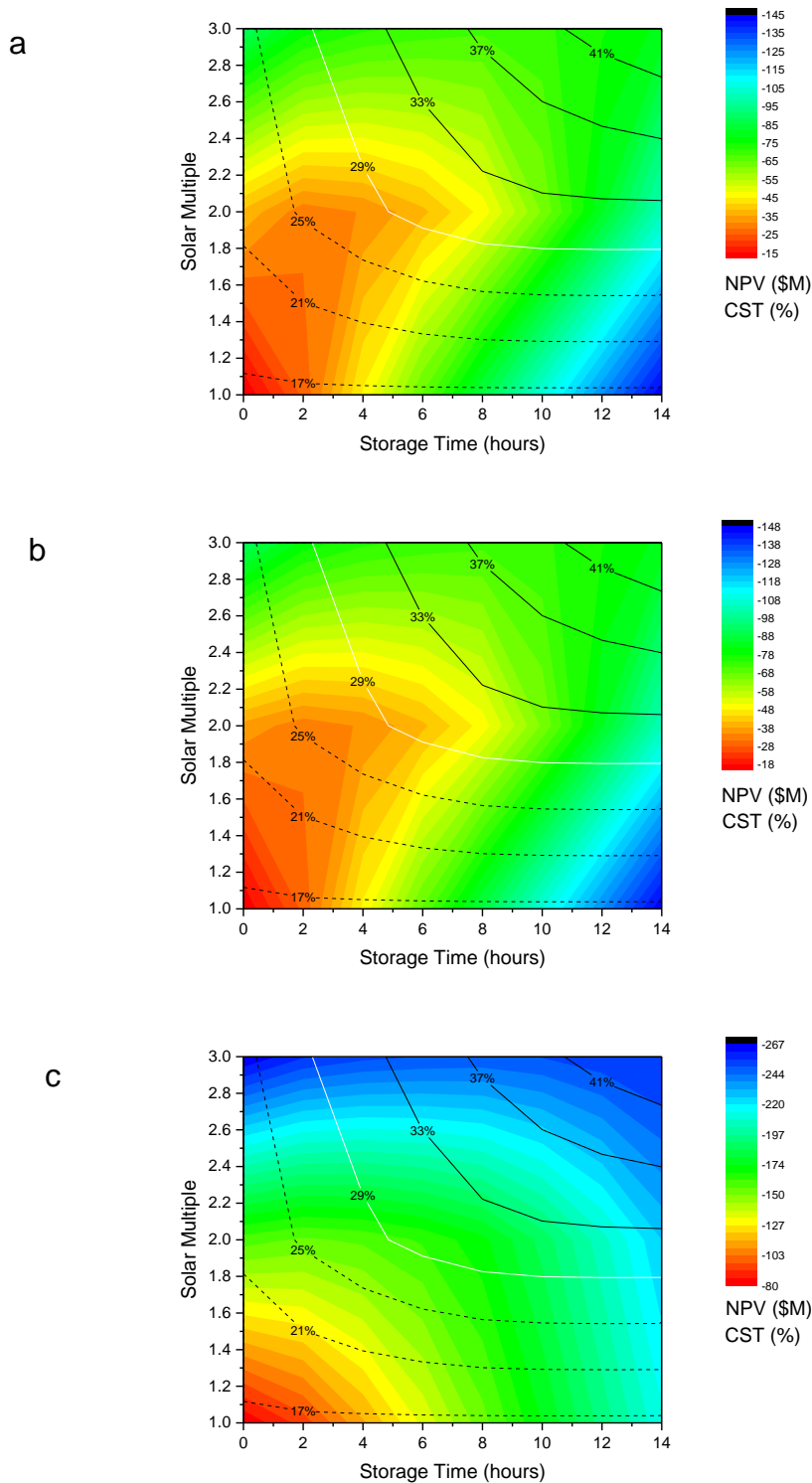


Figure 39 Net present value (NPV) and capacity factor (CST) of parabolic trough plants (392 MW_{th}) at the reference location using the cost models: a. best, b. combined and c. average.

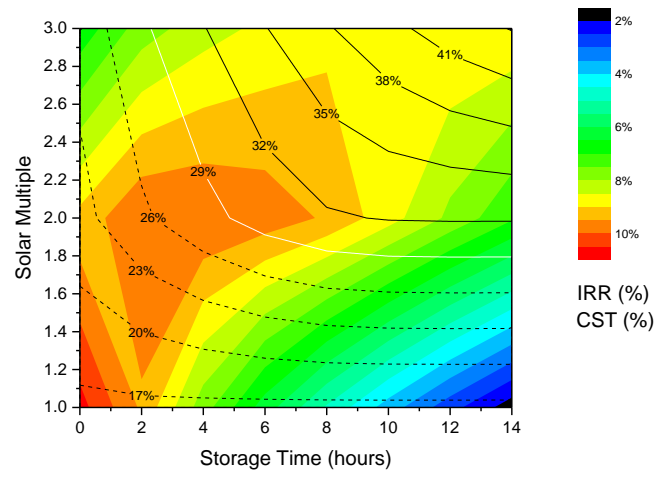


Figure 40: Internal rate of return (IRR) and capacity factor (CST) of parabolic trough plants (392 MW_{th}) at the reference location using the best cost model.

9.4.2. Tower system analysis

In Figure 41, the results of the financial analysis of the combined pilot and full scale plant construction and operation at the reference location are shown for central receiver plants using three different cost estimation models, as summarised in Table 10. The values shown are based on the cost models defined earlier as applied to a plant design with solar multiple of 2 and storage capacity of 8 hours. The best estimate cost model used in “b” represents the combination of component costs that appeared to provide the most realistic estimates of technology cost and the financial analysis indicates that an NPV of -\$96m exists at approximately solar multiple 2 with 8 hours of storage. This design should provide a CST input to the plant of approximately 38%, so comfortably achieves this project criterion.

In Figure 42 the IRR values are plotted versus the design conditions. Similarly to NPV, the highest IRR is obtained at solar multiple 2 and 8 hours storage. In this configuration, the IRR is 7.94%. This value is 1.85% lower than an equivalent trough system which is mainly driven by the larger investment required for the tower systems.

Table 10: Cost model values for full size plant – Tower systems.

| Item | Low “a” | Best estimate “b” | Average “c” | Units |
|--------------------|-------------|-------------------------|----------------|--------------------------|
| Site preparation | 21 | 21 | 21 | \$/m ² (refl) |
| Heliostats | 120.00 | 163.64 | 191.93 | \$/m ² (refl) |
| Tower - Fixed | 3,577,0340 | 3,577,034 | 4,195,548 | \$/m (height) |
| Tower - Scaling | 0.01130 | 0.01130 | 0.01130 | - |
| Receiver - RefC | 144,752,291 | 144,752,291 | 169,781,770 | \$ |
| Receiver - RefA | 1,571 | 1,571 | 1,571 | m ² |
| Receiver - Scaling | 0.7 | 0.7 | 0.7 | - |
| Thermal storage | 28.41 | 28.41 | 28.41 | \$/kWht |
| BOP | 22.78 | 22.78 | 35.52 | \$/kWt |
| EPC & Owner | 25 | 25 | 25 | % |
| O&M | 2 | 2 | 2 | % (CapEx) |

The lower financial performance of tower plants compared to trough plants was unexpected and may arise from the poor response of technology suppliers in this category, resulting in greater reliance on literature sources for the cost data. Thus, under a competitive tender for a real project this relative position may shift. Worldwide there has been significant increase in the planning and

construction of new tower plants, indicating that costs are being reduced. Most of these projects involve technology providers taking on project equity, which can obscure the real cost of components. In the case of tower technology, a major component cost is that of heliostats, which the best estimate cost model have at \$164/m² for large scale plants. Considerable research activity is ongoing worldwide into the development of better and lower cost heliostat designs, with ARENA-funded projects in Australia suggesting that targets of \$120/m² should be achievable for large scale plants. This figure has been used as the only change to the best estimate model when producing the low-cost model, for which the results are shown in “a”. These results in NPV of -\$52m and IRR of 9.57% with the same plant specification, so still considerably worse than achieved for the best parabolic trough plant. A third cost model using the average component costs was used to produce the average graph shown in “c”, which indicates the achievement of poorer NPV and IRR results. In these cases the plant cost is in the region of \$600m, so around 50% greater than for the trough plant, and the higher CST output is not sufficient to warrant this additional cost. Again, there is a tendency for the best NPV values to be achieved with smaller plants that don’t deliver the target CST output, but no cases were identified in this range of configurations that achieved even positive NPV results.

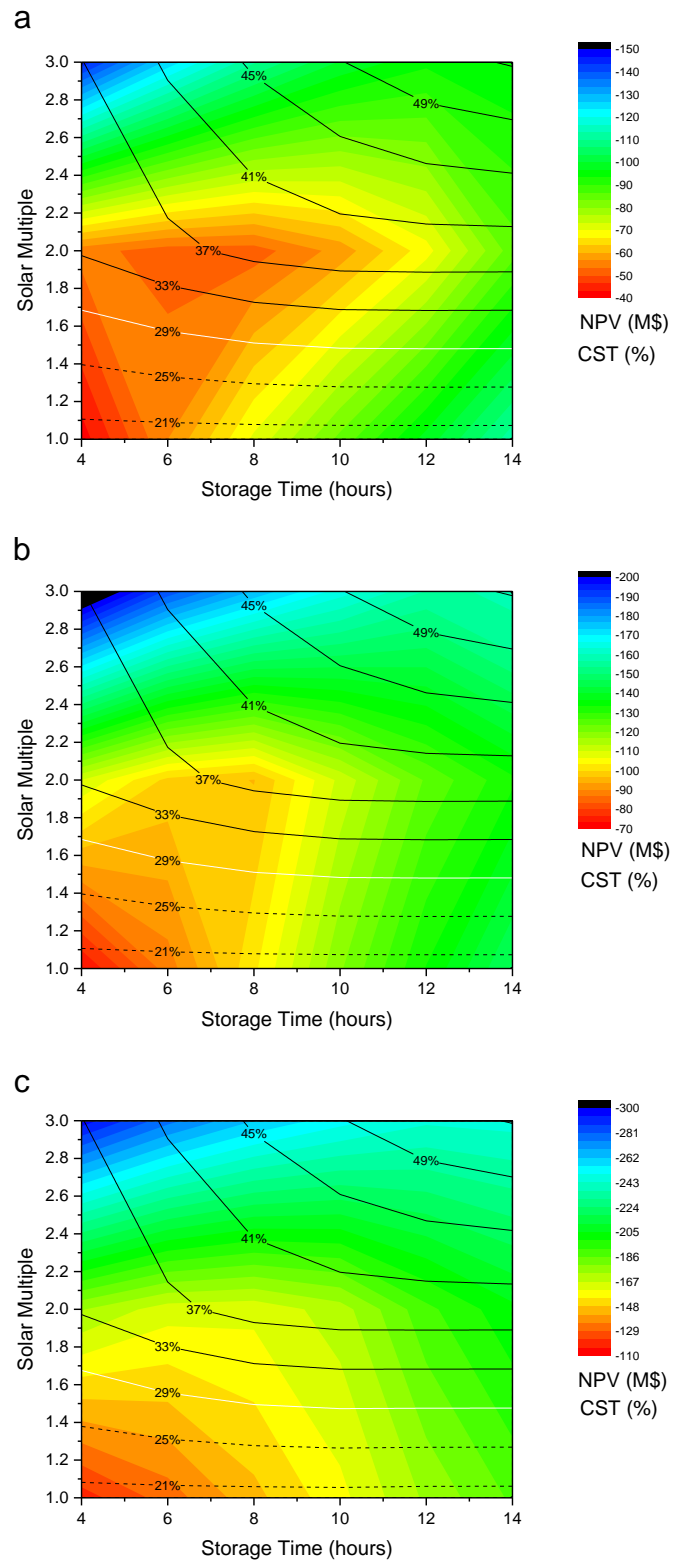


Figure 41: Net present value (NPV) and capacity factor (CST) of central receiver plants (392 MW_{th}) at the reference location using the cost models: a. low, b. best and c. average.

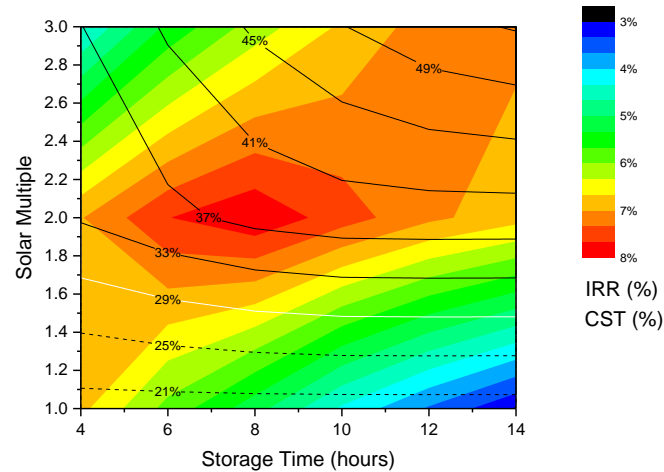


Figure 42: Internal rate of return (IRR) and capacity factor (CST) of central receiver plants (392 MW_{th}) at the reference location using the best cost model.

9.4.3. Fresnel system analysis

Fresnel system analysis

In Figure 43, the results of the financial analysis of the combined pilot and full scale plant construction and operation at the reference location are shown for linear Fresnel plants using the best estimate cost estimation model, as summarised in Table 11. The values shown are based on the cost models defined earlier as applied to a plant design with solar multiple of 2 and storage capacity of 6 hours. This represents the combination of component costs that appeared to provide the most realistic estimates of technology cost. Only a single cost model is presented for this technology due to the poor performance that is predicted, with considerably higher solar multiple being required to achieve the target CST output of 29% compared to the other technologies. The best design appears to be with solar multiple of approximately 2.1 with storage size around 4.5 hours with an NPV of -\$30m.

In Figure 43 the IRR values of Fresnel are also displayed. As expected from the NPV values the Fresnel IRR are slightly higher as compared to trough and tower systems. The linear Fresnel offer an 11.83% for solar multiple 1 and 0 hours of storage. However, the CST share achieved in these conditions is 13.74% which is 3 and 6 % lower than trough and tower respectively. The lower IRR is explained from the lower investment required for the Fresnel plant as compared to trough and tower under the same design conditions.

Table 11: Cost model values for full size plant – Fresnel systems.

| Item | Best estimate | Units |
|------------------|---------------|--------------------------|
| Site preparation | 33 | \$/m ² (refl) |
| Field | 103.58 | \$/m ² (refl) |
| HTF system | 32.47 | \$/m ² (refl) |
| Thermal storage | 40.34 | \$/kWht |
| BOP | 22.78 | \$/kWe |
| EPC & Owner | 25 | % |
| O&M | 2 | % (CapEx) |

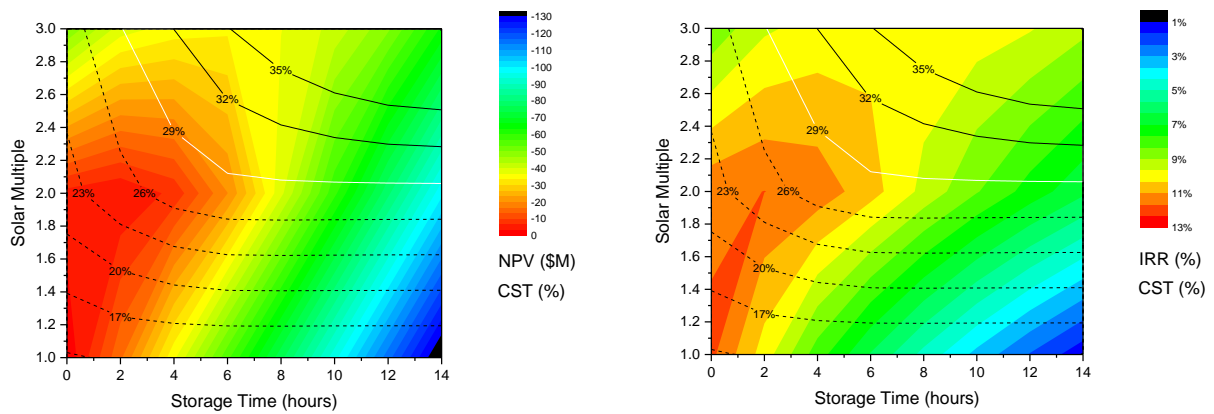


Figure 43: Net present value (NPV), internal rate of return (IRR) and capacity factor (CST) of linear Fresnel plants (392 MW_{th}) at the reference location using the best cost model.

9.5. Alternative scenarios

9.5.1. Capital cost reductions

There are several sources of predictions of the future costs of energy technologies, both internationally and specific to Australia. CST technology is more complex for cost and performance projections than most other energy technologies due to the variability in performance and cost at different sites and plant scales, plus the flexibility in selecting different thermal storage capacities. The relatively small number of installed plants worldwide and the range of plant specifications used require some analysis to interpret how the costs incurred relate to any new project.

Generically, IRENA²¹ assessed that there was a cost reduction in the technology of approximately 25% between 2010 and 2017. There has been a significant increase in the number and scale of new plants being planned and constructed worldwide, from which the Learning Rate method of cost projection suggests a significant reduction in the technology cost over the next 10 years. A CSIRO analysis prepared for AEMO²² assessed a range of energy technologies using a common modelling approach that predicted the likely uptake and cost improvements. This considered a CST system with 6 hours of storage as an electricity generation unit and identified likely cost reductions of approximately 30% from 2017 to 2025 based on technology uptake rates. The basis for the costs is on operation of the plant commencing in that year, so taking the cost data provided from suppliers as relevant to overnight construction in 2018, the reduction in cost for a plant commencing in 2021 would be approximately 10% and for 2026 it would be approximately 18%. The rapid cost reductions that appear to be happening with CST technologies make this a difficult field to make accurate predictions, as there could be significant fluctuations depending on the timing of the project and availability of specific equipment items or expertise, but these appear to be the current best estimates for Australia. These are also for electricity applications, so include a steam turbine system and other plant components that are omitted from a project for steam production only. These items are not subject to the same learning rate benefits due to the maturity of this part of the plant, so a solar steam production only project may be subject to higher cost reductions on the solar collector, receiver and storage components.

To illustrate the benefit of future cost reductions in CST technology, we have regenerated our previous results for the reference location with reduced CST costs. In this section we present a summary of results obtained for the reference location with a 20% reduction in capex (and concomitant reductions in O&M costs) by 2023, the projected start year for the implementation of a large-scale CST system.

²¹ Renewable Power Generation Costs in 2017, International Renewable Energy Agency, Abu Dhabi.

²² Hayward, J.A. and Graham, P.W. 2017, Electricity generation technology cost projections: 2017-2050.

The cost reduction between 2018 and 2023 is predicted based on the long-term growth rate in CSP technology worldwide of 19.6% pa²³ since the first plants were built in the 1980s and a learning rate of 15% per doubling of installed capacity. This learning rate is lower than that suggested by the IRENA of 30% based on historical data and somewhat higher than the rather conservative estimate of 10% by the IEA. With our estimated growth and learning rates, a cost reduction in CSP technology of around 20% by 2023 is predicted.

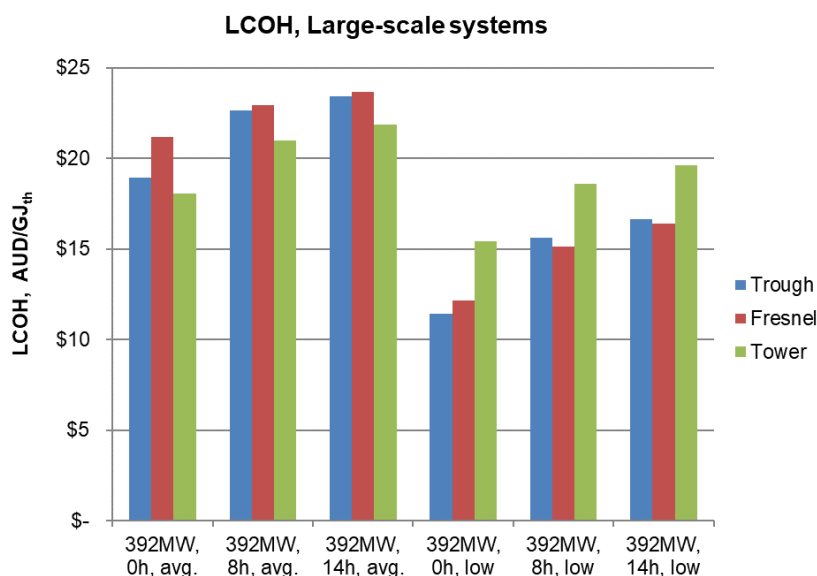


Figure 44: LCOH estimates for large-scale (392 MW_{th}) CST systems at the reference location with a 20% reduction in capex over today's costs for CST.

We adopt this number here, although the power block of a CSP plant may tend to experience slower cost decline (since it is mature technology) while solar field and thermal storage may tend to experience faster cost decline rates, which would result in larger cost reductions for a CST system for process heat (without power block).

Resulting LCOH, NPV and IRR for large-scale systems are shown in Figure 44 and Figure 45. The pilot system is projected to be built in the near future and cost reductions in this short timeframe are not further considered here.

LCOH decrease by around 19.5% compared to the base case. This decrease is slightly lower than the decrease in the capex of 20% due to the stronger scale effect in the O&M costs than in the capex of the overall system (O&M percentage is calculated as a function of capex).

²³ Higher growth rate up to ~40% pa over more recent time periods.

IRR increases significantly compared to the base case scenario, from around 4–7% in the base case to around 6–10% using average costs, and from around 6–13.5% in the base case to around 8.5–17.5% using low cost estimates.

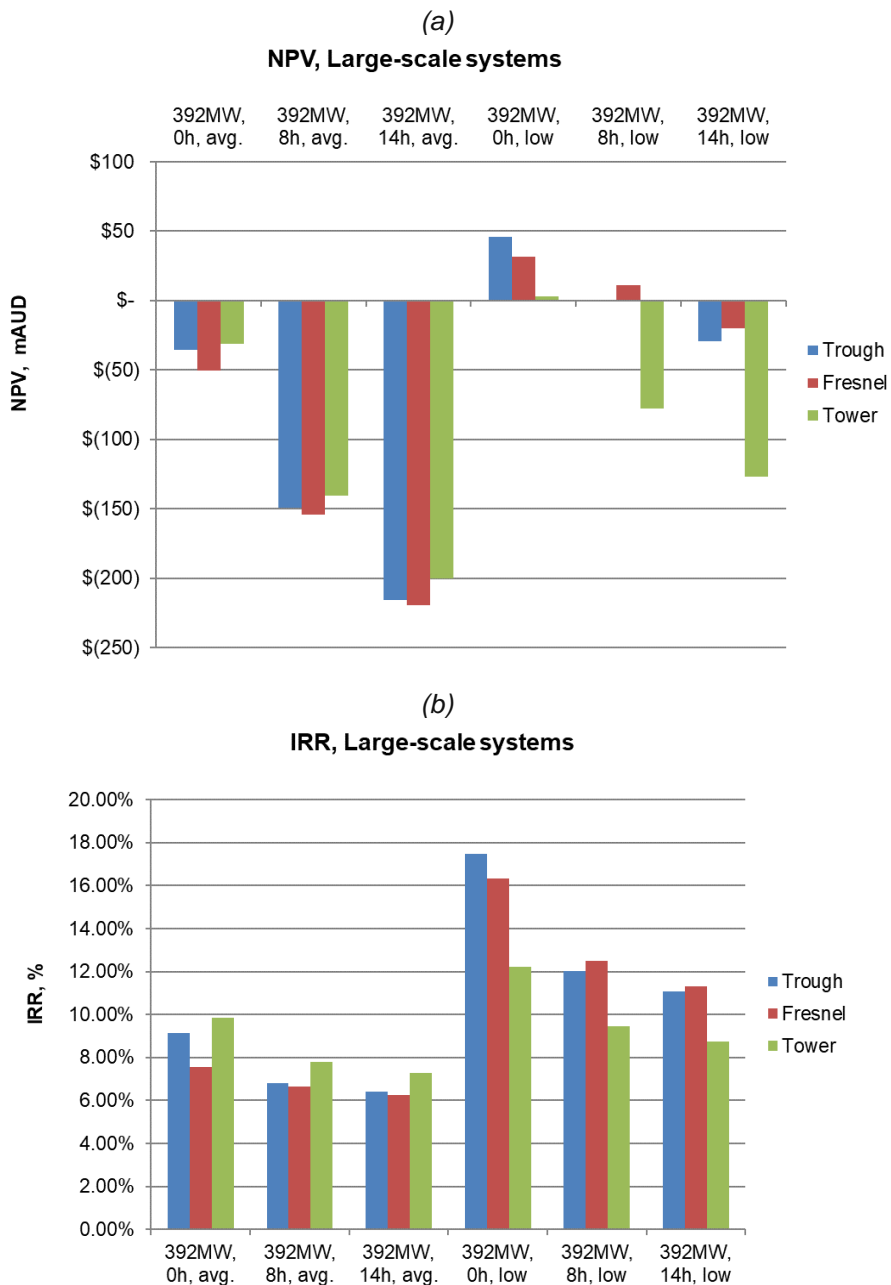


Figure 45: (a) NPV and (b) IRR estimates for large-scale (392 MW_{th}) CST systems at the reference location with a 20% reduction in capex over today's costs for CST.

NPV is positive for linear systems with up to 8 hours of TES and the tower system without TES under the low cost estimates, with highest NPV of \$46m estimated for a trough system without TES and \$31m for a Fresnel system without TES.

9.5.2. O&M cost reductions

O&M cost reductions may be achieved through synergies with existing operations at the reference site and future cost reductions resulting from innovations in mirror surface coatings and in the way CST plants are operated, e.g. through automated mirror cleaning and reduced staffing levels.

To illustrate the impact of O&M costs on the economics, LCOH, NPV and IRR results are presented in Figure 46 and Figure 47 for large-scale CST systems in the limiting case where no extra O&M expenditures are required for the CST system. This case illustrates the maximum possible effect of reducing O&M costs on the overall system economics.

LCOH decrease by around 6.5–11% compared to the base case results, which corresponds to the contributions of the O&M costs in the total LCOH.

IRR slightly increase compared to the base case scenario, from around 4–7% in the base case to around 5–8.5% using average costs, and from around 6–13.5% in the base case to around 7–15%.

NPV is positive for the linear systems without TES under the low cost estimates, with NPV of \$33m for a trough system and \$20m for a Fresnel system.

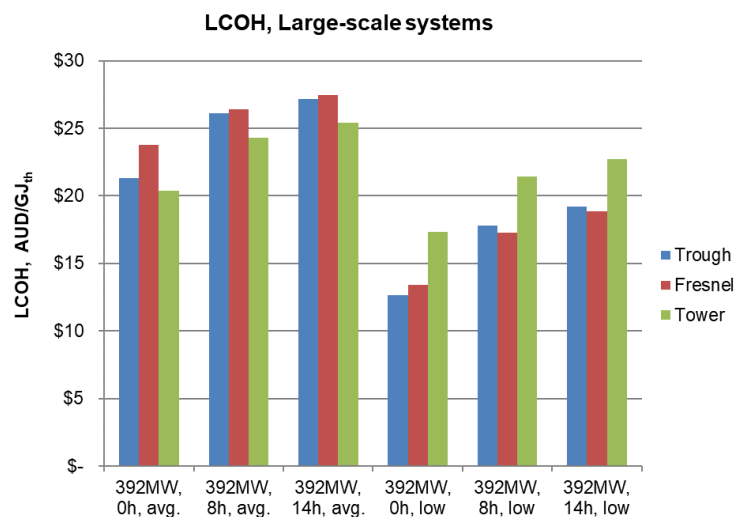


Figure 46: LCOH estimates for large-scale (392 MW_{th}) CST systems at the reference location, assuming no extra O&M costs incurred for the CST system compared to the refinery’s current O&M costs.

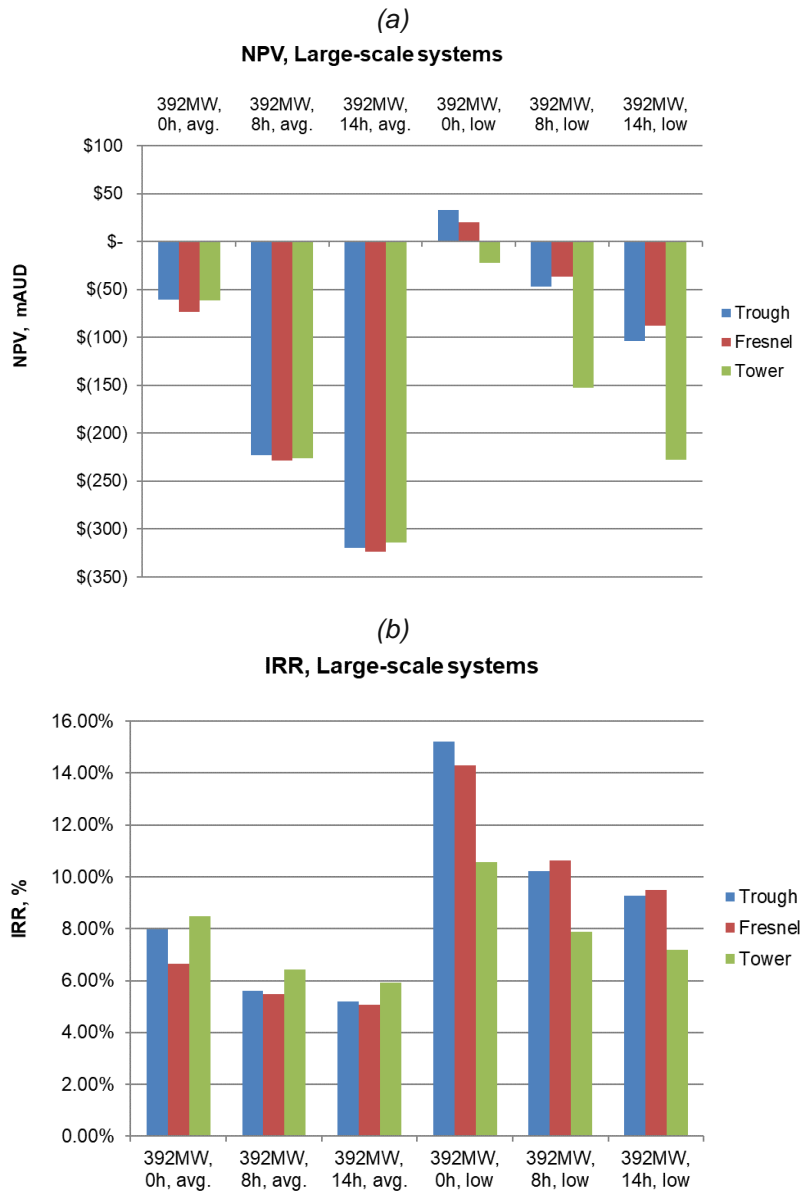


Figure 47: (a) NPV and (b) IRR estimates for large-scale (392 MW_{th}) CST systems at the reference location, assuming no extra O&M costs incurred for the CST system compared to the refinery’s current O&M costs.

9.5.3. Alternative plant locations

The emphasis in this analysis has been on a potential CST implementation at the reference facility, but there are other sites in Australia that are either linked to bauxite mining or processing, or could be considered as greenfield sites for future processing operations. The operations in WA are based on processing bauxite that is mined in the nearby Darling Range to produce alumina that is then shipped to markets for further processing to aluminium. This differs from the approach taken with the Weipa bauxite deposit in northern Queensland, where the bauxite is

shipped to Gladstone for refining to alumina which is either processed to aluminium locally or shipped to other locations, such as Tasmania. Gove in north-eastern Northern Territory has another bauxite mining operation with a currently inoperative refinery at Nhulunbuy, plus large deposits of bauxite have been identified in the extreme north of Western Australia at Cape Bougainville and Mitchell Plateau that are currently not mined. On this basis it appears reasonable to consider Gladstone and Darwin (as an available source for solar data similar to the northern bauxite deposits) as alternative plant locations. In addition, Learmonth on the coast of Western Australia in a high solar availability area provides an alternative greenfield option where there is nearby port (Exmouth) and natural gas access, but bauxite would need to be shipped to the site and, except in the unlikely event that aluminium production was also implemented, alumina would also have to be shipped from the nearby port.s

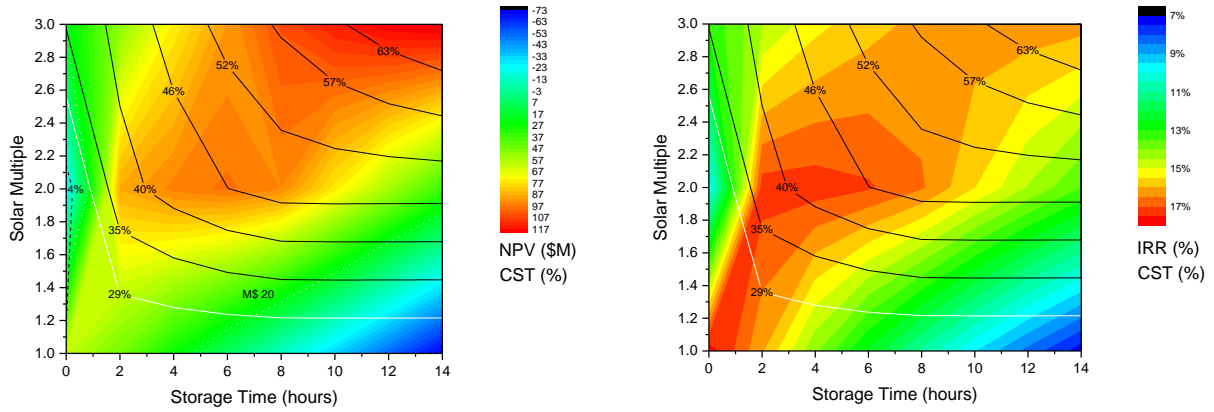
In a preliminary comparison of these sites with the reference location it is apparent that all are further to the north, so inherently should receive more even solar input through the year. However, both Gladstone and Darwin are in regions where seasonal weather conditions limit the benefits of this due to extensive rainfall events. The northern Australian sites represented by Darwin also present significant cyclone risk, which is likely to add considerably to the cost of some plant components, such as heliostats, that would need to be evaluated in more detail if a project appeared to be viable. This also applies to Learmonth, which is affected by sometimes intense cyclones but has a relatively low frequency of them in the historical record²⁴. It should be noted that damage from cyclones decreases significantly with distance from the coast and this could be used to reduce risk to the plant, but with some increase in transport costs to and from the plant.

The same modelling process used for the analysis at the reference location was used to determine the optimum plant configuration to meet the 29% CST input target and maximise the NPV, with the NPV including a pilot plant followed by the full 500t/h steam production plant.

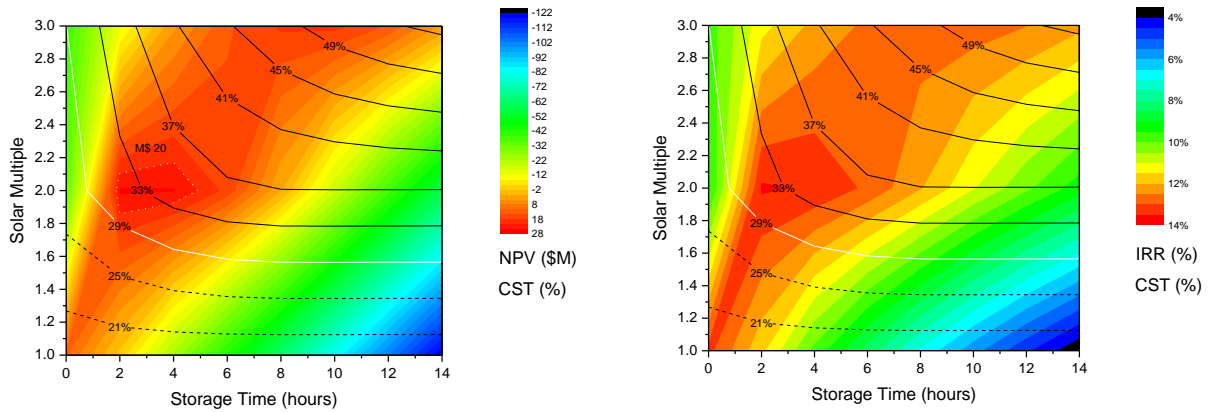
Results for trough systems at Learmonth, Gladstone and Darwin (a, b and c in Figure 48) show the benefits of a high solar availability location, with Learmonth easily achieving the target CST input of 29% at relatively small field and storage sizes and achieving positive NPV results that increase as the system size increases. Selection of the optimum at Learmonth is limited by the maximum CST input target of 45%, which occurs at solar multiple 2 with 6 hours of storage, the same specification that was determined at the reference location.

²⁴ <http://www.bom.gov.au/cyclone/history/wa/exmouth.shtml>.

(a)



(b)



(c)

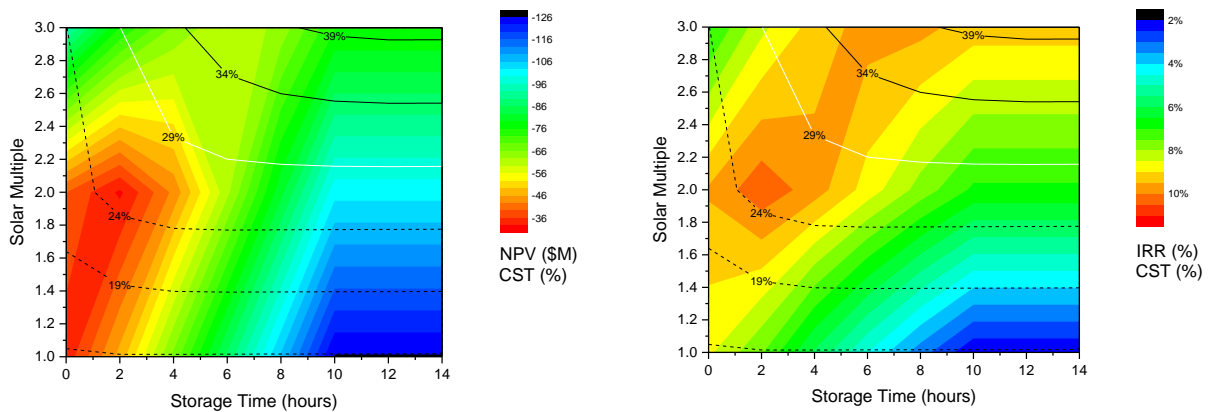


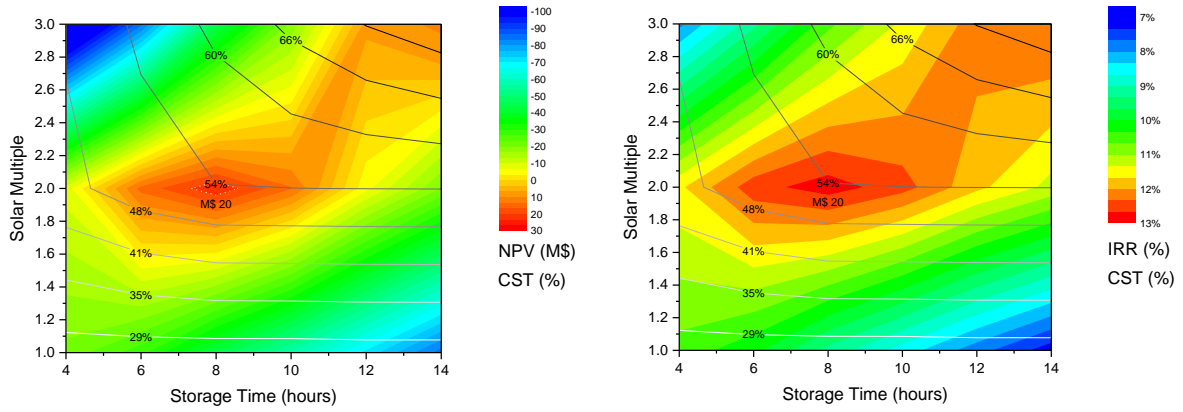
Figure 48: Net present value (NPV), internal rate of return (IRR) and capacity factor (CST) of parabolic trough plants (392 MW_{th}) using the best cost model at a. Learmonth, b. Gladstone and c. Darwin.

Gladstone also achieves good results, with a local NPV maximum at solar multiple 2 with 2 hours of storage providing a CST input of approximately 34%. Darwin, however, does not appear to be

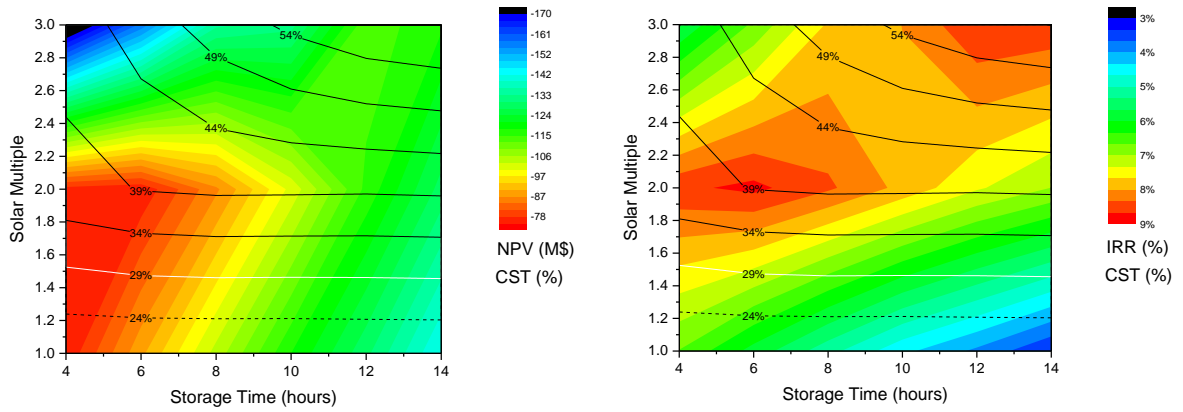
as promising for the technology and negative NPVs result from all combinations meeting the target CST input. The IRR values are over 12% in most of the design conditions for Learmonth and Gladstone. The maximum is localized in solar multiple 2 and 6 hours storage for Learmonth where the NPV is 17.0%. For Gladstone at solar multiple 2 with 2 hours of storage the IRR is 13.6%.

Results for tower systems at Learmonth, Gladstone and Darwin (a, b and c in Figure 49) show a good local NPV maxima, over \$20m for Learmonth at solar multiple 2 with storage of 8 hours that has a CST input above the target maximum of 45%. An unusual outcome is that reducing the size of the plant to reduce this to the target CST input will result in the NPV dropping below the target minimum. Both Gladstone and Darwin exhibit negative NPVs in the configuration where the target CST input share is achieved. There is an obvious movement of the optimum towards lower storage sizes at the lower solar availability sites, which is linked to the poor reliability of solar input reducing the capacity of the system to effectively fill the storage on a daily basis. IRR values are over 12% in the design conditions where the CST input share is over 41% for Learmonth. However, Gladstone and Darwin achieve lower IRR similarly to the reference location.

(a)



(b)



(c)

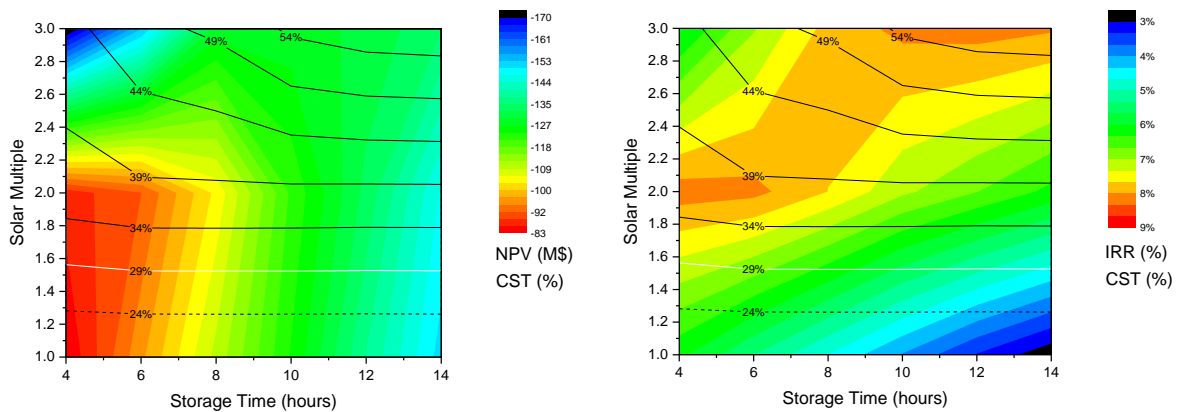


Figure 49 Net present value (NPV), internal rate of return (IRR) and capacity factor (CST) of central tower plants (392 MW_{th}) using the best cost model at a. Learmonth, b. Gladstone and c. Darwin

Results for the linear Fresnel system are shown only for Learmonth in Figure 50, as the system was identified as both having worse performance and higher costs than trough systems at the reference location, so only limited further assessments were undertaken. With the significantly higher solar availability at Learmonth the system performance is markedly improved and the NPV results are now positive across most of the plant designs. The optimum specification within the required criteria is solar multiple of approximately 1.5 with 2 hours of storage.

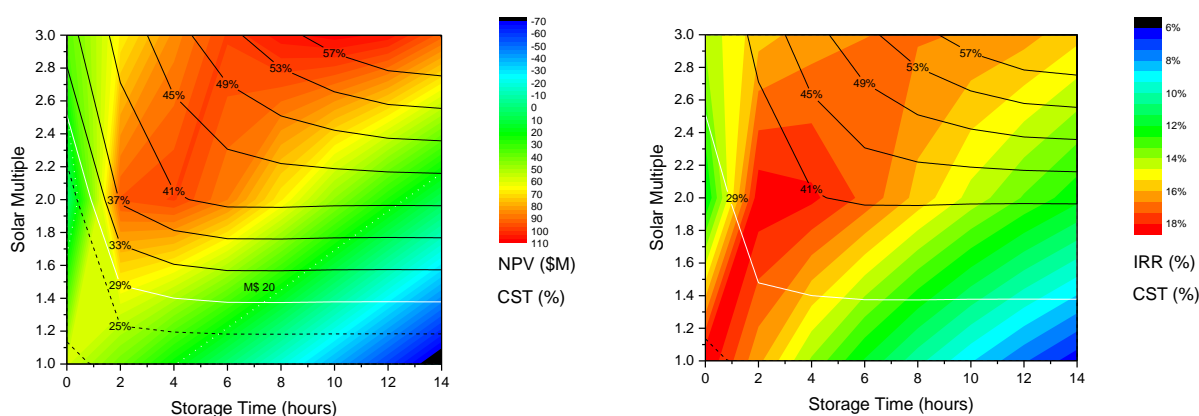


Figure 50 Net present value (NPV), internal rate of return (IRR) and capacity factor (CST) of linear Fresnel plants (392 MWth) using the best cost model at Learmonth

The results obtained in this study lead to the conclusion that the short-term configuration will be a parabolic trough plant with solar multiple 2 and 6 hours storage. However, in the long-term a central tower plant could be more appropriate because it can achieve larger CST % and larger NPV values if highest natural gas prices and larger CO₂ cost are achieved.

In Table 12 a summary of the best system results identified for the reference location and the three alternative locations is presented for the technology options assessed, all using the best estimate cost model and providing the design that matches the criteria for CST input share to the refinery and with the highest expected NPV. This indicates parabolic trough technology offers the best match to the requirements at all sites with this set of cost data, but fails to achieve the target NPV at the reference location. The benefits of using a site with higher solar availability are evident, with all technologies meeting the minimum requirements at Learmonth, and this should be considered when evaluating potential greenfield developments in technologies that require significant input of industrial heat. The failure to achieve the target NPV with trough technology at the reference location is relatively minor considering the large capital cost of the system and it is possible that further refinement of the system design could result in a successful project outcome. The uncompetitive costing of the tower technology is surprising, given the growing uptake in large scale projects worldwide and the reportedly rapid decrease in costs. No major technology

provider expressed interest in the project and this has resulted in a reliance on literature costs for the assessment, which may have resulted in an unintentional bias where the costs used for tower technology were more dated than for the other technologies. It is clear for the assessment that the use of tower technology allows for greater CST input due to improved winter performance and this may be an influencing factor in the future if a need for more significant input of renewable energy arises. Fresnel systems achieve the slightly higher IRR values in Learmonth and the reference location as compared with trough systems. However, Fresnel technologies are not demonstrated at the same scale and the risk of installing this technology is higher as compared with parabolic trough. In addition, Fresnel systems achieve the lowest CST input values of the study meaning that it requires a larger solar multiple to deliver the CST target.

Table 12: Summary of best system results for locations and technologies.

| Location | Technology | SM | Storage | Total CapEx | CST | NPV (m) | IRR |
|---------------|------------|----|---------|----------------|-------|----------|--------|
| Ref. location | Trough | 2 | 6 | \$ 452,322,240 | 30.2% | -\$28.48 | 10.36% |
| | Tower | 2 | 8 | \$ 734,898,488 | 38.4% | -\$79.9 | 8.3% |
| | Fresnel | 3 | 4 | \$ 496,555,776 | 32.0% | -\$24.68 | 10.6% |
| Learmonth | Trough | 2 | 6 | \$ 453,975,624 | 47.3% | \$106.78 | 17.5% |
| | Tower | 2 | 8 | \$ 739,353,792 | 53.8% | \$39.43 | 13.47% |
| | Fresnel | 2 | 4 | \$ 370,872,864 | 40.6% | \$103.38 | 18.5% |
| Gladstone | Trough | 2 | 2 | \$ 373,250,912 | 32.8% | \$31.70 | 14% |
| | Tower | 2 | 6 | \$ 706,154,696 | 39.2% | -\$60.36 | 9.5% |
| Darwin | Trough | 3 | 2 | \$ 518,370,048 | 29.7% | -\$64.70 | 8.5% |
| | Tower | 2 | 4 | \$ 691,021,392 | 36.8% | -\$72.15 | 8.8% |

9.5.4. Learmonth, WA

Following on from these screening results for three alternative locations, we have recalculated all economic metrics for a large-scale (392 MW_{th}) CST system with 0, 8 and 14 hours of TES for the exemplary greenfield plant location of Learmonth, WA. The average annual thermal output is

estimated using the “closest to average” year (in terms of DNI) between 2006 and 2015, year 2010 with an average daily DNI of 7.38 kWh/m²/day. This DNI is around 30% higher than that at the reference location (5.65 kWh/m²/day). Higher DNI directly translates into higher thermal output. In addition, Learmonth is 10° closer to the equator than the reference location, which leads to lower “cosine” (optical) losses in the solar field. The solar multiple is again optimised for each case as was done in the simulations for the reference location.

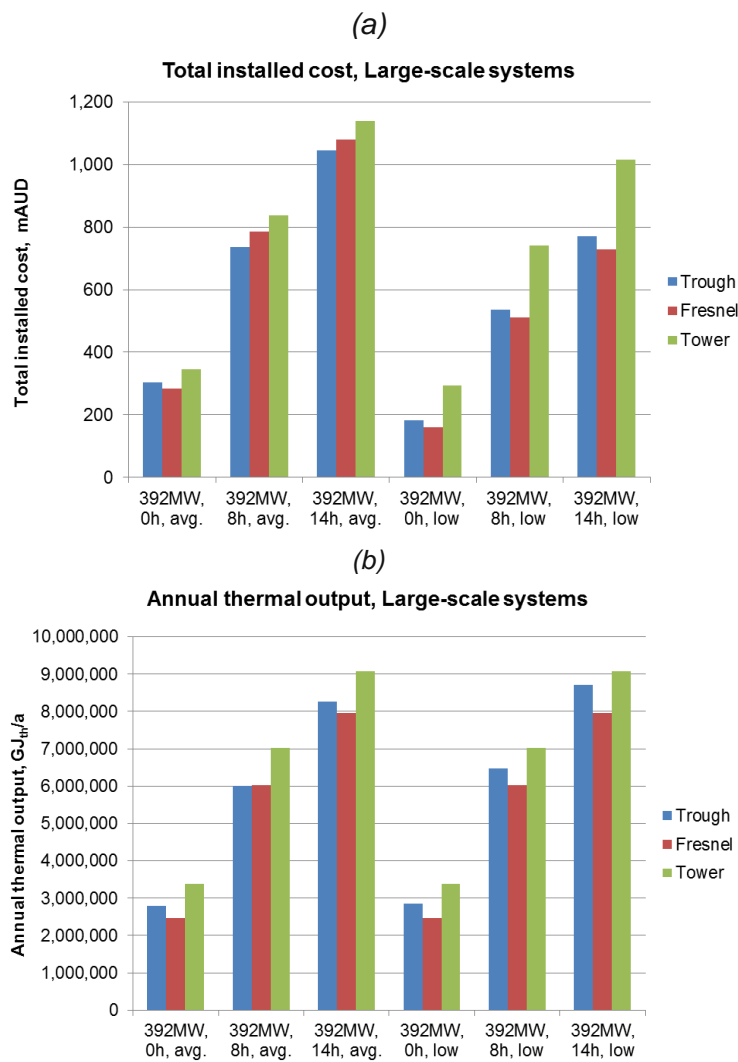


Figure 51: (a) Total installed cost and (b) annual thermal output estimates for large-scale (392 MW_{th}) CST systems in Learmonth, WA.

Figure 51 shows the total installed costs and annual thermal outputs. While the installed costs remain relatively unchanged compared to the reference location,²⁵ the thermal output increases by around 40 to 60% at Learmonth. This is mainly due to the better solar resource at Learmonth.

²⁵ Any differences in labour or transport costs between the reference location and Learmonth are not considered.

To a lesser extent the thermal output increases because the optimised systems feature larger solar field relative to TES at Learmonth than at the reference location. As a result, LCOH are predicted to be 28 to 35% lower at Learmonth than at the reference location (Figure 52).

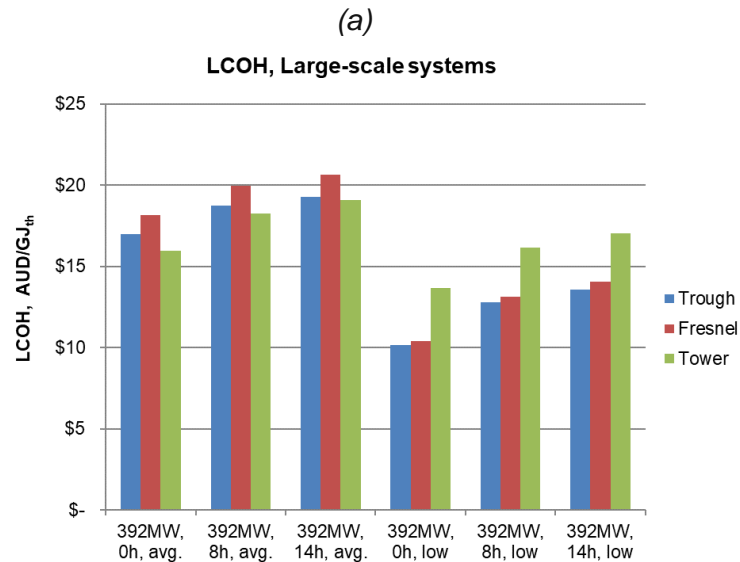


Figure 52: Levelised cost of heat estimates for large-scale (392 MW_{th}) CST systems in Learmonth, WA.

The better CST system performance at Learmonth combined with the low-cost estimates results in positive NPVs >AUD20m for all configurations involving linear systems (Figure 53a).

Interestingly, despite the monotonically increasing LCOH with TES size, due to scale effects in the O&M costs, the NPV increases with increasing TES up to 8 hours for the linear systems and low-cost models, reaching around \$98m for trough and \$80m for Fresnel.

With current average cost estimates, IRR values are around 8–11.5%, while with low cost estimates they are around 11–19.5% (Figure 53b). These results are based on today’s cost estimates and do not include any future cost reductions in CST technology.

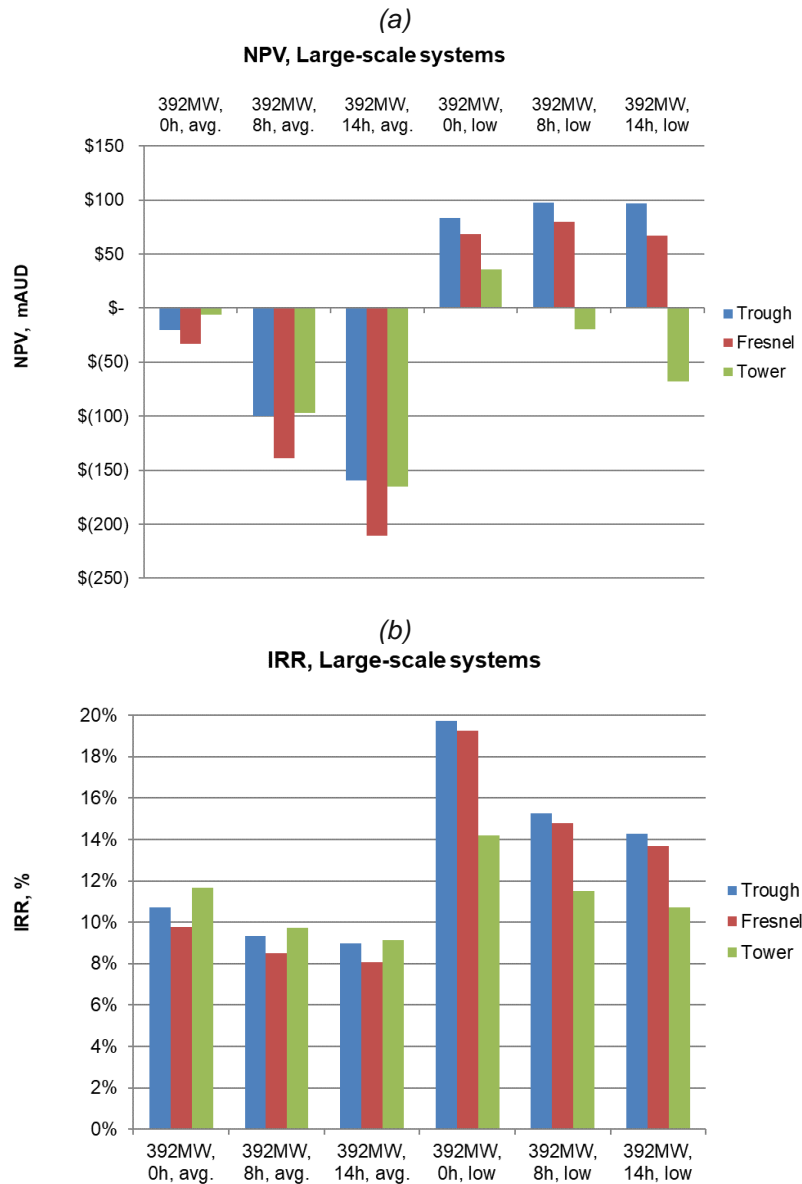


Figure 53: (a) NPV and (b) IRR estimates for large-scale (392 MW_{th}) CST systems in Learmonth, WA.

The higher DNI and the closer proximity to the equator of Learmonth result in significantly higher capacity factors compared to the reference location, ranging from 20–27% for systems without TES to 64–73% for systems with 14 hours of TES (Figure 54a).

Nevertheless, the output of CST systems with 14 hours of TES remains below the thermal energy demand by the refinery (392 MW_{th} continuous, corresponding to 1030 TJ_{th}) in all months (Figure 54b-c). While in the summer half year, the CST system delivers 80% or more of the thermal energy demand of the refinery, its output is reduced significantly during the winter months. Somewhat higher availability is reached with tower compared to trough technology, particularly during winter months, where tower systems experience lower cosine losses.

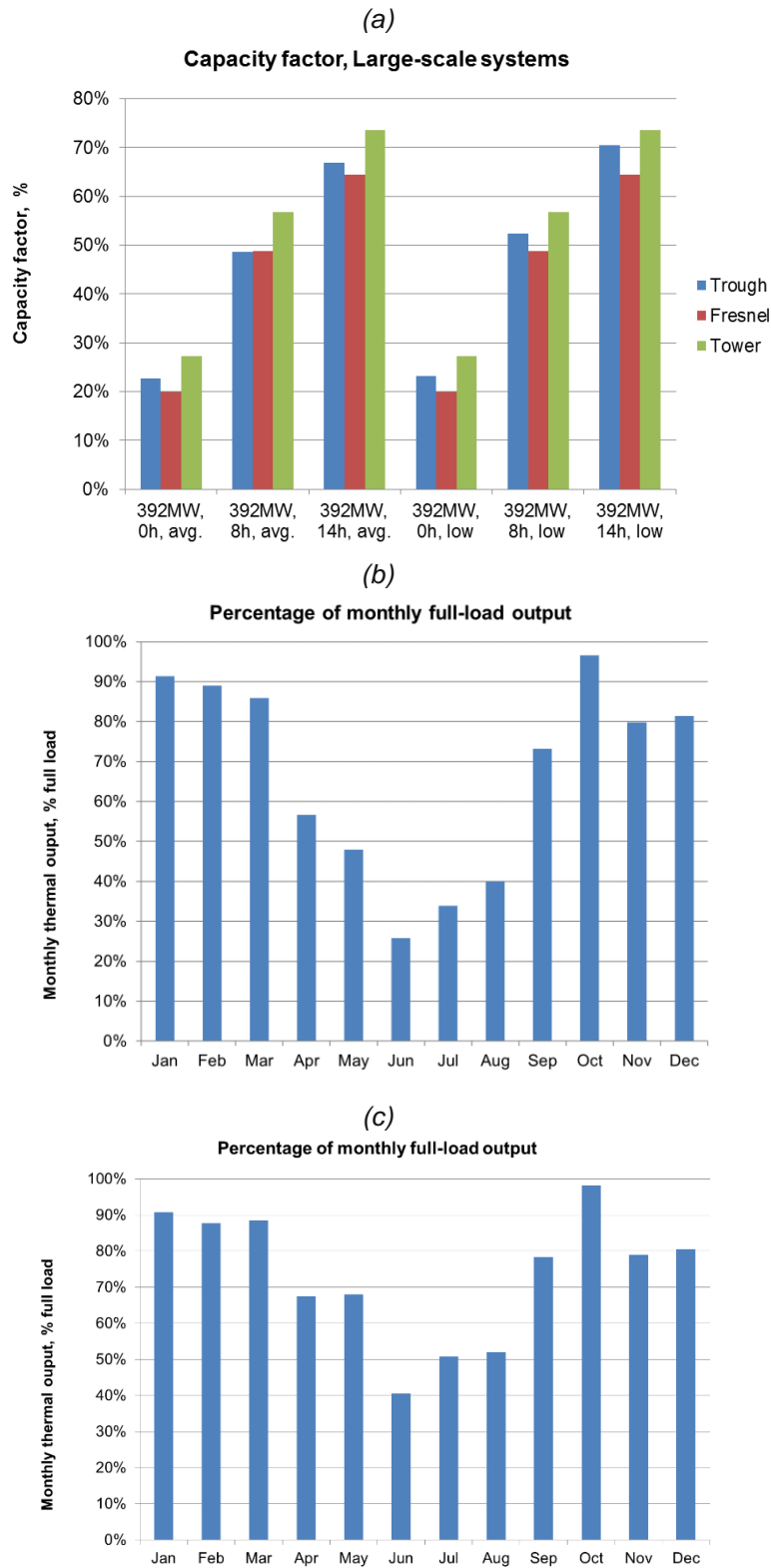


Figure 54: (a) Capacity factor estimates for large-scale (392 MW_{th}) CST systems; (b-c) month-by-month variation in thermal output relative to design output for (b) a trough and (c) a tower system with 14 hours of TES, for Learmonth, WA.

9.6. Resource requirements

9.6.1. Water

Water is mainly required for cleaning of the CST system. Typical water use for mirror cleaning is approximately in the range of 50 to 100 m³/GWh_{th}, with Fresnel systems reported to use somewhat less water. Fresh water costs are typically several AUD per m³. Hence, for a pilot system with a 50 MW_{th} solar field (solar multiple = 2.5), the water demand would be in the order of 4,000 to 8,000 m³/a resulting in costs of around 8,000 to 16,000 AUD/a. These costs are relatively minor compared to the overall costs and are already factored into the O&M cost data used. Sourcing the required amount of water required is not a problem at the reference location.

9.6.2. Land

Average land cover factor for the 3 technologies under consideration are listed in Table 13. As can be seen, there is a large difference in the land use among the technologies, with Fresnel technology requiring about four times less land area than tower and about half the area of trough. The size of a CST system is also influenced by the solar field collection efficiency at the design point, expressed as the thermal power collected per unit mirror area in Table 13.

The linear technologies require significantly less land than tower and have the additional benefit of flexible arrangement of their modules on the available land, while tower solar fields are less flexible in terms of the solar field shape.

Comparing these land requirements to the land available around the reference facility, there is clearly enough land available for the size of a large-scale CST plant. However, the preferred site to the southwest of the refinery, site 1, would likely only be able to accommodate a large-scale system of the trough or Fresnel technologies. A large-scale tower system with TES would likely have to be built on site 3, which is further away from the refinery. Civil works would likely be required in this case to make enough space for a heliostat field.

Table 13. Mean land cover factors and required land areas for pilot and large-scale CST systems. Land area ranges are for systems with 0 to 14 hours of TES.

| Technology | Land cover factor | Optical performance at design, kW _{th} /m ₂ | 20 MW _{th} | 392 MW _{th} |
|------------|-------------------|---|----------------------------|--------------------------|
| Trough | 34% | 0.68 | 0.091-0.25 km ² | 2.2-6.3 km ² |
| Fresnel | 64% | 0.63 | 0.06-0.14 km ² | 1.1-3.2 km ² |
| Tower | 21% | 0.58 | 0.34-0.64 km ² | 4.7-12.3 km ² |

Parabolic trough systems are modular, with the troughs occupying narrow rectangular areas of land running in north-south orientation and tracking the sun from east to west through each day. This allows for efficient use of areas of land that are shaped approximately in rectangles. This would require the land to be levelled, which is included in the costing as site preparation on the basis that no unusually difficult issues will arise.

The tower systems are less modular than trough systems and need to conform approximately to the shape of the optimised heliostat field, which results in a challenge in fitting large tower plants on restricted land areas. The site for the large heliostat field may require some stabilisation of residue storage areas, but it is possible to relocate groups of heliostats to neighbouring areas to vacant land between the pilot and large heliostat fields without significantly impacting on plant performance.

9.6.3. O&M requirements / manning levels / relationship to ongoing operations

Although not yet fully evaluated, in contrast to a new standalone CST system, adding a CST system to an existing refinery bears the potential of significant synergies in plant operations. Typically, a CST system requires a team of system operators to monitor and control the system, as well as a team of field operators to clean and maintain the solar field. It is conceivable that the control systems of the CST system (essentially a set of computers with data acquisition and control software and electronics connected to the CST system) be spatially integrated in the existing refinery operations, which could reduce the number of extra staff required to operate the CST system.

There is a wide range of forecasts for staffing levels when developing and operating CSP plants and it varies depending on the country. Furthermore, there will be significant variations depending on the system size, technology type and local supply chains and logistics. There is publicly available data from CSP plants developed in the US over the last few years that provides a good overview for different technology types including solar tower and parabolic trough and sizes ranging between 50-390MW_e (100-1,000 MW_{th}).

Using Estela and ESMAP data an assessment has been undertaken comparing the jobs created during the construction and operation phase for the different CSP plants (including both tower and trough plants). The plant construction and operation jobs per unit of energy (here electricity) produced are plotted in Figure 55. The trend lines show how clear scale effects in the number jobs created by a CST plant. The scale effects are more notable for the construction employment than for the operation. Based on this data, a large scale (392 MW_{th}, corresponding to around 150 MW_e) CST system would create approximately 1,000 jobs during construction and require around 150 staff for O&M.

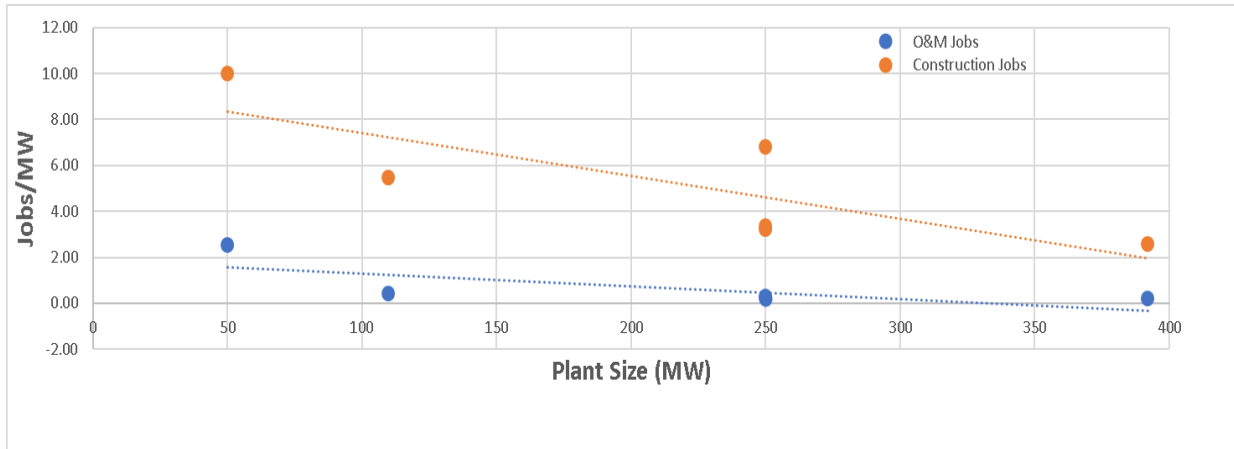


Figure 55: Construction and O&M jobs created by CST systems per unit of installed capacity (here electricity) as functions of plant size (MW_e).

9.6.4. Construction time

Typically, a 100MW_{th} trough plant takes approximately 18 months from ground breaking to connection. First of a kind projects that represent new technology configurations typically take up to twice as long as this and also have much more extended commissioning and de-bugging phases.

In addition to this, proponents need to factor in the time required for approvals and to reach financial closure, which can be extensive. Figure 56 gives an indicative timeline for a 150MW_e/400MW_{th} trough plant project.

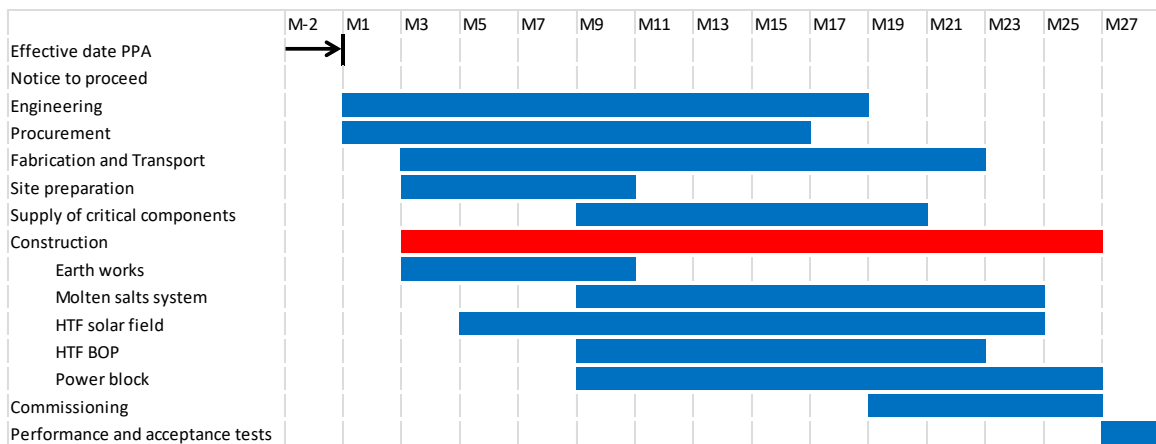


Figure 56: Exemplary CST project timeline for a 150 MW_e/400MW_{th} plant (redrawn from Aries for the Ouarzazate project (2012)).²⁶

²⁶ https://www.esmap.org/sites/default/files/esmap-files/ESMAP_IFC_RE_Training_Aries_Ingenieria_Sistemas_Perez.pdf

9.6.5. Requirements during construction

During construction of a CST system, the implementation company will require certain contributions from the client that would be expected to include:

- Land area and eventual leveling
- Consumables such as water and electricity
- Storage facilities, nearby storage and open laydown area
- Security fencing and security personnel
- Site lighting
- Personal facilities such as toilet, bath, changing rooms, dining facilities etc.

9.7. Environmental impact

9.7.1. Glare

Although routinely dealt with in large-scale CST plants, misalignment or defocussing of heliostats or secondary reflections can result in a glare hazard in the surroundings of a CST system, particularly in case of tower plants. Hence, a safety gap between solar field and any surrounding roads or houses should be allowed for. Exact safety distance depends on a number of factors and should be determined in the framework during the engineering stage.

9.7.2. Impact on local flora, fauna and communities

Past CST projects have suffered from delays and associated high costs due to required relocation of local protected fauna. Hence, it is good practice to ensure from early on that the land is available and free of protected species, or that appropriate relocation plans are implemented prior to construction start. The acceptance of new large-scale technology by local communities may also impact the construction process of a new large-scale plant. Appropriate communication with the local community and council and collection of feedback should also be conducted from the early stage of a project.

9.8. Discussion and Recommendations

9.8.1. Economics

We have collected and used recent cost data (from period 2016-2018) for the main components of a CST system for process heat (solar field, thermal storage and balance of plant) for all the main commercial CST technologies (trough, tower, Fresnel) from several sources (technology suppliers, NREL SAM cost model, public data). We have estimated the annual thermal power output and costs of CST systems at the reference location, WA, for both small (20 MW_{th}) and large (392 MW_{th}) CST plants with thermal storage capacities covering the probable range from 0 to 14 full-load hours and optimised solar field size (for given rated power and storage capacity).

Based on our results, we conclude that, at present, there is no CST system configuration for the reference location with a lifetime of 20 years that would meet the economic criterion of NPV>AUD20m with a WACC of 5% for a 20 MW_{th} pilot system and 12% for a 392 MW_{th} large-scale system. Highest NPV of \$16m is estimated for a large-scale trough system without TES, based on today's low cost estimations.

There are several scenarios in which a CST system is likely to achieve the target of NPV>AUD20m target.

Future cost reductions. CST is still a relatively new technology and has experienced rapid cost reductions over the past several years, despite relatively slow uptake of the technology by the market. However, several major CST projects are currently underway worldwide which will further advance the technology along its experience curve. In addition, CST technology is currently receiving a major boost through new public R&D funding initiatives, such as the recently finalised USD72m CSP Gen3 funding round by the US Department of Energy.²⁷ With a moderate learning rate of 15% cost reduction per doubling of installed capacity and growth rate of installed capacity estimated based on current projects underway, we predict a reduction in CST costs of about 20% by 2023. This cost reduction leads to an approximately 20% reduction in LCOH and an increase in all NPV and IRR results, with the highest predicted NPV value of AUD 46m obtained for a 392 MW_{th} trough system without TES (Figure 45).

Lower solar share. The current project requirement is to reach a solar share of 29–45%. CST systems with TES are readily capable of reaching this target range. However, our results clearly show that LCOH decreases and hence the economic viability (NPV and IRR) improves with decreasing TES size. A TES helps increase the availability of a CST system²⁸ and improve its controllability. However, a TES does not add any extra energy generation capacity to the system, while it does add extra costs. As a result, adding TES capacity generally leads to increasing

²⁷ <https://www.energy.gov/eere/solar/generation-3-concentrating-solar-power-systems-gen3-csp>

²⁸ A TES improves the number of operating hours of a CST system per day and its dispatchability, i.e. the flexibility of when energy is supplied. However, a TES does not reduce the variation in thermal output of a CST system over the course of a year (from month to month).

thermal energy costs.²⁹ Reducing the solar share requirement would allow taking into consideration CST systems with smaller TES that could nearly match the NPV target set in this project, based on today's lowest cost estimates at the reference location (Figure 28).

Better plant location. Compared to the sunniest locations in Australia, the solar resource at the reference location, WA of around 2000–2100 kWh/m²/year is relatively low. Regions in Australia with the highest solar resource reach up to 40% higher solar resource than at the reference location. An increase in the solar resource leads to a correspondingly higher energy output by the CST system, or to a corresponding reduction in total installed costs. To illustrate the benefit of a location with very good solar resource, we have presented results for a CST system in Learmonth WA, showing that with today's costs, a large-scale (392 MW_{th}) CST plant with a TES size between 0 and 14 hours would be likely to meet the NPV>AUD20m requirement and could lead to IRR values of up to 20% (Figure 53).

O&M cost reductions. Potential reductions in O&M costs may be achieved through synergies between the operations of the existing refinery and the CST system and as a result of innovations in the plant operation and maintenance. To illustrate the impact of the O&M costs on the economics of large-scale CST systems, we recalculated the results for the reference location by excluding O&M costs from the analysis. These results show that cost reductions in the O&M costs can reduce the LCOH by up to around 6.5–11% (Figure 46–Figure 47).

Higher natural gas price. The NPV results are sensitive to the cost of natural gas displaced with the CST system. Even a 10 or 20% higher gas price than assumed in this study could tilt the analysis for certain cases towards feasible economics. Similarly, a slight decrease in the gas price could be enough to render a previously viable CST system uneconomical.

Additional factors that may improve the economics of a CST system include: *i)* longer system lifetime (25-30 years), *ii)* lower WACC and *iii)* additional income from large generation certificates (LGCs).

Comparing the three different CST technologies (trough, tower and Fresnel), we find that the two linear technologies (trough and Fresnel) tend to show similar economics. Trough shows somewhat better economics than Fresnel for systems without TES. But for all cases with 8 or 14 hours of TES, both at the pilot and large scales and with both average and low-cost estimates, trough and Fresnel perform almost identically. There is no clear distinction between the two technologies in terms of their economics.

Economic performance of tower technology is somewhat distinct from the two linear technologies. Based on average cost estimates, tower technology leads to better economics (in terms of LCOH and IRR) compared to linear systems, mainly due to its higher annual thermal output (and hence

²⁹ The situation is different here compared to a CST power plant, where the power block and balance of plant represent a major share in the total plant costs and the overall system economics may improve through the addition of a TES due to the higher utilisation of the power block and balance of plant.

higher capacity factor), except for a small system size of 20 MW_{th} without TES, where tower showed a deterioration in thermal performance. On the other hand, using our low-cost estimates, the linear technologies result in significantly better economics than tower. So much so, that with an IRR expectation of 5%, a 20 MW_{th} trough or Fresnel pilot system with up to 8 hours of TES may be feasible at the reference location without any or with only a small (<AUD 2m) financial grant (Figure 30a).

9.8.2. Technologies and suppliers

Technology status and maturity. To date, trough technology is by far the most mature and most proven of the three CST technologies. Experience with trough plants dates back to the 1980s and currently 85% of all CSP plants (for power generation) use trough technology. However, there has been a shift in interest towards tower technology in recent years, primarily due to its ability to reach significantly higher temperatures than trough. In addition, tower technology suffers less from cosine optical losses than trough and Fresnel and therefore generates a higher and more uniform thermal output over the course of a year. Current forecasts indicates a higher deployment rate of tower than trough technology in the coming years. In addition, tower technology is currently receiving the highest priority in R&D, both in Australia and internationally. The increasing deployment and R&D efforts in tower technology, together with its lower maturity may mean that tower technology costs will decline more rapidly in the coming years than those of trough and Fresnel. On the other hand, tower is a less proven technology than trough and therefore may be considered as a higher risk investment. So far, Fresnel technology has only taken a few percent of the CSP market and no new large-scale projects are currently under development. There is one major CSP project in the world using Fresnel technology (Puerto Errado 2) that is currently fully operational, in addition to several smaller projects. This project has had positive coverage. In Australia, Fresnel technology has had a short appearance in the solar boost projects at Kogan Creek and at Liddell power station, which however are both not operational.

Molten salt heat transfer fluid. One shortcoming with trough and Fresnel technology is that both technologies can only be operated at temperatures of up to 500°C when molten salt is used as a heat transfer fluid. However, there are no large-scale reference systems in the world to demonstrate the technical feasibility of using molten salt in trough or Fresnel collectors. Both trough and Fresnel collectors have been tested with molten salt at the pilot scale, however, due to the lack of operational data, salt-based trough and Fresnel systems must be considered as technologically unproven.

9.8.3. Way forward

While a CST system at the reference location is not fully economically viable at the moment based on the given investment criteria, there are configurations where positive IRRs and NPVs are possible. This is likely to further improve within the next few years. It may take several years to develop, build and fully evaluate a pilot CST system, before a large-scale system can be

planned. Hence, it may be a good time now for further investigation and for the development of a demonstration project. Solar thermal process heat for industrial applications is one of the main priorities of the Australian Renewable Energy Agency and the climate to receive a grant to co-fund a first-of-its-kind demonstration plant for solar process heat in Australia is favourable at the moment.

When planning a CST system, it should be kept in mind that the economics improve with increasing lifetime of the CST system. Existing CST systems such as the SEGS III to IX plants in California have been operating for up to 30 years.³⁰ Hence, CST projects should ideally be projected for at least 25-30 year. Other major factors that impact the economics are the plant location (solar resource), date of construction (future cost reductions), plant size (scale effects in total installed and O&M costs), natural gas price and WACC. Concessional loans as offered by the Clean Energy Finance Corporation may be one way of reducing the WACC for the project.³¹ A steam off-take agreement with a renewable energy provider may be another potential path to pursue. Finally, an actual bidding round may bring forth lower bids than in our initial non-binding Request for Information.

³⁰ https://www.nrel.gov/csp/solarpaces/project_detail.cfm/projectID=30

³¹ <https://www.cefc.com.au/enquiries/faqs/#2287>

10. MECHANICAL VAPOUR RECOMPRESSION

Previous work has indicated that a CST system configured for replacement of the 470°C/80 bar steam currently produced by gas fired boilers has good potential to offer a positive IRR. It is however unlikely to meet the IRR hurdles for investment. It will also only offer a partial (although significant) replacement of gas fired steam production. Nonetheless this is encouraging and offers the possibility of progressing a project by offering an offtake agreement for steam and awarding this based on a competitive process among consortia who could build own and operate such as system on the back of an offtake agreement.

Before considering this further, other technological options for de-carbonising the low temperature side of the process are considered. There are no plausible geothermal or bioenergy resources that might readily be used at large scale at the reference location. A strong plausible contender however is mechanical vapour recompression (MVR) of the low-pressure steam that exits the system. Mechanical vapour re-compression can be driven by renewable electricity from the grid.

The MVR option has been analysed in detail for comparison with CST options.

10.1. Overview of MVR

Mechanical vapour compression can be used when a process requires steam to drive it and has a waste vapour stream at another point that is at lower pressure and temperature than the process requires. The waste vapour can be compressed to raise its condensation temperature and pressure to that required by the process. The units themselves are essentially steam turbines operating in reverse with electric motor drives. Overall the system is a vapour compression heat pump using steam as the working fluid and using the waste heat stream as the heat source. Low pressure steam has little thermodynamic value of its own but it embodies large amounts of enthalpy from the presence of water in the vapour phase.

The basic principles and their application to industrial processes are review in an information sheet produced by the US Department of Energy³².

It is suggested that MVR typically requires around 5% to 10% of the energy required to raise an equivalent amount of steam in a boiler. A pressure ratio of less than 2 can be expected from a single stage compressor, so multi stage system would be required for more substantial increases. Adiabatic compression of close to saturated steam increases the amount of superheat as the pressure is increased. If the overall goal is to increase steam pressure and achieve steam at

³² <https://www.energy.gov/eere/amo/downloads/use-vapor-recompression-recover-low-pressure-waste-steam>

close to the new saturation temperature, multistage compression is used with water injecting desuperheaters applied to lower the temperature to just above saturation at each pressure stage.

Howden turbo fans are an example of a specialist provider of MVR systems³³.



Figure 57. Single stage MVR unit from Howden.

10.2. Application to reference refinery

MVR is analysed here as an option for steam production, integrated into the existing energy supply system at the reference facility.

³³ <https://www.howden.com/en-gb/applications/mechanical-vapor-recompression-mvr>

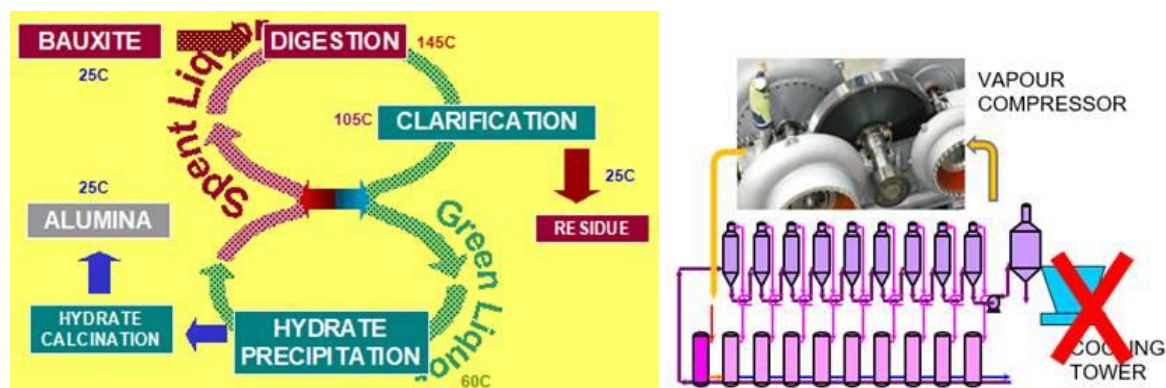


Figure 58. Schematic on introducing MVR to digester train.

At present, process steam is injected to the highest temperature digester unit and then a sequence of flash tanks cascades steam down in temperature and pressure heating each progressively lower temperature digester in turn before finally exiting for condensation in a cooling tower for return to the boilers. In an MVR scenario, the cooling tower is removed and the lowest pressure steam is to be recompressed to the pressure of the process steam input for re-injection.

It is assumed that MVR generates steam suitable for direct input to the digestion process, at conditions of approximately 215°C and 8.9 bar.

Note that MVR would not be suitable to generate steam at 80 bar and 470°C for input to the steam turbine. Effectively, this would mean that steam is compressed by an electrically driven compressor followed by expansion in the steam turbine back to the digester conditions, which would not result in a gain in power generation compared to generating steam for direct input to the digestion process.

MVR is compared to solar thermal steam generation from feedwater at 80 bar and 120°C, heated to 470°C. This is considered the preferred process for use of CST, as the technology is readily able to achieve 470°C. Using CST to generate steam at 215°C would result in only marginally lower costs of steam produced, while resulting in a substantial decrease of the steam turbine power output.

It should be noted that MVR is a potential option when there is low grade steam in the process that can be upgraded which would otherwise be lost to the environment. On the other hand, solar thermal energy is applicable to generate steam via evaporation of compressed feedwater. Hence, the two technologies are not necessarily mutually exclusive, as their applications are different. They may be used side-by-side, depending on the availability of upgradable low-grade steam and the process steam requirements.

- Solar thermal energy as a substitute for natural gas currently used in gas boilers to generate steam has been analysed previously. Here we describe the analysis of MVR applied to low-grade steam and compare the economics of the two approaches.

MVR systems have been investigated with equipment suppliers for a range of conditions and established model for estimating installed cost.

Further, 160,000m³/h is considered near the upper limit on inlet volume flow so for flows above this, multiple units in parallel will be required.

For the reference refinery, the parameters in Table 14 have been collected and used to analyse the thermo-economics of MVR.

Table 14. Input parameters for MVR system analysis.

| Parameter | Value | Source/comments |
|------------------------------------|--|---------------------------|
| Steam inlet conditions | 52°C/0.136 bar (sat) | Internal communication |
| Steam outlet conditions | 215°C/8.92 bar (175°C sat) | Internal communication |
| Exit Steam generation rate | 500 tph / 4.38 million tpy | Based on existing boilers |
| Operating hours of MVR system | 8322 h/a | 95% capacity factor |
| Pressure ratio below 1 bar | 1.35 | Supplier information |
| Pressure ratio above 1 bar | 1.95 | Supplier information |
| Isentropic efficiency below 1 bar | 80.5% | Supplier information |
| Isentropic efficiency above 1 bar | 88% | Supplier information |
| Overall drive efficiency | 95% | Supplier information |
| Lifetime | 20 year | assumption |
| Construction start/time | 2020/1 year | assumption |
| WACC | 12% | assumption |
| Natural gas price (real, constant) | 10 \$/GJ-HHV (0.0439 \$/kWh-th) | assumption |
| Fixed O&M cost | 2% capital cost/year | assumption |
| Gas boiler efficiency | 82% | Internal communication |
| CO ₂ emissions costs | 29 \$/tCO ₂ in 2020 to 131 \$/tCO ₂ in 2050 (0.0065 to 0.03 \$/kWh-th) | Internal communication |
| Electric energy cost | 0.07 to 0.12 \$/kWh-e | Variable parameter |

10.3. Analysis

MVR replaces steam generation in the gas boilers and hence mitigates costs related to gas consumption and CO₂ emissions. On the other hand, an MVR system incurs an upfront capex, yearly opex (currently neglected) and yearly electric energy costs to run it. In addition, an MVR system would result in a reduction in the steam mass flow through the steam turbine and hence in the steam turbine system power output. This loss in power generation is assumed to be replaced with additional electricity purchases from the grid.

10.3.1. Reduction in steam turbine power output

Nominal (full load) steam turbine mass flow rate is 900 tph, resulting in a power output of around 130 MW-e (net), assuming a full-load isentropic turbine efficiency of 95%. If the steam flow rate through the turbine is reduced, the power output decreases, i) due to the lower mass flow rate, ii) due to reduced part-load turbine efficiency. The change in efficiency is estimated based on the following equation (Patnode, 2006):

$$\eta_{part\ load} = \left(1 - \left(0.191 - 0.409 \left(\frac{m}{m_{ref}} \right) + 0.218 \left(\frac{m}{m_{ref}} \right)^2 \right) \right) \eta_{full\ load}$$

At a reduced mass flow rate of 400 tph, the part load isentropic efficiency is 90%. The power output is reduced to 55 MW-e, a reduction of 75 MW-e.

This results in the requirement for additional electricity purchases of \$46.0 to \$78.8 million pa. (depending on electricity price) to replace the loss in power output from the steam turbine. These additional costs are taken into account in the NPV and IRR calculations for MVR.

10.3.2. Gas and CO₂ emission cost savings

Thermal power demand to generate 500 tph of steam at 80bar/470°C from compressed feedwater at 120°C—the current process in the gas boilers— requires 392 MW-th, or 3.4 GWh-th/a (12.7 million GJ/a).

In addition to the fuel costs, it is assumed that CO₂ emissions from natural gas combustion in the gas boilers will be taxed in future. The CO₂ emission costs are estimated to range from 29 \$/t in year 2020 to 131 \$/t in 2050 (Australian Treasury modelling), corresponding to a range of 0.0065 \$/kWh-th to 0.03 \$/kWh-th.

10.4. Results and Discussion

Table 15 and Figure 59 summarise results of the thermo-economic analysis of MVR, based on the input parameters in Table 14. The unit (levelized) cost per ton of useful steam (LCOS) at 8.9 bar /215°C produced with MVR increases approximately in proportion to the increase in electricity price, from 6.6 \$/t at 0.07 \$/kWh-e to 11.1 \$/t at 0.12 \$/kWh-e. For comparison, gas related costs (fuel and CO₂ emission costs) to produce steam at 80 bar / 470°C are 43.4 \$/t (avg. over period

2021 to 2040). Note that these LCOS results do not include the indirectly incurred costs to replace the loss in power output from the steam turbines. Alternatively, those additional electric energy costs could be factored into the LCOS for MVR.

The NPV for MVR is strongly positive, as the electric energy costs incurred are substantially lower than the mitigated gas-related costs, while the capex is negligibly small compared to the energy-related costs.

Due to the relatively small upfront capex and the large gas-related cost savings, the IRR is strongly positive, ranging from 169% at an electricity cost of 0.12 \$/kWh-e to 259% at 0.07 \$/kWh.

Table 15. Results from MVR system analysis.

| Parameter | Value | Source/comments |
|--|-------------------------------|--|
| Inlet massflow | 389 tph | Combines with de-superheat water to give 500 tph at exit |
| Number of stages | 10 | |
| Pressure ratio stages 1 - 6 | 1.35 | Limit for low p stages |
| Pressure ratio stages 7 | 1.52 | Adjusted to give final p=8.9b |
| Pressure ratio stages 8 -10 | 1.95 | Limit for high p stages |
| Electric power input to MVR | 115.35 MW-e | |
| Effective thermal power | 385.25 MW-t | Relative to 20°C water |
| Total MVR installed cost | \$482m | |
| Annual electric energy consumption of MVR | 960 GWh-e/a | |
| Electricity cost for MVR | \$67.2 to \$115.2 million pa. | at 0.07 to 0.12 \$/kWh-e |
| Loss in steam turbine power output | 75 MW-e | |
| Annual electric energy loss from steam turbine | 606 GWh-e/a | |
| Electricity cost for ST loss | \$42.4 to \$72.7 million pa. | at 0.07 to 0.12 \$/kWh-e |
| Levelised cost of steam (\$/t) | 33.88 to 45.4 \$/t | at 0.07 to 0.12 \$/kWh-e |
| Levelised cost of steam (\$/GJ) | 12.2 to 16.4 \$/GJ | at 0.07 to 0.12 \$/kWh-e |
| Net present value | -\$21.8 to -\$606 million | at 0.07 to 0.12 \$/kWh-e |
| Internal Rate of Return | 11% to negative | at 0.07 to 0.12 \$/kWh-e |

For comparison, the IRRs are compared for MVR and solar thermal. Generating 500 tph of steam at 470°C/80bar from feedwater at 120°C requires around 392 MW_{th}, corresponding to 2.82 GJ/t.

The energy costs of CST depend on technology, TES size, timing and cost model assumptions made. Here we use tower technology with i) 14 hours of storage, year 2018 average costs, ii) no TES, lowest cost estimates for year 2023. For NPV and IRR calculation, NG price is assumed to be 10 \$/GJ-HHV.



Figure 59. IRR for MVR compared to 2 CST tower configurations.

It is apparent that the MVR system has the same IRR value as a CST plant with no storage at an electricity cost of .066\$/kWh and as a plant with 14 hrs of storage at an electricity cost of .083\$/kWh.

This range of electricity cost is approximately the cost seen for electricity at present so the technologies by this comparison are economically comparable.

10.5. Next steps

To fully assess the comparison of the MVR vs CST options, a projection of the costs of renewable electricity needs to be considered. This is a complex issue. It can be observed that many studies are beginning to indicate that average renewable electricity costs in a 100% RE scenario may be very close to the same average price as present. There are further complexities however as the increasing penetration of PV and wind is likely to see wholesale prices fall to quite low levels when such generation is at high levels but rise significantly when it is not. This will be investigated further.

A possibility that may prove to be optimal is reducing the capacity factor of operation of an MVR system to cover only those hours when electricity costs are low and constructing a CST system with storage to deliver its energy at times when the price of electricity is likely to be highest.

When this analysis is complete, further steps are dependent on the assessment of the overall attractiveness and if and how it might consider going to market to obtain binding offers with more certainty than the present cost estimates.

11. CONCLUSIONS

For Program 1 of the present project, we have considered possibilities of integrating concentrated solar thermal energy into the low-temperature stage of the Bayer alumina process. Based on the steam demand of the reference refinery, we have defined several CST system design options. We have received preliminary cost estimates from suppliers for linear (through and Fresnel) CST technologies, while for point-focussing tower systems, none of the large technology providers responded with cost information. Supplier data has been complemented with cost models from the NREL System Advisor Model (SAM) which also provides a basis to estimate a cost breakdown for the major cost components of the plant.

The available data has been used to derive size-dependent component cost models for solar field, thermal energy storage and balance of plant. These models were used in SAM to estimate economic performance for pilot and large-scale CST systems. SAM can be used to calculate the annual thermal power generation of CST systems and the total installed costs of each system configuration. The results have been used to evaluate the economic feasibility of a CST system for steam generation at the reference location.

While configurations with positive NPV could be identified, none of the CST system configurations studied for the reference location reached the economic target of $NPV > AUD20m$ with WACC of 12% and today's cost estimates for CST. The values of IRR were estimated to be in the range of around 3.5-7% based on the average costs provided by suppliers and 6-13.5% based on the current low-costs provided by suppliers, depending on thermal energy storage size and CST technology. Several factors, including further CST cost reductions in the coming years and better solar resource, have been identified with strong potential to lead to greatly improved economics for future systems. To illustrate the effect of solar resource on the CST system's economic performance, we repeated our analyses for the location of Learmonth, WA, which receives very high solar resource. For this location, NPV values of AUD97m and IRR of 19.7% have been predicted even with today's CST costs.

The three main CST technologies showed comparable economic performance, although the tower system offers the highest solar contribution to the total energy. Very similar economic performance was obtained for trough and Fresnel, while tower technology tends to result in somewhat better economic figures than the linear technologies, under current average cost estimates. If low cost estimates are used, significantly better economics are obtained with linear systems, however with less established technology.

In addition to the economics, we have considered several additional aspects in our feasibility analysis, including available technology suppliers, resource requirements and environmental impact.

Based on our comprehensive analysis, we conclude that:

- 1) Although a large-scale CST system at the reference location would currently not meet the economic requirements for investment for a typical alumina producer, it could nonetheless potentially be built with a positive IRR, even with the cost estimates from present technology.
- 2) Better CST system economics are expected in the future due to ongoing reductions in CST costs (capex and opex), better plant location, lower solar share, longer projected system lifetime, higher gas price and lower WACC. These factors, individually or combined, are likely to yield attractive economics for a CST system.
- 3) Some level of thermal energy storage capacity (≥ 2 hours) is considered to be likely to be necessary to allow an operator to manage the inherent variability of solar energy. Furthermore, significant thermal storage will be essential to capitalise on the opportunity identified to offer greatest potential to operate with 100% renewable energy - that of a hybrid with an MVR system operated from a renewable electrical network.
- 4) Land and resources at the reference location would be appropriate for construction of a pilot followed by a large-scale CST system.

Based on the outcomes of this initial study, we conclude that further investigation into the integration of a CST system for the Bayer process is warranted and we recommend that further analysis be conducted.

Potential alternative renewable technology options besides CST for steam generation have been screened. While the potentials of bioenergy and geothermal have been deemed low for this large-scale application, mechanical vapour recompression of waste steam currently discarded at around 53°C and 0.14 bar, driven by renewable grid electricity, has been identified as a potentially viable alternative, although further development of this technology is considered to be necessary to meet the requirements of an alumina plant.

Consequently, an economic analysis of MVR has been conducted, via performance modelling and cost estimations based on up-to-date supplier data. The cost and the economics of MVR strongly depend on the assumed average electricity price over the plant operation life. If a reduction in future average electric energy prices to below ~7 c\$/kWh can be achieved, MVR may be more economical at the reference location in the short- to mid-term than current CST costs. On the other hand, above around 8 c\$/kWh, CST with storage may be more cost effective than MVR even at today's costs of CST energy at the reference location.

Electrically driven grid connected MVR can potentially offer higher potential renewable contributions than an on-site CST system alone. For full renewable operation it seems likely that an optimised combination of the two will offer the best financial performance. Further work to analyse this approach is recommended.

APPENDIX A. STEAM GENERATION HEAT EXCHANGERS

The steam generation heat exchangers are not included in all cost estimations from vendors. Therefore, we derive the approximate costs for a heat transfer fluid (HTF) to water/steam heat exchanger train here. It is assumed that feedwater preheating, evaporation and superheating (for high-temperature steam) are conducted in separate units, as shown schematically in Figure 60. HTFs are assumed to be oil and molten salt for low and high temperatures, respectively.

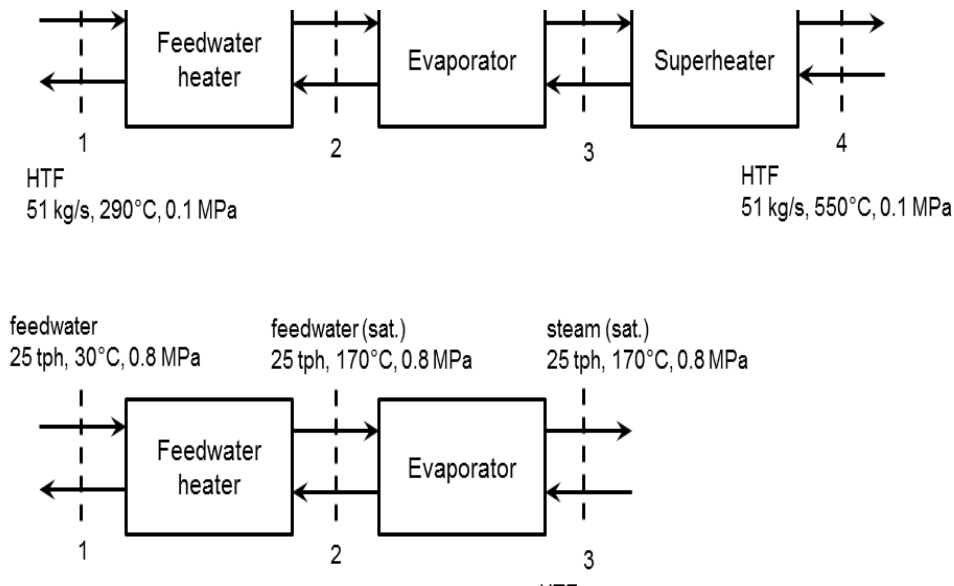


Figure 60. Schematic of layout and modelling assumptions for steam generation heat exchanger design calculations (top: high-temperature steam; bottom: low-temperature steam). State points are numbered (1, 2, 3, ...).

Intermediate HTF temperatures are found from equation:

$$\dot{Q} = \dot{m}_c (h_{c,o} - h_{c,i}) = \dot{m}_h c_{p,h} (T_{h,i} - T_{h,o})$$

Water/steam state points are known and HTF mass flow rates and specific heats are determined based on SAM simulations for 20 MW_{th} systems. Required heat transfer areas are estimated based on:

$$\dot{Q} = UA\Delta T_{lm}$$

where ΔT_{lm} is the log-mean temperature difference and overall heat transfer coefficients are estimated based on data available in Seider, 2009³⁴, to be 1 kW/m²/K for preheater and evaporator and 3 kW/m²/K for superheater. Heat exchanger costs are then estimated based on the heat transfer areas for floating head shell-and-tube heat exchangers, including cost factors for material (Monel, corrosion resistant Ni-alloy) and pressure. Finally, costs are updated from their 2006 cost base (CI cost index 500) to 2017 (CI cost index 567) and converted from USD to A\$ (USD/A\$ = 1.31391; 2017-11-28). The resulting heat transfer areas and heat exchanger costs are summarised in Table 16.

Table 16. Estimated heat exchanger areas and costs for the pilot-scale CST system design variants 3, 4, 7 and 8 in Table 2.

| CST design variant | Preheater | Evaporator | Superheater | Totals |
|-----------------------|--------------------|--------------------|------------------|--------------------|
| 3, 4 (470°C, 8 MPa) | 44 m ² | 62 m ² | 9 m ² | 115 m ² |
| | A\$156,000 | A\$172,000 | A\$130,000 | A\$458,000 |
| 7, 8 (210°C, 0.8 MPa) | 122 m ² | 582 m ² | - | 704 m ² |
| | A\$158,000 | A\$394,000 | - | A\$552,000 |

³⁴ Seider et al., *Product and Process Design Principles*, 3rd ed., 2009.

APPENDIX B. COST MODELING

B.1. Methodology

Cost data sources used to derive cost models include:

- data obtained from technology providers
- internal data
- SAM default cost data (v. 2017.9.5)
- recent study by H. Price, 2017 (lead: Solardynamic LLC) on behalf of US Sunshot, for a solar thermal peaker plant

Cost information has been obtained with varying levels of detail, ranging from one-line cost quotations to detailed breakdowns of component costs. In addition, quoted cost data was based on varying system sizes, thermal storage capacities, operating temperature ranges, design DNI, etc. s

Subject of this section is the consolidation of the received data and information for each main system component in order to bring it onto an equal basis for comparison purposes and to determine size scaling law model parameters.

B.1.1. Data consolidation

The CST system is divided into the main system components:

- Solar field
- Thermal energy storage
- Balance of plant

Cost data is divided into these three categories. Indirect costs are not included in these component cost models; they are added as an additional 25% to the direct component costs. Where the scope of the balance of plant did not include the steam generation heat exchangers, they were added in according to the estimations in Appendix A.

The received cost data was adjusted for the following parameters:

- Currency
- Operating temperature range
- Design DNI

Currencies were converted as: USD/AUD = 1.333, EUR/AUD = 1.6.

The operating temperature range of the solar field influences its collection efficiency. For linear collectors (trough and Fresnel), the efficiency curve of a parabolic trough evacuated tube receiver is used to convert the quoted design solar field output at the design temperature range used in the quote to the design temperature ranges used in this project. For tower systems, the blackbody efficiency at the HTF outlet temperature from the receiver is used as temperature correction. For low- temperature (0.8 MPa, 210°C) and high-temperature steam (8 MPa, 470°C), the solar field operating temperature ranges were set to 200-300°C and 300-500°C, respectively (section 5.2). The solar field design output is additionally corrected by the design DNI. The design DNI is set to 950 W/m² in this project.

In addition, the solar field operating temperature range is equal to the temperature difference in the thermal storage and hence influences the amount of storage material required per unit of energy storage, according to:

$$U = c_v \rho V \Delta T$$

Assuming specific heat and density to remain approximately constant with temperature, the required volume of storage material per unit of stored energy scales with $\frac{1}{\Delta T}$. Hence, to a first approximation, it is assumed that the thermal storage capacity is inversely proportional to the temperature difference across the storage system.

The thermal storage cost is mainly due to the storage material with a minor fraction due to the container, valves, etc. Further assuming the cost of the storage material to scale linearly with its volume (i.e. zero economies of scale; see size law analysis below), the thermal storage costs then scale inverse-proportionately to the temperature difference across the storage system. Quoted thermal storage costs are adjusted accordingly for the above design operating temperature ranges.

After the above adjustments, unit solar field cost data are initially expressed in AUD per MW_{th} of design solar field thermal output and grouped according to collector type: trough, Fresnel, tower. For linear concentrators, solar field costs include costs for concentrator, receiver and HTF system (incl. HTF). For tower systems, solar field costs include costs for heliostats, tower and receiver.

Initially, the solar field costs were further grouped according to the design operating temperature range used in the quotation. However, it turned out that there is no clear distinction between collectors aimed to operate at different temperatures (e.g. an oil-based or molten-salt based parabolic trough collector). Hence, this grouping was not further maintained.

Thermal storage cost data was compiled across all technologies – thermal storage technology depends on temperature but is independent of collector technology. Unit costs are expressed in AUD/MWh_{th} (in agreement with SAM input parameters).

Balance of plant costs are used from the quotations for linear concentrators as no specific information for BOP for tower technology could be obtained. As for thermal storage, costs are not expected to depend on the collector technology used. Unit BOP costs are expressed in AUD per MW_{th} of design system thermal output. Note that the solar field output is what the thermal power delivered by the solar field both as output to the user and to the thermal energy storage. In contrast, the system thermal output is the output to the user alone. The ratio of solar field output to system output is the solar multiple.

B.1.2. Reference system

A reference system is defined with the following specifications:

| Reference parameter | Reference unit cost |
|-------------------------------------|---|
| System design thermal output | 20 MW_{th} |
| Solar multiple | 2.5 |
| Thermal energy storage capacity | 300 MWh_{th} / 15 hours |
| Design DNI: | 950 W/m^2 |
| Design operating temperature ranges | low-temperature steam: 200-300°C high-temperature steam: 300-500°C |

Cost models are defined relative to this reference system.

B.1.3. Overview of cost models

Total installed costs are composed of:

$$C_{TOT} = C_{SF} + C_{TES} + C_{BOP} + C_{Indirects}$$

where:

C_{SF} , C_{TES} , C_{BOP} , $C_{Indirects}$ are costs for solar field, thermal storage, balance of plant and indirect costs. Indirect costs cover contingencies, EPC and owner costs and taxes. They are fixed at 25% of the total of $C_{SF} + C_{TES} + C_{BOP}$.

The component cost models for C_{SF} , C_{TES} , C_{BOP} are summarised in Table 17. The exponent x (0...1) of the size-dependence power law reflects the level of economies of scale that can be obtained by increasing a system component; the smaller x , the larger the size dependence and vice versa, with $x = 1$ indicating that there are no size benefits (marginal unit costs of the system component remain constant with size).

Table 17. Component cost models.

| | Reference unit cost | Size parameter | Reference size parameter | Size power law exponent |
|---|--|--|--|--|
| Solar field | | | | |
| $C_{SF} = c_{SF}(\dot{Q}_{SF})\dot{Q}_{SF}$, where: $c_{SF}(\dot{Q}) = c_{ref}(\dot{Q}_{ref})\left(\frac{\dot{Q}}{\dot{Q}_{ref}}\right)^{x-1} \frac{\text{AUD}}{\text{MW}_{th}}$ $\bar{C}_{SF} = \bar{c}_{SF}(\dot{Q}_{SF})\dot{Q}_{SF}$, where: $\bar{c}_{SF}(\dot{Q}) = \bar{c}_{ref}(\dot{Q}_{ref})\left(\frac{\dot{Q}}{\dot{Q}_{ref}}\right)^{x-1} \frac{\text{AUD}}{m^2}$ | $c_{ref}(\dot{Q}_{ref})$: unit solar field cost at reference size, \dot{Q}_{ref} , AUD/MW _{th} $\bar{c}_{ref}(\dot{Q}_{ref})$: unit solar field cost at reference size, \dot{Q}_{ref} , AUD/m ² | \dot{Q} : actual solar field rating, MW _{th} | \dot{Q}_{ref} : reference solar field rating, 50 MW _{th} | $x = 0.9$ (postulated) |
| Thermal energy storage | | | | |
| $C_{TES} = c_{TES}(Q_{TES})Q_{TES}$, where: $c_{TES}(Q) = c_{ref}(Q_{ref})\left(\frac{Q}{Q_{ref}}\right)^{x-1} \frac{\text{AUD}}{\text{MWh}_{th}}$ | $c_{ref}(Q_{ref})$: unit thermal storage cost at reference size, Q_{ref} , AUD/MWh _{th} | Q : actual thermal storage size, MWh _{th} | Q_{ref} : reference thermal storage size, 300 MWh _{th} | $x = 1$ postulated (spec. TES cost independent of size) |
| Balance of plant | | | | |
| $C_{BOP} = c_{BOP}(\dot{Q}_{BOP})\dot{Q}_{BOP}$, where: $c_{BOP}(\dot{Q}) = c_{ref}(\dot{Q}_{ref})\left(\frac{\dot{Q}}{\dot{Q}_{ref}}\right)^{x-1} \frac{\text{AUD}}{\text{MW}_{th}}$ | $c_{ref}(\dot{Q}_{ref})$: unit BOP cost at reference size, \dot{Q}_{ref} , AUD/MW _{th} | \dot{Q} : actual system power rating, MW _{th} | \dot{Q}_{ref} : reference system power rating, 20 MW _{th} | $x = 0.7$ postulated |

B.2. Component cost modelling

B.2.1. Solar field

Linear concentrators

Specific solar field cost data points (in AUD/MW_{th}) for linear concentrators (Fresnel and trough) are shown in Figure 61. No clear distinction can be observed between trough and Fresnel technology. This should not surprise, as the two technologies compete for similar temperature applications on a per unit energy cost basis. Hence, it could be expected that both technologies provide similar unit costs. An initial differentiation into low- and high-temperature cases also did not show a clear differentiation, indicating that there is no significant difference between oil- and molten salt-based systems geared at different temperature levels. Hence, the solar field model was developed without taking the temperature application range of the technology into account.

A distinct group of lower-cost offers has been identified, with specific costs around half of those of other major suppliers at the same solar field size. This clear distinction of these cost data points may have several reasons. It may be a reflection of the companies' more innovative technology

that achieves cost savings compared to the state-of-the-art technology. While state-of-the-art technology may be more proven, novel technology may achieve lower costs, at the expense of a higher technical risk associated. It may be a reflection of different component costs, depending on where they are sourced and with what quality they are associated. It may reflect differences in estimated labour and other local costs. It may also reflect differences in the level of interest in/priority for the project and hence “how hard” suppliers are bidding and hence how conservative their bids are. This may be due to different levels of commercial development of their technologies, differences in the companies’ experience and commercial engagement levels (“how hungry” they are for a new project of this type and scale) and whether and how far into the future they projected their technology’s costs and with what certainty (e.g. new storage medium with much reduced unit costs may be in principle feasible but not yet proven at large scale). For these reasons, we consider the low-cost data points the “best case” scenario for the near future, associated with additional technical and financial risks. These technologies would need to be put through a more thorough trial during the pilot system operation phase than the more mature technologies, to ensure that they perform as expected over an extended period of time.

Two cost models are derived, one that is a fit to all data points, considered as a realistic average estimate of the expected costs, and a model that is a fit to the low-cost data points, reflecting the “best case option”. Using both models in the economic feasibility analysis helps determine how likely it is that a CST system will be economically attractive today or in the near future.

Further, a size-dependence can be observed in the data in Figure 61. The size dependence exponent, x , has been previously determined to be around 0.9 for solar fields and is fixed at this value here. The sole free model parameter is then the specific solar field cost at the reference size, $c_{\text{ref}}(\dot{Q}_{\text{ref}})$. A root mean square minimisation is applied to fit the model curve to the data points, to obtain $c_{\text{ref}}(\dot{Q}_{\text{ref}})$. The resulting models fitted to all data points and to the low-cost data points, respectively, are given in Figure 61 and Table 18.

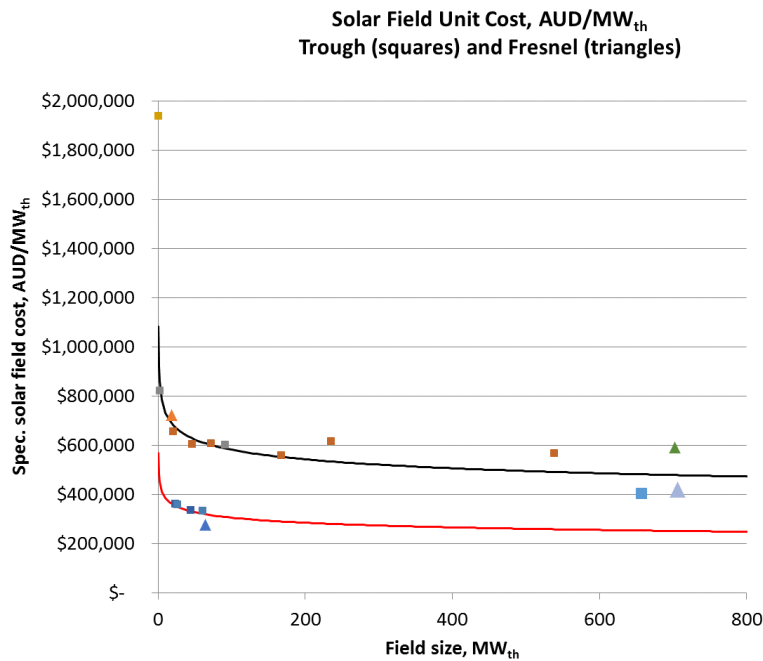


Figure 61. Linear concentrators, specific solar field costs per MW_{th} design output (normalised to T -range 200-300°C).

Table 18. Linear concentrators, solar field model parameters for T -range 200-300°C (AUD/MW_{th}); RMSE: root mean square error.

| Set of data points | Ref. spec. cost, AUD/MW_{th} | Exponent | RMSE |
|----------------------|--------------------------------|----------|-----------|
| All | \$622,586 | 0.9 | \$261,046 |
| Low-cost data points | \$326,361 | 0.9 | \$20,537 |

Solar field unit costs per unit of concentrator aperture area (AUD/m^2 , as required by SAM) are obtained from:

$$\bar{c}_{SF} = c_{SF}\eta_{SF}$$

where η_{SF} is the solar field performance (MW_{th}/m^2) at design. The solar field performance is obtained as the rated solar field thermal output at design divided by the specified solar field size:

$$\eta_{SF} = \frac{\dot{Q}_{SF}}{A_{SF}}$$

The solar field performance for all data points is shown in Figure 62. It can be observed that there is no significant size dependence, as would be expected for linear concentrators. Data for troughs

is scattered over a narrow band with a mean of 0.682 kW_{th}/m² (Table 19). Performance data for Fresnel technology scatters over a larger band, with a deviation of approximately 15% from the mean of 0.631 kW_{th}/m². As would be expected, Fresnel reaches a lower thermal performance compared to trough due to its approximated concentrator optics with increased optical losses compared to troughs.

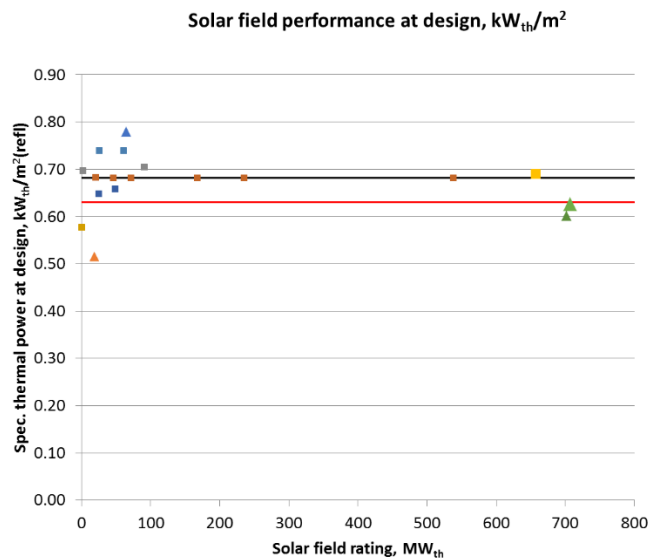


Figure 62. Linear concentrators, solar field design performance at T-range 200-300°C (squares: trough; triangles: Fresnel).

Table 19. Average thermal performance for trough and Fresnel technologies (at T-range 200-300°).

| Technology | Th. performance, avg, kW _{th} /m ² |
|------------|--|
| Trough | 0.682 |
| Fresnel | 0.631 |

The specific solar field costs for linear concentrators per unit of solar field area and model fits to the data are shown in Figure 63 with associated model parameters in Table 20. As a result of the differing thermal performance, a distinction can be made between trough and Fresnel unit costs per m². Consequently, individual models are created for average and low-costs for trough and Fresnel.

Note that specific solar field costs in AUD/MW_{th} depend on the design solar field operating temperature range (as higher temperatures lead to lower thermal output) and design DNI (higher design DNI results in lower AUD/MW_{th}) while costs in AUD/m² are independent of operating temperature and DNI.

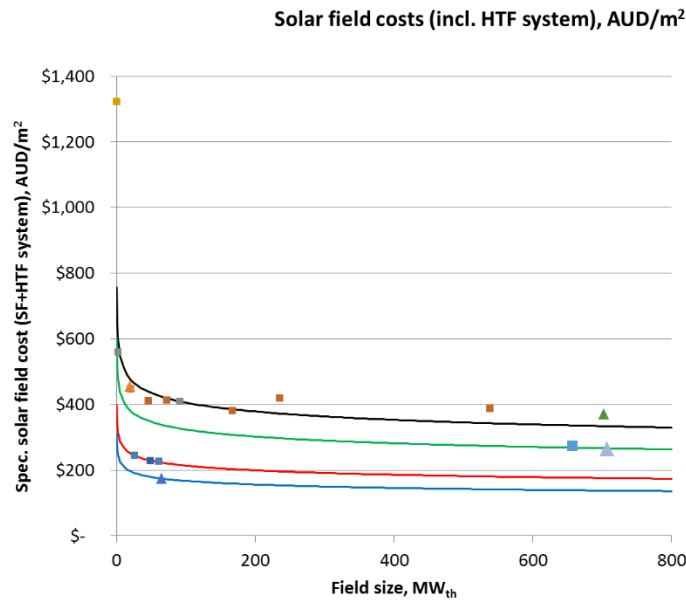


Figure 63. Linear concentrators, specific solar field costs per m² mirror area.

Table 20. Linear concentrators, solar field model parameters (AUD/m²); RMSE: root mean square error.

| Set of data points | Ref. spec. cost, AUD/m ² | Exponent | RMSE |
|--------------------|-------------------------------------|----------|-------|
| Trough, All | \$435 | 0.9 | \$191 |
| Trough, low-cost | \$229 | 0.9 | \$2 |
| Fresnel, all | \$347 | 0.9 | \$104 |
| Fresnel, low-cost | \$179 | 0.9 | \$0 |

Tower concentrators

Available data for tower systems are scarcer than for linear concentrators. Of the six tower technology companies contacted in our RFI, only one data point was received. In addition, component cost data are used from a recent ITP study (basically reflecting the Aurora plant cost), from SAM and from a recent study by Solar Dynamics LLC for the US peak power market. Solar field cost models were generated in AUD/MW_{th} and AUD/m², analogously to linear concentrators.

Average design thermal performance of the tower systems was 0.58 kW_{th}/m² normalised to T-range of 200-300°C). The resulting model curves are given in Figure 64-Figure 65 and Table 22-Table 21.

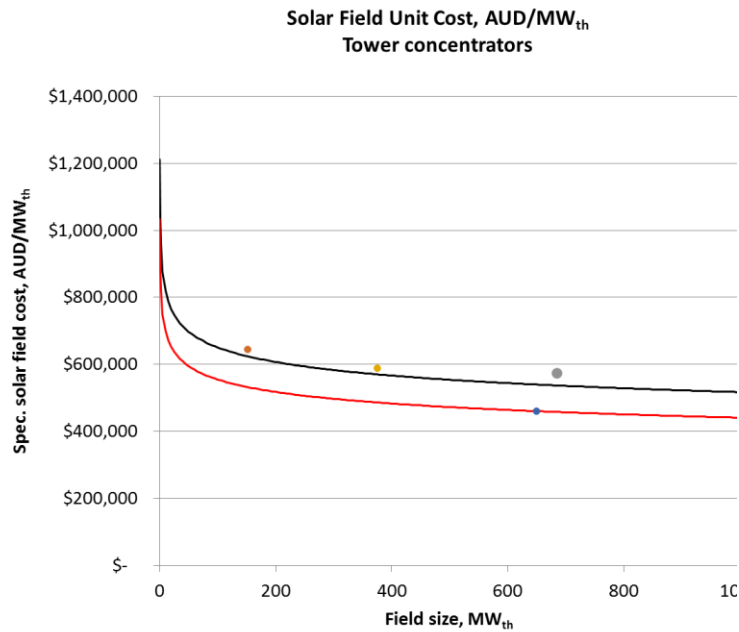


Figure 64. Tower concentrators, specific solar field costs per MW_{th} design output (normalised to T-range 200-300°C).

Table 21 Tower concentrators, solar field model parameters (AUD/MW_{th}) for T-range 200-300°C; RMSE: root mean square error.

| Set of data points | Ref. spec. cost, AUD/MW _{th} | Exponent | RMSE |
|--------------------------|---------------------------------------|----------|----------|
| All | \$697,236 | 0.9 | \$45,934 |
| low cost (Solar Reserve) | \$594,448 | 0.9 | \$0 |

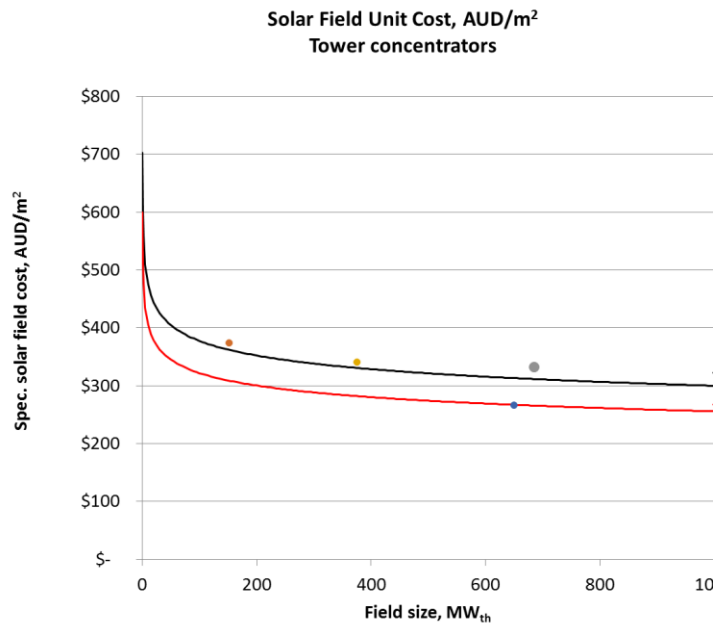


Figure 65. Tower concentrators, specific solar field costs per m² mirror area.

Table 22. Tower concentrators, solar field model parameters (AUD/m²); RMSE: root mean square error.

| Set of data points | Ref. spec. cost, AUD/m ² | Exponent | RMSE |
|--------------------------|-------------------------------------|----------|-------|
| All | \$405 | 0.9 | \$127 |
| low cost (Solar Reserve) | \$345 | 0.9 | \$0 |

Figure 66 compares the unit solar field costs (in AUD/m²) for all modelled cases at reference solar field size (50 MW_{th}). Average unit costs are comparable across all three concentrator technologies, while low cost options exist for trough and Fresnel that are around 50% lower in cost. It should be noted that annual thermal energy generation varies across technologies with tower concentrators suffering from lower cosine optical losses and hence higher annual output per m² compared to linear concentrators.

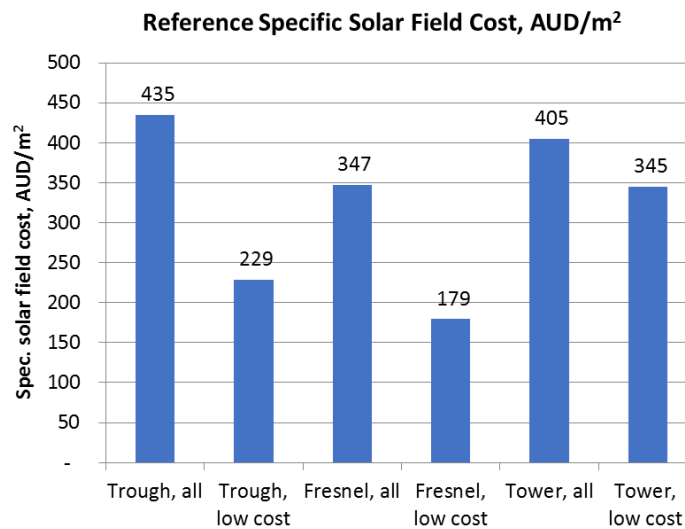


Figure 66. Specific solar field cost at 50 MW_{th} solar field size, across all technologies.

B.2.2. Thermal storage

Data points and model results for the thermal storage system are shown in Figure 67 and Table 23. Data points include oil- and salt-based TES systems, both from linear and tower type solar systems.

The amount of storage medium required is inversely proportional to the temperature difference over which the storage system operates (hot to cold tank; assuming the specific heat capacity is constant with temperature). Since the storage system costs are mainly determined by the costs for the storage medium, to an approximation storage system costs also scale inversely with storage amount (as long as there is no size dependence of the medium costs).

All data points (as well as the model) are adjusted with regard to the temperature difference of the TES system. The data shown in Figure 67 is presented for a temperature difference of 100°C (in accordance with the low-temperature steam application). For the higher temperature steam application, where the solar thermal system operates between 300 and 500°C, the storage unit costs are half of those shown in Figure 67.

Based on the data shown, there are no clear cost trends with regard to any of the following parameters:

- type / permissible operating temperature of storage medium (oil, salt)
- status of technology provider
- storage size (capacity)

Consequently, a model was created that captures all data points. In the absence of a clear size dependence, $x = 1$ was set.

As seen in Figure 67, a low-cost mineral oil TES medium is proposed for low-temperature applications. This oil can operate up to 315°C and would result in a step change in TES costs. A second model was generated to represent this low-cost TES option for low-temperature steam generation.

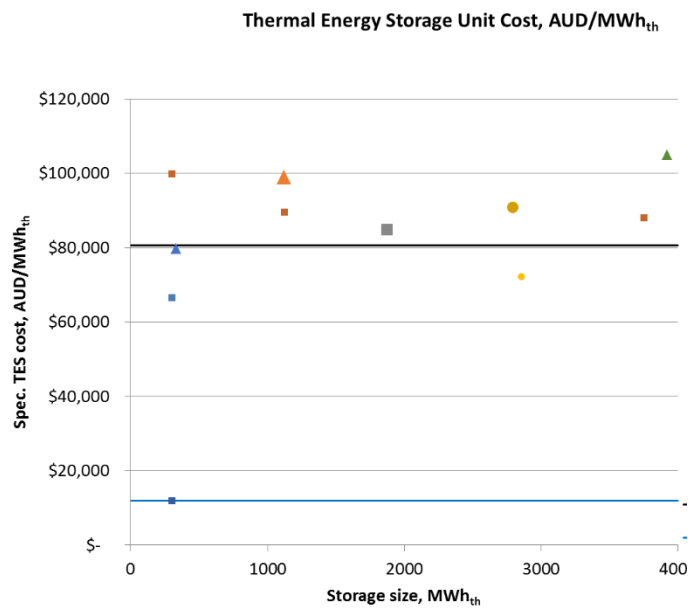


Figure 67. Specific TES costs per MWh_{th} of capacity, normalised for T-range 200 to 300°C.

Table 23. Thermal energy storage model parameters (AUD/MWh_{th}), for a temperature difference of 100°C between hot and cold storage tanks; RMSE: root mean square error.

| Set of data points | Ref. spec. cost, AUD/MWh _{th} | Exponent | RMSE |
|--------------------|--|----------|----------|
| All | \$80,685 | 1.0 | \$24,393 |
| mineral oil | \$11,916 | 1.0 | \$0 |

B.2.3. Balance of plant

Balance of plant unit costs and model results are shown in Figure 68 and Table 24. The size dependence exponent, $x=0.7$, has been previously determined and is fixed at this value here. Similarly as for the solar field, a set of low-cost data points can be observed. Consequently, two

models are generated, one representing all data points and one model fitted to the low-cost data points. Again, the latter model is considered as the “best case” scenario for the near future.

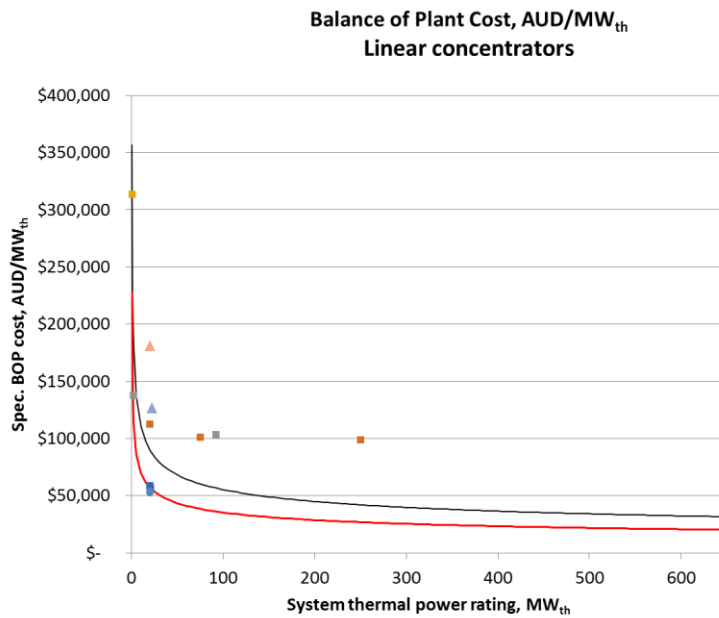


Figure 68. Specific BOP costs per MW_{th} design system output.

Table 24. Balance of plant model parameters (AUD/MW_{th}); RMSE: root mean square error.

| Set of data points | Ref. spec. cost, AUD/MW _{th} | Exponent | RMSE |
|--------------------|---------------------------------------|----------|----------|
| All | \$89,578 | 0.7 | \$46,805 |
| Low-cost offers | \$57,150 | 0.7 | \$5,336 |

B.3. Operation and Maintenance costs

O&M costs are mainly due to the labour costs for supervising the plant performance and for mirror field cleaning. Additional costs arise from component replacements (receivers, mirrors), cleaning equipment, and water usage.

O&M cost data has been obtained from several sources, including literature, SAM and technology suppliers, for all CST technologies. Data has been converted to AUD/MWh_{th} and is plotted in Figure 69. There is a relatively large spread in the O&M costs among different data sources. The mean is AUD12.34/MWh_{th}. No clear trend could be seen with regard to:

- CST technology (concentrator type, heat transfer fluid)

- status of technology provider

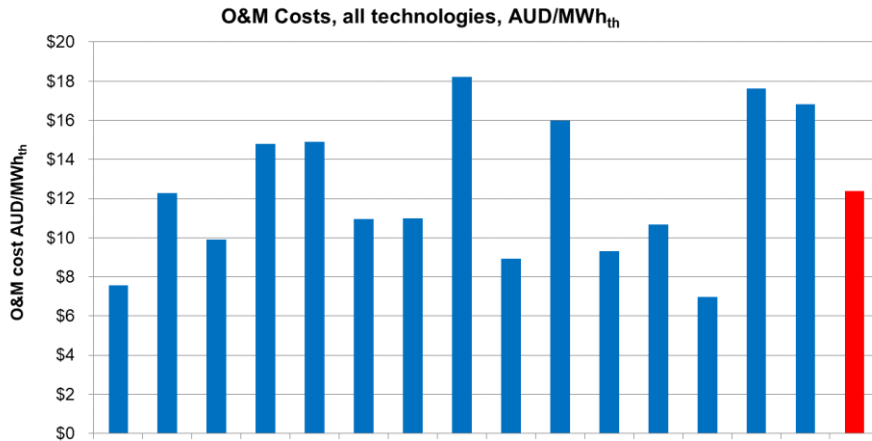


Figure 69. O&M costs across all technologies, per MWh_{th} thermal output.

Figure 70 shows the annual O&M cost data expressed as a percentage of the estimated total installed system costs for eleven data points (for which total installed costs are available) from Figure 69. There seems to be a dependence of O&M costs on system size (measured here in terms of CAPEX).

Fitting the data points with a 0.7 power law (black curve) results in the model parameters listed in Table 25. The model predicts O&M costs of 2.05% for a system CAPEX of AUD100m, declining to 1.03% for a CAPEX of AUD1bn. This model is used the economic study to determine the O&M costs of each plant configuration.

Table 25. O&M cost model parameters (% of capex pa.).

| Ref. size, mAUD | O&M % of capex at ref. size | Exponent |
|-----------------|-----------------------------|----------|
| 100 | 2.05% | 0.7 |

Based on the data points, systems with CAPEX ranging from 50 to AUD500m have annual O&M costs ranging from 2% to 1.25% of CAPEX pa. For smaller systems, the O&M percentage increases rapidly.

The data point Zhu '14 is based on data for a CSP system and may over-estimate the actual O&M costs of a process heat plant of this size, for two reasons. One, the O&M percentage of CAPEX is calculated using the total O&M costs of the CSP plant divided by the CAPEX of the system without the power block. This calculation assumes that all the O&M originate from the

solar system and the O&M costs of the power block are negligible in comparison. Two, the data point is 4 years old and lower O&M costs may be achieved today.

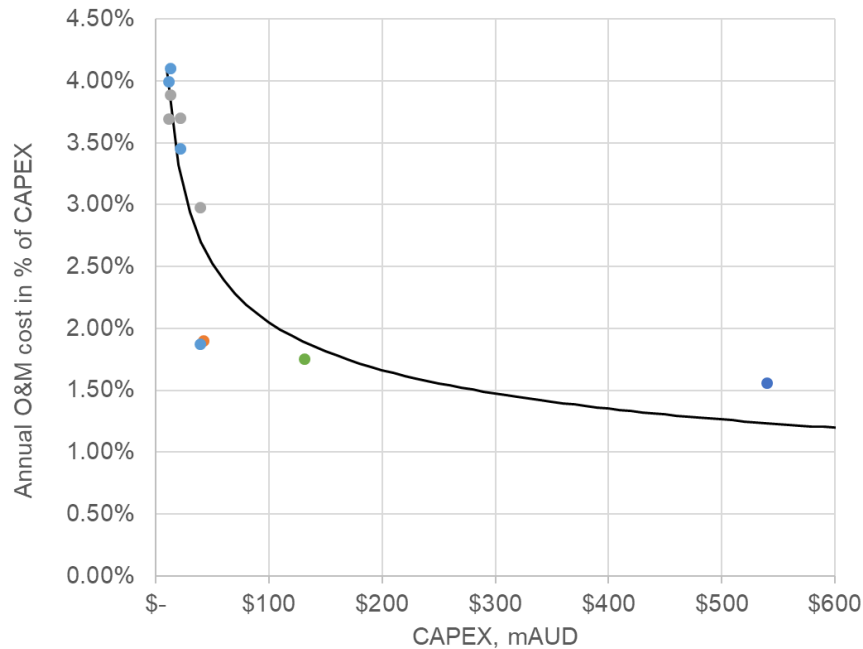


Figure 70. Annual O&M costs in % of CAPEX as a function of system size (in terms of CAPEX).

Synergies may exist between the operations of the alumina refinery and the CST plant that may reduce the O&M costs at the reference site.

In addition, ongoing R&D on anti-soiling mirror coatings and automated solar field monitoring and cleaning may lead to reductions in the O&M cost in the future (possibly with an effect on existing plants).

For these reasons, we present another set of results where O&M costs are set to zero. These results illustrate the potential impact of O&M cost reductions on the solar energy unit costs, compared to the base case scenario.

B.4. Model verification

To verify the cost models and obtain an estimate of their accuracy in reproducing the available cost data, SAM models have been generated to reproduce the available data, using cost input parameters generated with the above component cost models. Original data points and SAM model results are compared in terms of the sum of the component costs, $C_{SF} + C_{TES} + C_{BOP}$. The results are presented in Figure 71-Figure 73 for the system operating temperature ranges of 200-

300°C and 300-500°C (negative data points correspond to underpredictions of the real costs by the model).

The sum of the component costs is calculated by combining the component cost models for SF, TES and BOP in three ways: 1) by using the “average” cost models for SF, TES and BOP; 2) by using the “low-cost” models for SF, TES and BOP; 3) by using the low-cost models for SF and BOP and the “average” cost model for TES.

Note that in all systems the same medium is used both as the HTF and as the TES medium (either both oil or both molten salt). There are no systems that combine oil HTF with molten salt TES.

As can be seen from the results in Figure 71-Figure 73, the models are able to reliably reproduce the data points across a range of sizes from 0.2 MW_{th} up to several hundred MW_{th} and across all CST technologies, with a typical error below 20%. In particular, costs of systems at smaller scales are reproduced with reasonable accuracy. With this level of confidence, the models are expected to be useful tools for an initial feasibility assessment, in particular for a near-term pilot-scale project on the order of several MW_{th}.

Only one data point for a large-scale Fresnel system is not well represented by the models, which is quoted significantly higher than any other system in the same size range. One reason for that may be that the BOP costs are quoted for a CSP system and hence are significantly higher than those of a process heat system.

Based on these results, state-of-the-art systems should be modelled with the average cost models. The low-cost models can be used to estimate current/near-term best-case costs for oil-based trough systems operating at up to ~300°C. The combination of low-cost SF and BOP models and average cost TES model can be used to estimate current best-case costs for salt-based systems operating at up to 500°C.

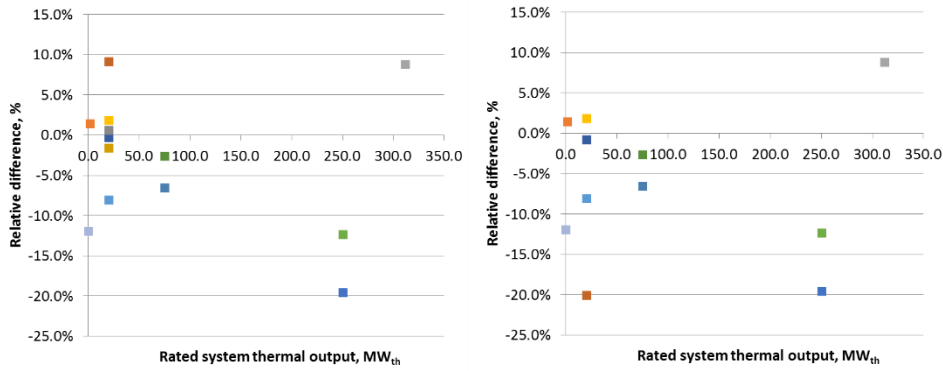


Figure 71. Trough-based systems, relative difference of model results and cost data points, left 200-300°C, right 300-500°C.

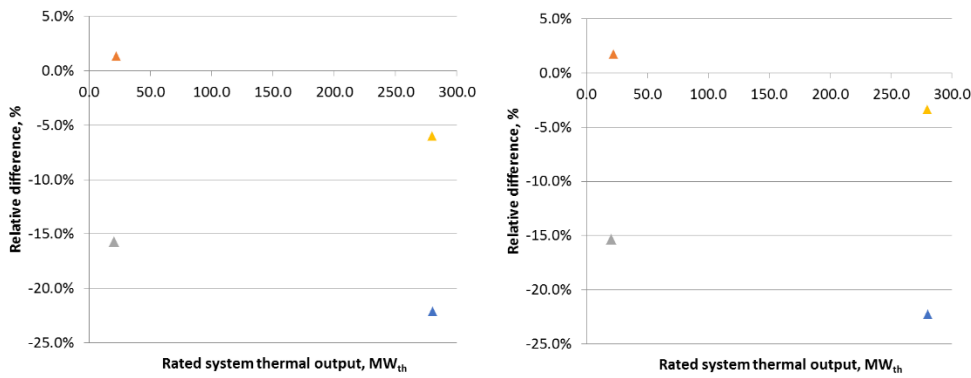


Figure 72. Linear Fresnel-based systems, relative difference of model results and cost data points, left 200-300°C, right 300-500°C.

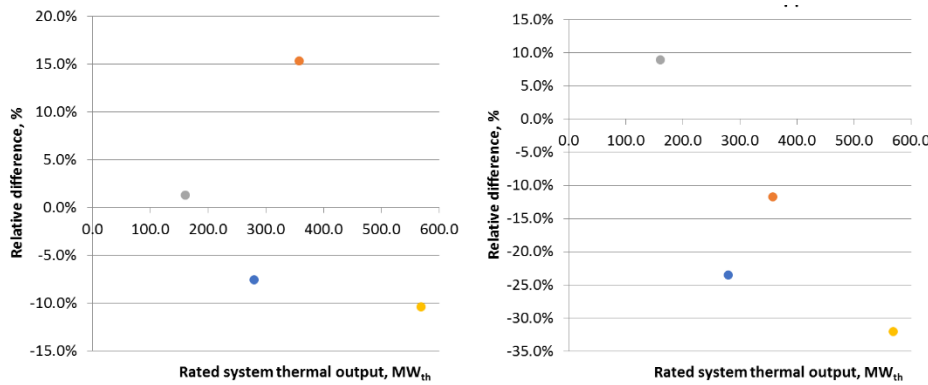


Figure 73. Tower-based systems, relative difference of model results and cost data points, left 200-300°C, right 300-500°C.

ITP Thermal Pty Ltd

Office: Level 1, 19-23 Moore St
Turner ACT 2612

Postal: PO Box 6127
O'Connor ACT 2602
Australia

Email: info@itpau.com.au
Phone: +61 (0) 2 6257 3511

itpthermal.com